Laser Diagnostics in Turbulent Combustion Research

Jeffrey A. Sutton

Department of Mechanical and Aerospace Engineering
Ohio State University

Princeton-Combustion Institute Summer School on Combustion, 2019

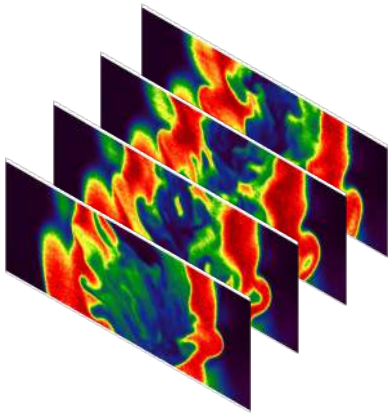

Lecture 9 – Absorption and Basic Laser-Induced Fluorescence Principles

Overview and Outline of Lecture

Goal: Provide an Overview of the Fundamentals of Absorption and Laser-Induced Fluorescence

- Brief Discussion of the Absorption Process and Absorption Spectroscopy
- Development of the LIF Rate and Fluorescence Signal Equations

In the Last Lecture…

- Last lecture we spent time examining basic spectroscopy – which included developing a means to understand which transitions are "allowed", why they are allowed, and "where" to tune your laser to for diagnostic applications
- For example, OH absorption:

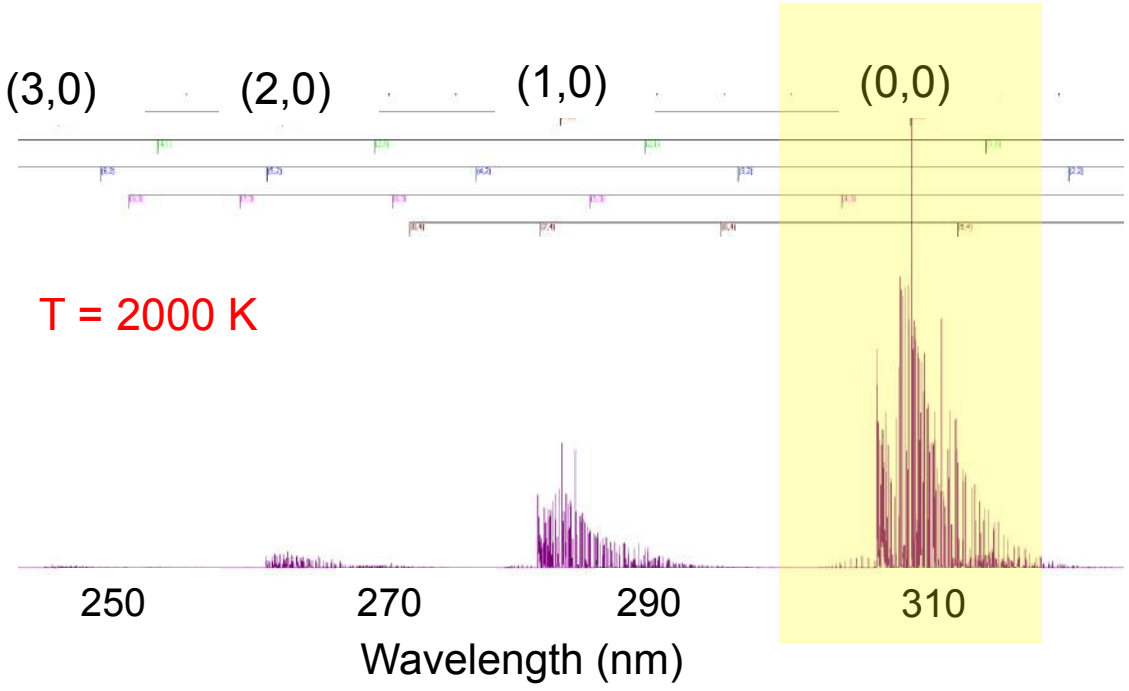

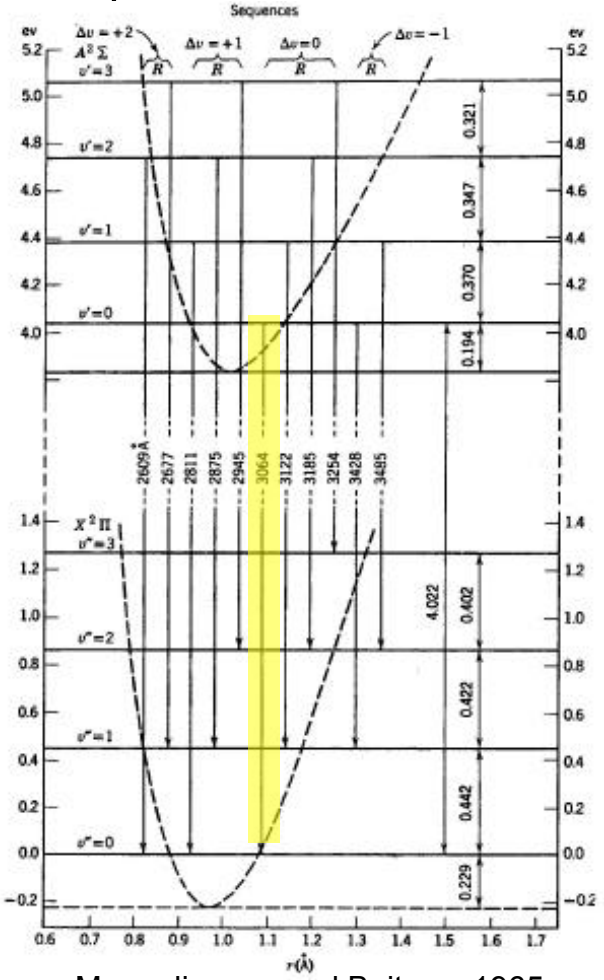

In the Last Lecture…

- OH absorption (in more detail):

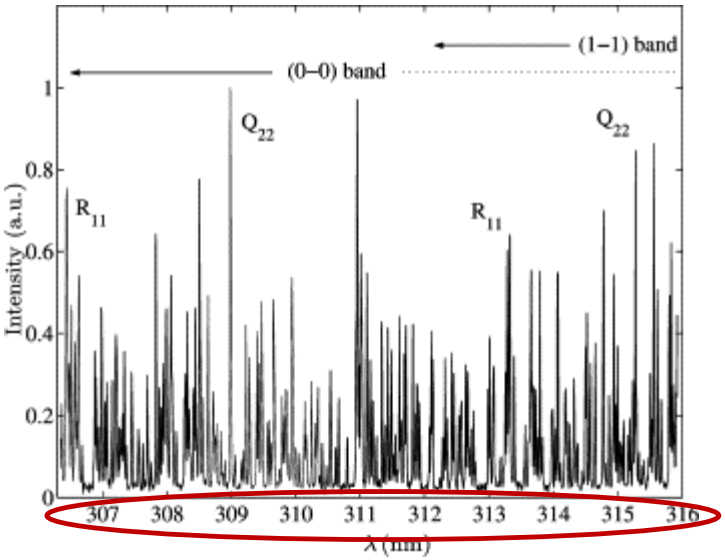

Singla et al., CNF, 2006

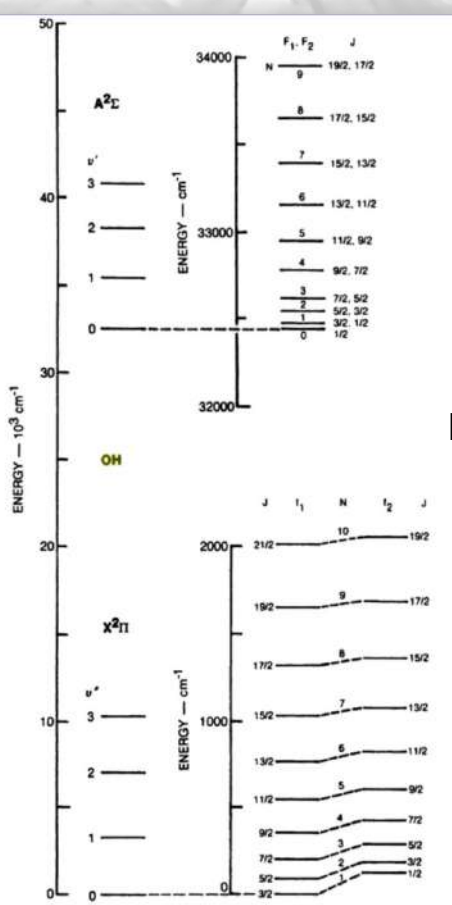

Eckbreth, 1996

- If you think about it, we spent an entire lecture discussing the “x axis”!
- More specifically, what frequencies in which electronic, vibrational, and rotational transitions occur – i.e., where to tune your laser for absorption or LIF!

This Lecture…

- So, what about the y-axis?
- We need to understand how the energy is distributed (i.e., how the individual transitions are populated) and what determines the relative intensities of each rotational line

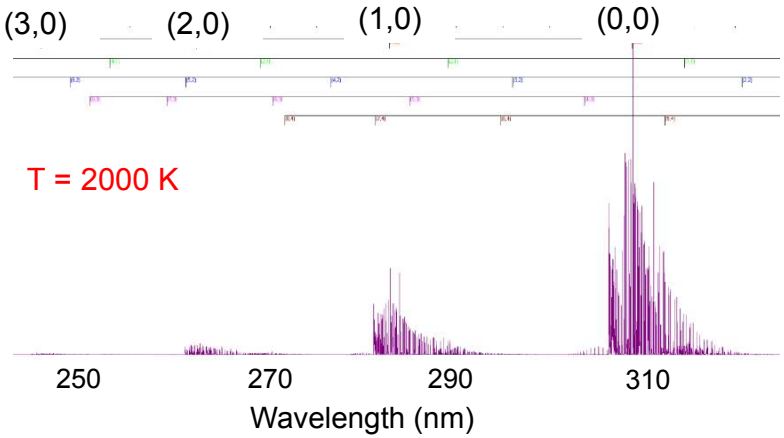

- However, I think it is informative to develop the basic theoretical foundation behind absorption and laser-induced fluorescence (LIF) first.
- After the development of absorption and LIF equations, then we can go back and focus on the "y-axis" (from a spectroscopic point-of-view) as this is very important in choosing the appropriate transitions for LIF measurements as we ultimately want to use LIF techniques in various turbulent flame situations.

Electric Dipole

- An electric dipole is a separation of positive and negative charges, which is characterized by their dipole moment ($\vec{p}$):

$$\vec{p} = q \cdot \vec{d} \qquad \textbf{(100)}$$

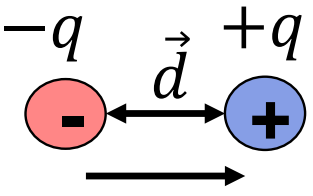

where *q* is the magnitude of the charge and $\vec{d}$ is the separation between the two charges or "displacement vector".

- From a physical point-of-view, we know that there is a charge distribution within an atom or molecule. For molecules there can be non-uniform distributions of positive and negative charges and thus, the molecules have dipole moments. We refer to these as "molecular dipoles".
- Molecules can be classified as having a "permanent dipole" when two atoms in the molecule have different electronegativity ("force" of electron attraction). These molecules are called "polar molecules".
- In addition, a dipole moment can be "induced" in a molecule by an external electric field

Molecular Dipole Model

- Recall, the electric field oscillation drives a polarization in the molecule (we discussed this in Lecture 3)
- A realistic medium (i.e., a gas) has a large number of dipoles. The density of the dipoles is represented by a total count within a unit volume, *N* [#/m^3]. Assuming an average dipole moment of $q \cdot \vec{d}$, then the summation of the all of the dipole moments within the unit volume is

$$\vec{P} = N \cdot q \cdot \vec{d} = \varepsilon_o \chi \vec{E} \qquad \textbf{(21)}$$

- A polarization is a coherent oscillation between two electronic states; that is, the external electric field (laser light) induces an oscillating dipole within the molecule. How?
- When an external electric field interacts with molecules, the local electron cloud is perturbed (the electron orbits are disturbed). The oscillation of the electron cloud results in a periodic separation of charges and an induced dipole moment. The dipole also is a source of emitted EM radiation (we'll look at this when discussing Rayleigh/Raman scattering)
- The type of induced dipole depends on the wavelength (frequency) of the light! Assuming that the optical frequency of the laser overlaps an allowed transition (subject to selection rules), then absorption can occur.

Transitions and Absorption

- Optical electromagnetic radiation (i.e., laser light) permits transitions among electronic states

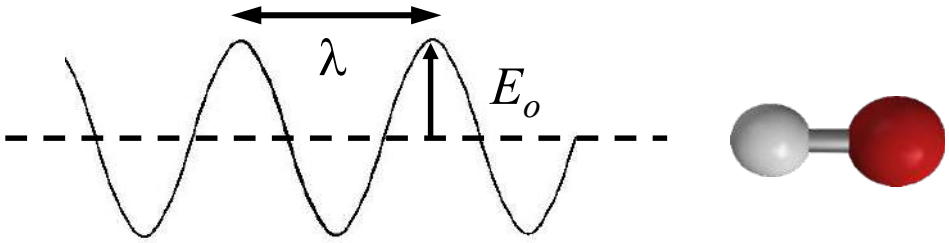

- If $\lambda = hc/\Delta E$ corresponds to a vibrational energy gap, then the radiation will be absorbed, which will results in a molecular vibrational transition.
- If $\lambda = hc/\Delta E$ corresponds to an electronic energy gap, then radiation will be absorbed and the electron will be promoted from the highest occupied molecular orbit (HOMO) to the lowest unoccupied molecular orbit (LUMO)

Pictorial of Absorption

Absorption: induced oscillation of a dipole; the rotation of the molecule is accelerated by the electric field of an incident photon to a higher frequency ("orbit" at higher energy); the molecule ends up in an excited electronic state. This "removes" a photon from the incident field.

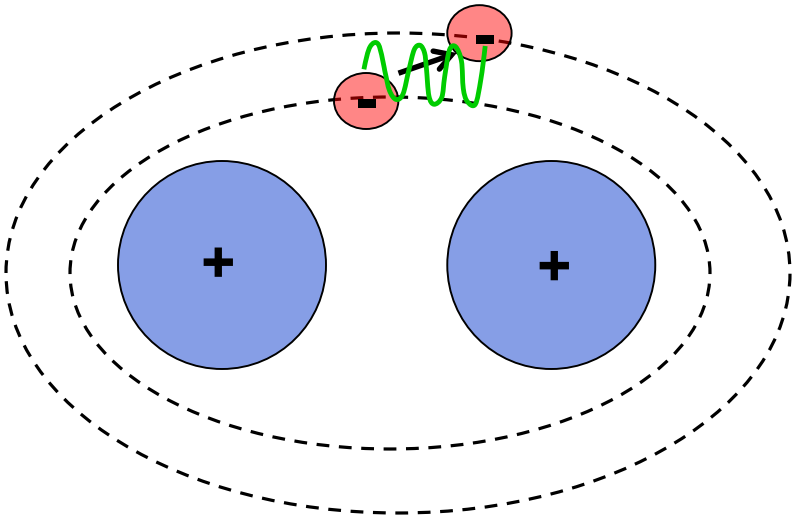

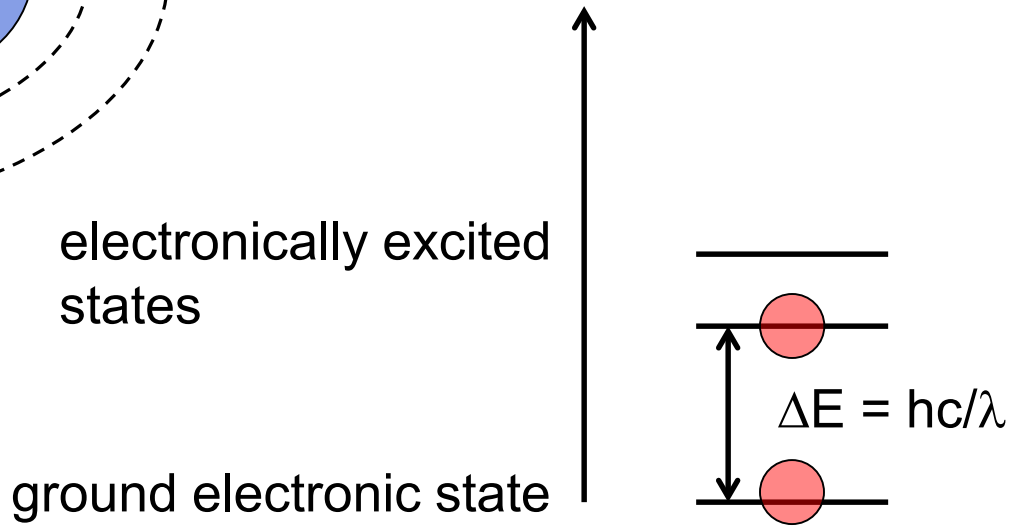

Absorption Principles

- in the early 20th century, Einstein proposed that the absorption and emission of photons can be treated in a similar manner to a collisional process, described by the product of a rate coefficient and the concentrations of the molecules and photons

- The overall rate at which absorption occurs (per volume) can be written as $W_{12}n_1$, where n_1 is the number density of the ground state and the absorption rate per molecule between states 1 (initial i) and 2 (final f) is

$$W_{12} = \int_{\nu} B_{12} I_{\nu}(\nu) Y(\nu) d\nu \qquad \textbf{(107)}$$

  where B_{12} is the Einstein B coefficient for absorption, $I_{\nu}(\nu)$ is the laser spectral irradiance lineshape, and $Y(\nu)$ is the absorption lineshape (more on this later)

- For a laser source which is spectrally broad compared to the absorption linewidth, Eq. (107) reduces to

$$W_{12} \approx B_{12} I_{\nu} \qquad \textbf{(108)}$$

  where I_{ν} is the laser spectral irradiance at the center of the absorption line

Absorption Principles

- The Einstein B coefficient can be calculated from

$$B_{12} = \frac{8\pi^3 \vec{p}_{fi}}{3ch^2 g_1} \qquad \textbf{(109)}$$

where g_1 is the degeneracy of the initial state 1, defined as (2J+1), J is the total angular quantum number, and $\vec{p}_{fi} = \int \psi_f^* \vec{p} \psi_i d\tau$ is the dipole transition moment

- For molecules the Einstein B coefficient is a function of the electronic, vibrational, and rotational states. The Einstein B coefficient can be calculated from Eq. (109) if a solution to the Schrödinger equation for the wave function of the molecular system of interest has been obtained. Typically, the Einstein coefficients are determined experimentally.

- Note that the relationship between the Einstein B coefficient in spectroscopic units to SI units is

$$B_{12}[s^{-1}(W/cm^2/cm^{-1})^{-1}] = c^{-1} B_{12}[s^{-1}m^2 J^{-1}] \times c^{-1} \times 10^2 \qquad \textbf{(110)}$$

Absorption Principles

- As photons are absorbed, there is attenuation of the laser beam as it propagates through the absorbing medium. This is "desired" for absorption spectroscopy, but considered as "loss mechanism" for LIF

- The absorption of a collimated beam is proportional to the laser spectral irradiance and the distance traveled (dx) as

$$-dI_\nu = \alpha I_\nu dx \qquad \textbf{(111)}$$

  where the proportionality coefficient, α, is known as the absorption coefficient

- Eq. (111) can be integrated to yield the portion of the spectral irradiance that is transmitted through the medium

$$I_\nu = I_{\nu,0} e^{-\alpha x} \qquad \textbf{(112)}$$

  where $I_{\nu,0}$ is the incident spectral irradiance

- It is common to write the absorption coefficient as

$$\alpha = S_{12} Y(\nu) \qquad \textbf{(113)}$$

  where S_{12} is the linestrength for a given transition

Absorption Principles

- Moving forward with absorption (or LIF) we need to consider what type of model we will use for the molecular system.
- First, let's just consider a two-level model describing only the levels coupled by the laser radiation (ground, electronic state and excited, electronic state), where the lower state has population n_1 and the upper state has population of n_2.
- To calculate the absorption coefficient, consider a collimated beam of irradiance I_ν between frequencies $\nu + d\nu$ over a pathlength of dx
- Only a fraction of the absorbers in the lower state can absorb in the frequency range of $\nu + d\nu$. This fraction is denoted as δn_1 and is represented by the interaction of n_1 with the absorption lineshape:

$$\delta n_1 = n_1 Y(\nu) d\nu \qquad \textbf{(114)}$$

- In a volume of length dx there will be $\delta n_1 dx$ absorbers with an absorption rate of W_{12} and a total number of absorption transitions per second of

$$R_A = I_\nu B_{12} \delta n_1 dx \qquad \textbf{(115)}$$

Absorption Principles

- The total amount of energy absorbed over a length dx is

$$-dI_\nu d\nu = h\nu c(R_A - \underbrace{B_{21} I_\nu \delta n_2 dx}) \quad \textbf{(116)}$$

Due to stimulated emission

- If the population in the excited state (n_2) is small, Eq. (116) is reduced to

$$-dI_\nu d\nu = h\nu c(I_\nu B_{12} \delta n_1 dx) = n_1 h\nu c I_\nu Y(\nu) dx d\nu \quad \textbf{(117)}$$

- Comparing Eq. (117) to Eq. (111), we see that the absorption coefficient can be written as

$$\alpha = n_1 h\nu c Y(\nu) B_{12} \quad \textbf{(118)}$$

and the linestrength as

$$S_{12} = n_1 h\nu c B_{12} \quad \textbf{(119)}$$

- Thus, the fractional portion of the laser irradiance that transmits through the absorbing medium can be written as

$$I_\nu / I_{\nu,0} = \exp(\underbrace{-\tau}) = \exp(\underbrace{-k(\nu)L}) = \exp\left(-n_1 h\nu c Y(\nu) B_{12} L\right) = 10^{-A} \quad \textbf{(120)}$$

Optical depth $k(\nu) = S_{12} Y(\nu)$ *absorbance*

- This is the Beer-Lambert law in several common forms!!!

TDLAS

- Most common application of absorption spectroscopy is **T**unable **D**iode **L**aser **A**bsorption **S**pectroscopy (**TDLAS**); ***TDLAS*** = *absorption spectroscopy with tunable diode laser*
- Laser is tuned over the absorption line by changing diode current. At each wavelength, an absorption measurement is made
- Typically, this is done quite rapidly – scan rates as high at 10 GHz (allows averaging for high SNR and high sample rates)
- Biggest disadvantage of TDLAS or any absorption technique is that it is a line-of-sight (path-integrated) measurement!

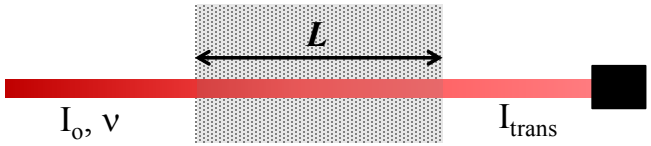

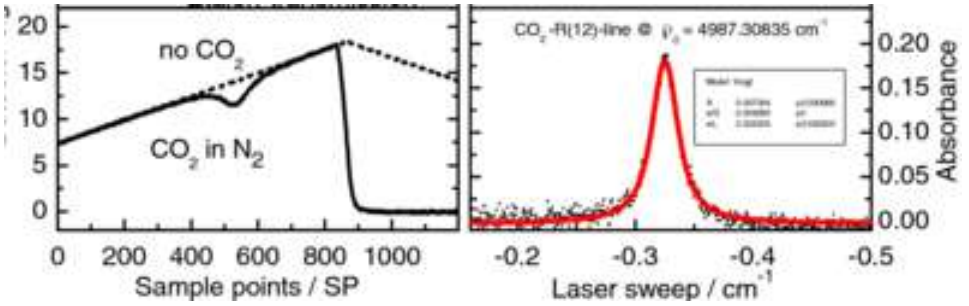

Nwabhoh, et al., 2013

Applications of TDLAS

- Laboratory experiments: Flow reactors, flames, shock tubes
- Ground test facilities: model scramjets, arcjets, shock tunnels, and other high-enthalpy facilities
- Engines: IC engines, gas turbine engines, pulse detonation engines
- Pool fires, explosions, and detonations
- Industry environments: boilers and coal gasifiers
- Scramjet flight test (i.e., AFRL, 2012)
- Atmospheric applications
- Sensitive leak or pollutant detection

Example: kHz-Rate Water Vapor (IC engine)

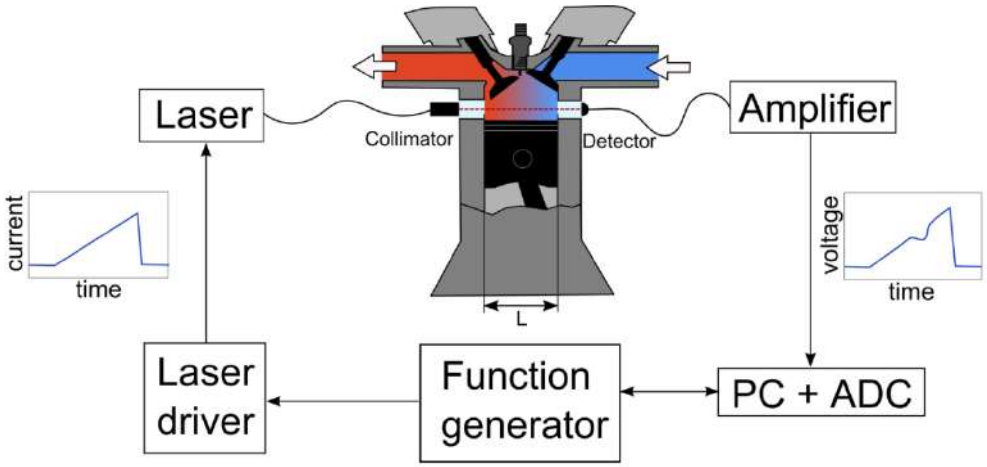

Witzel, et al., 2013

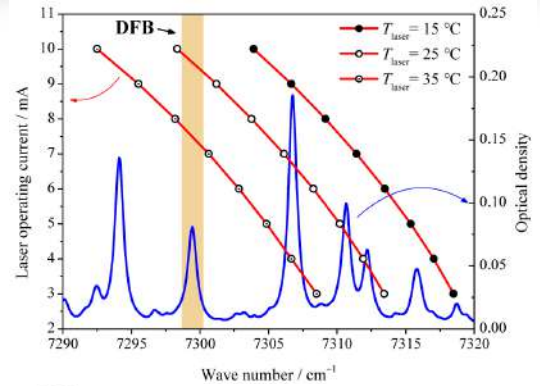

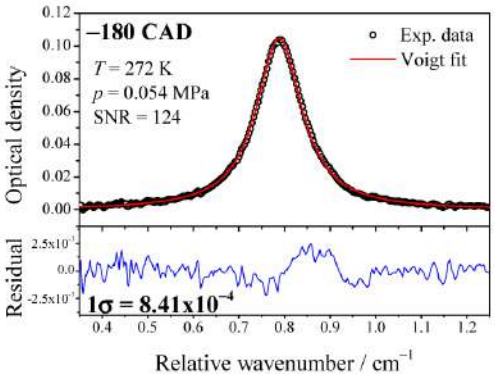

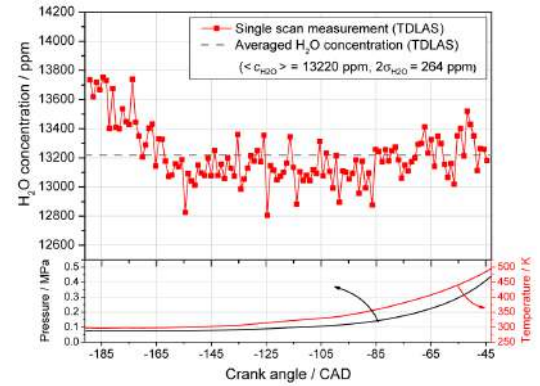

- TDLAS H_2O concentration measurements (1.4 μm) under motored conditions – EGR characterization
- 10-kHz acquisition rate (1.2 crank angle degree resolution)
- SNR > 30 for all measurements

LIF Background

- In its simplest form, LIF can be described as the absorption of laser light at an allowed optical transition followed by a “spontaneous” emission of radiation in the form of UV, visible, or IR light

- Thus, it is a resonant, two-step process: (1) absorption and (2) emission

- After absorption, molecule is in excited state (has “absorbed” energy)

- Molecule quickly loses excess vibrational energy through collisions and falls to lowest vibrational level of excited state

- From this level, the molecule can return to any vibrational level in the ground state – energy loss is in the form of spontaneously-emitted photons, i.e., <u>fluorescence</u>

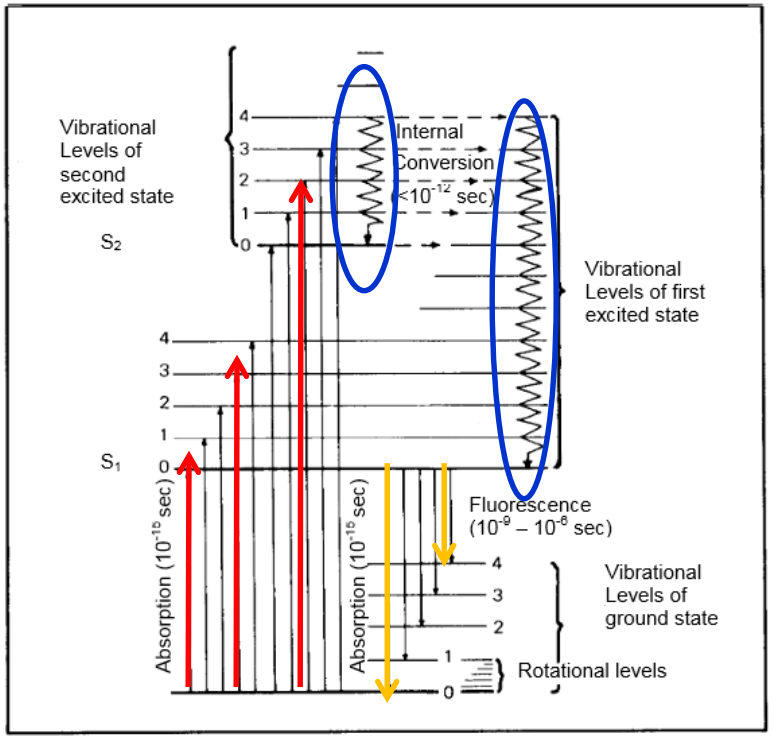

“An Introduction to Fluorescence Spectroscopy” (2000)

- Thus, fluorescence is <u>NOT</u> instantaneous (absorption is!)

LIF Rate Equations

- The LIF equation will be developed based on the semi-classical rate equation analysis first developed by Piepmeier in 1972.
- This approach is conceptually and mathematically easier than quantum mechanical descriptions (but may neglect certain processes and limit broad applicability)
- The photophysics governing LIF for a multi-level molecule can be quite complex - upon excitation, the absorber may undergo several de-energizing processes before it emits photons, which produces the LIF signal

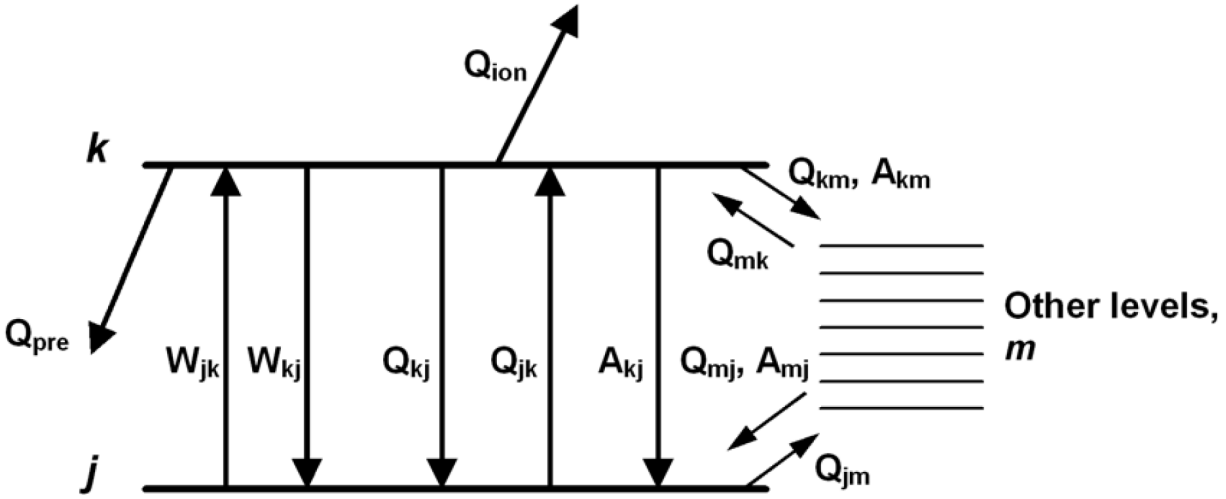

LIF Rate Equations

- Assuming a lower-energy level j and an upper-energy level k *(the laser-coupled states)*, a fraction of the absorbers are transferred to the excited state through stimulated absorption at a rate of W_{jk}.
- The molecule also can be returned to its original quantum state by stimulated emission at a rate of $W_{kj} \approx B_{ij} I_\nu$
- Photo-ionization can occur when additional molecules are absorbed and excite higher molecular states, including ionized levels. Ionization occurs at very high laser irradiances and serves as a population sink. The rate coefficient is $Q_{ion} = \sigma_{2i} I_\nu / h\nu$, where σ_{2i} is the photo-ionization cross section for level 2.

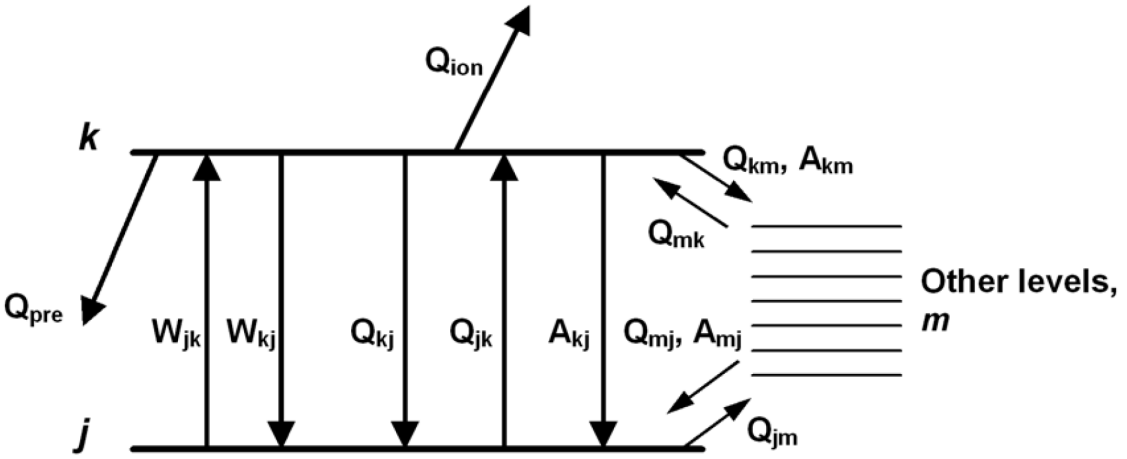

LIF Rate Equations

- Dissociation can occur by the absorption of a second photon. Internal collisions of the atoms can lead to internal energy transfer and cause the molecule to dissociate. When dissociation is produced by a change from stable to a repulsive arrangement, it is called predissociation (rate Q_{pre})

- Depopulation also can occur through inelastic collisions with other molecules producing rotational, vibrational, and electronic energy transfer (rates Q_{kj}, Q_{km}, Q_{mj}). Rotational energy transfer (RET) is the fastest and vibrational energy transfer (VET) is the slowest. Electronic energy transfer rates (also called "quenching" rates) vary significantly for different excited species and collision partners. Quenching is both temperature and pressure dependent

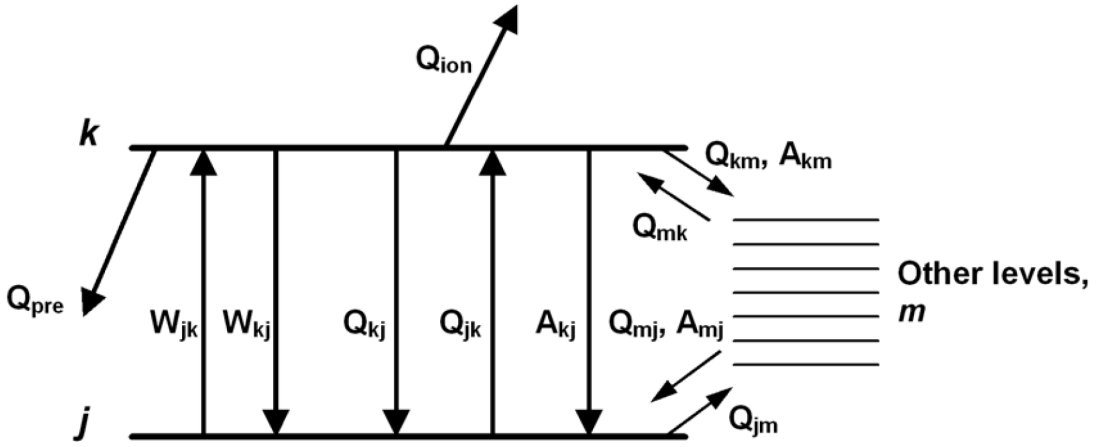

LIF Rate Equations

- After laser excitation, the excited-state molecules can change vibrational and/or rotational levels through RET and VET directly and then radiate light OR they can electronically transfer energy (collisional quenching) and then change vibrational and/or rotational levels
- Finally, the original upper state (laser-populated state) and other nearby upper states which were populated through collisions and RET and VET processes fluoresce isotropically (rates A_{kj} or A_{mj}) producing LIF scattered power, which is proportional to LIF signal

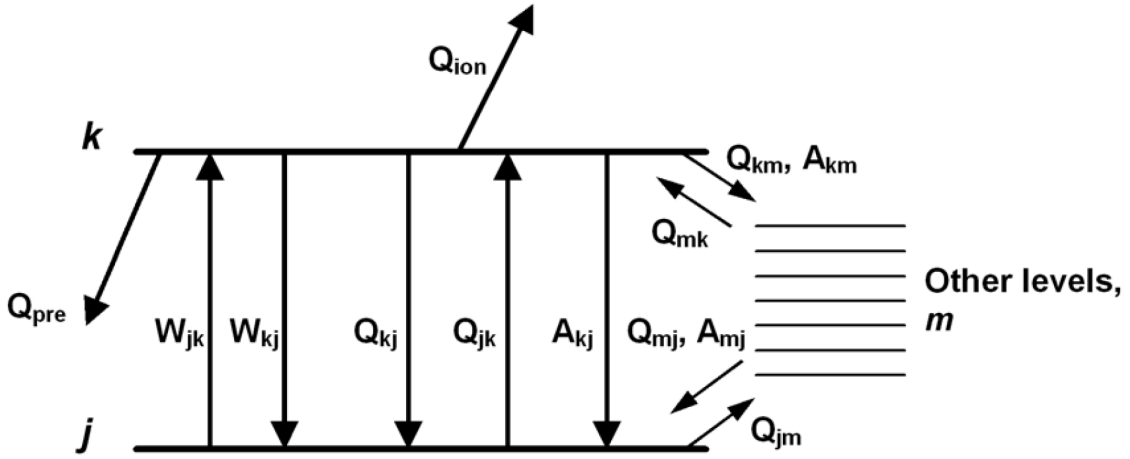

LIF Rate Equations

- The excitation process is modeled by a set of time-dependent rate equations, relating the change of population of a specific quantum state i to the rate at which collisions and radiative processes populate and depopulate state i

$$\frac{dn_i}{dt} = \sum_{i \neq j} n_j (Q_{ji} + W_{ji}) + \sum_{j>i} n_j A_{ji} + \sum_{j<i} n_i A_{ij} - n_i \sum_{i \neq j} (Q_{ij} + W_{ij}) - n_i (Q_{pre} + Q_{ion}) \quad \textbf{(121)}$$

- Q_{ji} and Q_{ij} are the rates at which collisions populate and depopulate state i, respectively through quenching, RET, and VET. A_{ij} and A_{ji} are the Einstein A coefficients for spontaneous absorption and emission, respectively. Q_{ion} and Q_{pre} are the ionization and predissociation rates, respectively.

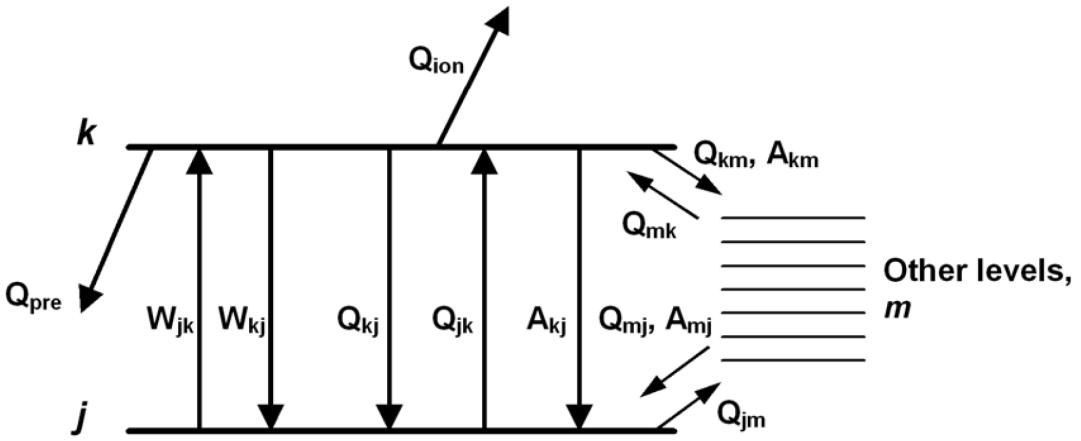

Which Model to Use?

- We need to model the molecular system – to account for the absorption and emission processes between the two laser-coupled states; collisional energy transfer; collisional excitation; photo-ionization; and predissociation. How many "levels" to use?

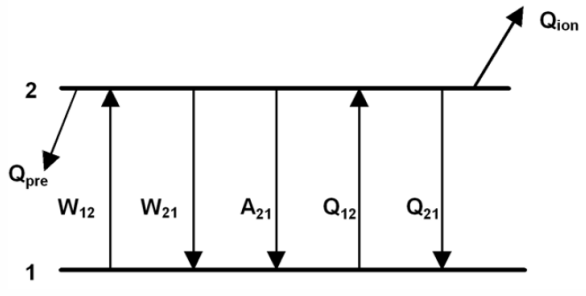

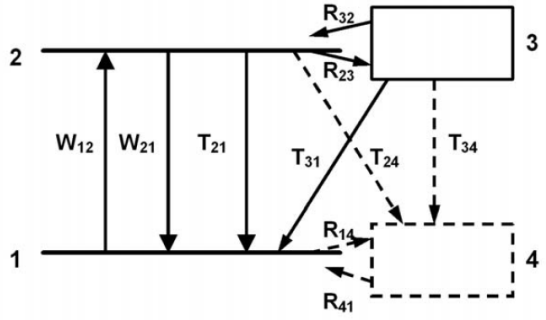

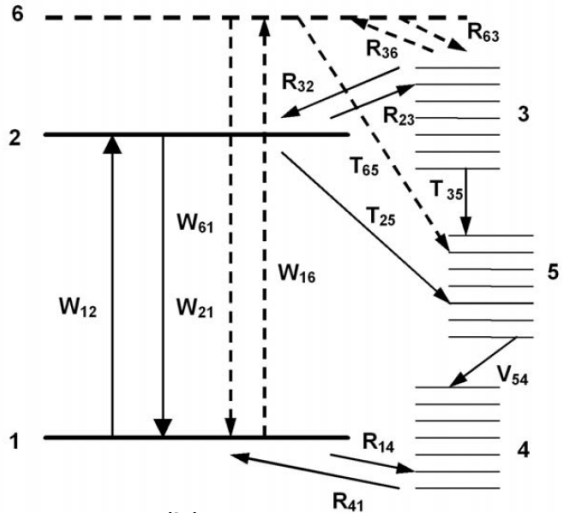

Two-level model **3- and 4-level model** **5- and 6-level model**

- We will develop the LIF equation for a two-level model and discuss where it is accurate and applicable

Rate Equations

- Assuming the LIF process is described only by the two laser-coupled states then the set of rate equations is reduced to:

$$\frac{dn_1}{dt} = -n_1(W_{12} + Q_{12}) + n_2(W_{21} + A_{21} + Q_{21}) \quad \textbf{(122a)}$$

$$\frac{dn_2}{dt} = n_1 W_{12} - n_2(W_{21} + A_{21} + Q_{21} + Q_{ion} + Q_{pre}) \quad \textbf{(122b)}$$

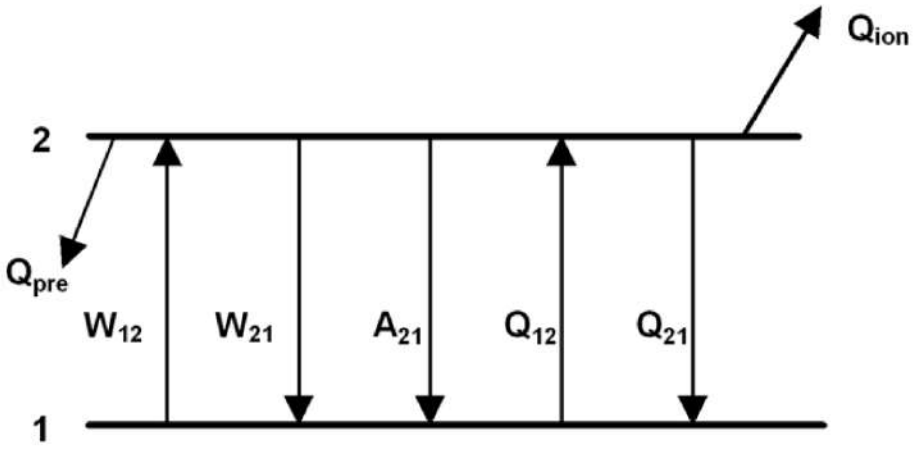

Figure: Two-level model of the energy transfer process during a laser-induced fluorescence (LIF)measurement. Shown are the rate coefficients for spontaneous emission (A_{21}), stimulated absorption (W_{12}) and emission (W_{21}) between the two laser-coupled states, collisional excitation (Q_{12}) and collisional energy transfer, i.e. "quenching" (Q_{21}), photoionization (Q_{ion}), and predissociation (Q_{pre}).

Rate Equations

- To solve this set of equations some assumptions need to be made: (1) Collisional excitation rate Q_{12} is neglected (2) The upper level has a negligible population prior to laser excitation (n_2 ($t<0$) = 0). This allows an initial condition of $n_2(t=0)$ = 0. (3) The total population is conserved (no chemical reactions occur during the measurement). Thus, Q_{pre} = Q_{ion} = 0

- These assumptions reduce the set of equations described by Eq. (122) to

$$\frac{dn_1}{dt} + \frac{dn_2}{dt} = \frac{d}{dt}(n_1 + n_2) = 0 \qquad \textbf{(123a)}$$

$$n_1 + n_2 = constant = n_1^0 \qquad \textbf{(123b)}$$

  where n_1^0 is the initial population of state n_1

- Substitution of Eq. (123b) into Eq. (122b) yields

$$n_2(t) = \frac{W_{12} n_1^0}{r}(1 - e^{-rt}) \qquad \textbf{(124)}$$

  where r = W_{12}+W_{21}+A_{21}+Q_{21} and it is assumed that W_{12} and W_{21} are zero for $t \leq 0$ and constant for $t > 0$.

Rate Equations

- We will define two terms: (i) the fluorescence rate, F_R [photons/cm^3/sec] and (ii) the total number of fluorescence transitions, F [photons/cm^3], which is just the integrated fluorescence rate
- The fluorescence rate is given by $F_R = n_2 A_{21}$, which can be written as

$$F_R = n_2 A_{21} = \frac{W_{12} n_1^0 A_{21}}{r}(1 - e^{-rt}) \qquad \textbf{(125)}$$

- Integrating over the duration of the laser pulse, the total number of fluorescence transitions occurring during the laser pulse is

$$F(0 < t \leq t_l) = \int_0^{t_l} F_R \, dt = \frac{W_{12} n_1^0 A_{21}}{r} t_l \left[1 - \frac{(1 - e^{-rt_l})}{rt_l}\right] \qquad \textbf{(126)}$$

- After the laser pulse, the population n_2 decays from $n_2(t_l)$ to zero with a decay constant of $(A_{21}+Q_{21})^{-1}$, leading to

$$F(t_l < t < \infty) = n_2(t_l) A_{21} \int_{t_l}^{\infty} e^{-(A_{21}+Q_{21})t} \, dt = \frac{n_2(t_l) A_{21}}{A_{21} + Q_{21}} \qquad \textbf{(127)}$$

Rate Equations

- Substituting Eq. (124) for n_2 yields:

$$F(t_l < t < \infty) = \frac{W_{12} n_1^0}{r} A_{21} \left[\frac{(1 - e^{-rt})}{A_{21} + Q_{21}} \right] \qquad \textbf{(128)}$$

- Combining Eqs. (124) and (128) yields the total number of fluorescence transitions:

$$F_{Tot} = \frac{W_{12} n_1^0 A_{21}}{r} \left\{ t_l + (1 - e^{-rt_l}) \left[\frac{r - (A_{21} + Q_{21})}{r(A_{21} + Q_{21})} \right] \right\} \qquad \textbf{(129)}$$

- Define the saturation spectral irradiance as

$$I_\nu^{sat} = \frac{Q_{21} + A_{21}}{B_{12} + B_{21}} \qquad \textbf{(130)}$$

and the general analytic solution for the total number of fluorescence transitions is

$$F = \frac{W_{12} n_1^0 A_{21}}{A_{21} + Q_{21}} \left(1 + \frac{I_\nu}{I_\nu^{sat}} \right)^{-1} \left[t_l + \frac{(1 - e^{-rt_l})}{r} \frac{I_\nu}{I_\nu^{sat}} \right] \qquad \textbf{(131)}$$

Steady-State Solution

- If the laser pulse is long compared to the characteristic time, $t_l >> r^{-1}$, then steady-state has been achieved. In this case, the total number of fluorescence transitions is represented by

$$F_{SS} = \frac{W_{12} n_1^0 A_{21}}{A_{21} + Q_{21}} \left(1 + \frac{I_\nu}{I_\nu^{sat}}\right)^{-1} t_l \qquad \textbf{(132)}$$

- As an example, let's compare the general and steady-state solutions for NO (λ_{exc} = 226 nm) at P = 1 atm and T = 1500K

- Rate coefficients and quenching rates are taken from the literature and the incident irradiance is chosen to match common experimental values.

- It is clear that the steady-state approximation is valid for typical flame conditions and pulse lengths longer than a few ns.

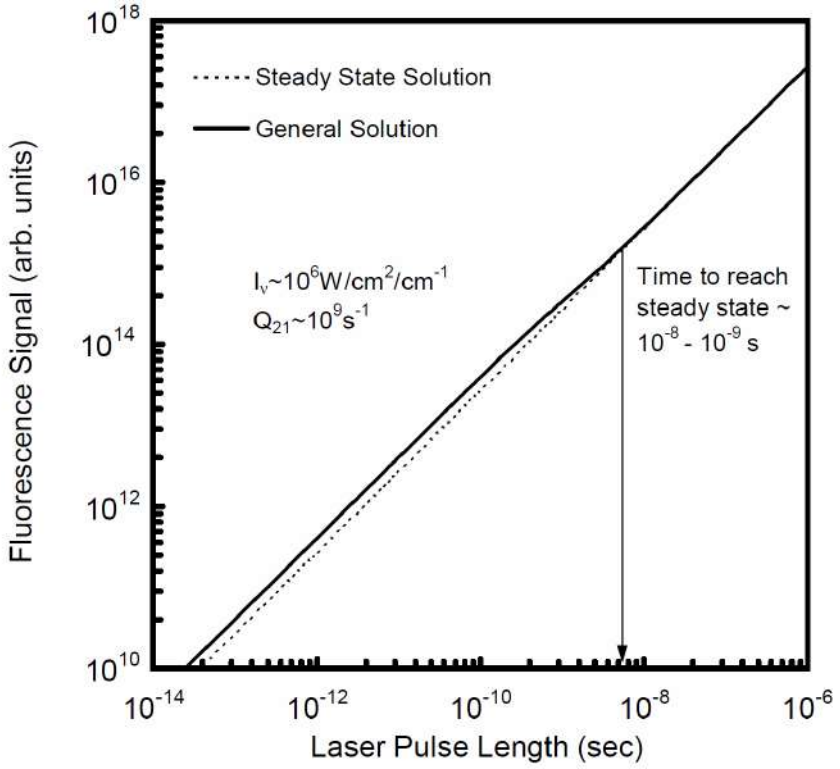

Linear Solution

- In many experiments, the laser irradiance is much less than the saturation irradiance ($I_\nu \ll I_\nu^{sat}$), especially in imaging situations
- Thus, as $I_\nu / I_\nu^{sat} \rightarrow 0$, the low-irradiance solution of the integrated fluorescence rate is written as

$$F_{linear} = W_{12} n_1^0 \frac{A_{21}}{A_{21} + Q_{21}} t_l \qquad \textbf{(133)}$$

- This equation is often termed the “linear fluorescence equation” since F scales linearly with W_{12}, which is linearly proportional to the laser irradiance.
- The term $A_{21}/(A_{21}+Q_{21})$ is the Stern-Volmer function and represents the ratio of the transitions that produce fluorescence photons to the total number of transitions. Sometimes referred to as the “quantum yield”

Linear Solution

- We can compare the general analytic and linear solutions for the same previous conditions: NO (λ_{exc} = 226 nm) at P = 1 atm and T = 1500K
- The solution is obtained with a 6-ns laser pulse length
- For low values of laser irradiance, there is a linear increase of fluorescence signal (proportional to F) with increasing laser irradiance and the linear approximation is valid
- As laser irradiance increases, the relationship between F and the laser irradiance becomes non-linear and the regime is said to be "partially saturated" or "fully saturated" when the response of F is flat with increasing irradiance
- The irradiance that satisfies the linear solution has to be determined for each molecule/environment!

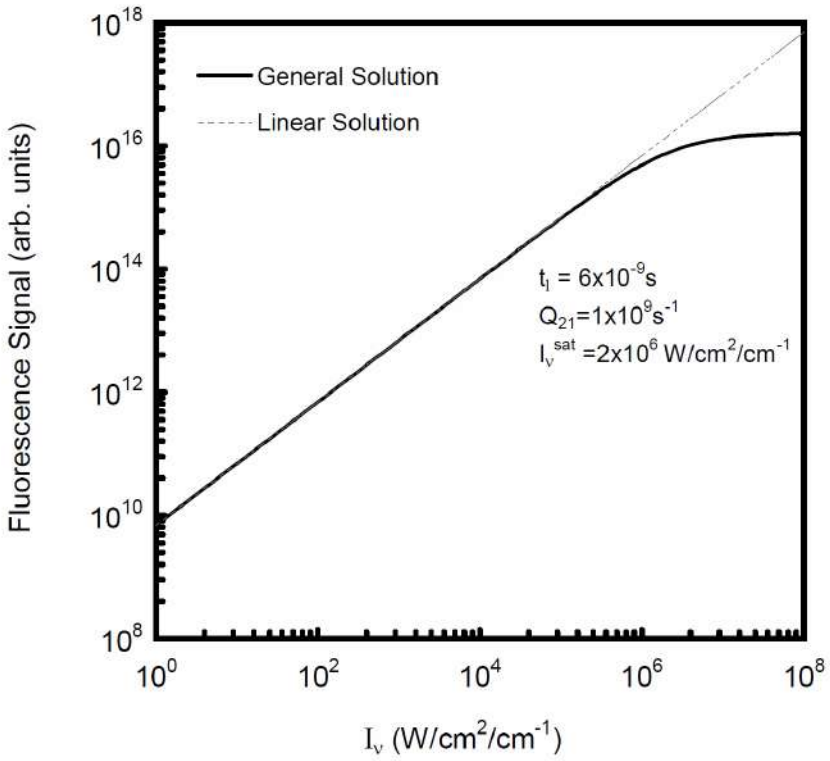

Linear Solution

- For example, here is a measurement for OH signal response as a function of laser energy within a laminar, premixed flame
- In this test, a spectrally narrow 282-nm laser beam was focused to a point ($d \approx 200$ μm). Hence the low laser energies lead to large spectral irradiance ($W/cm^2/cm^{-1}$) values

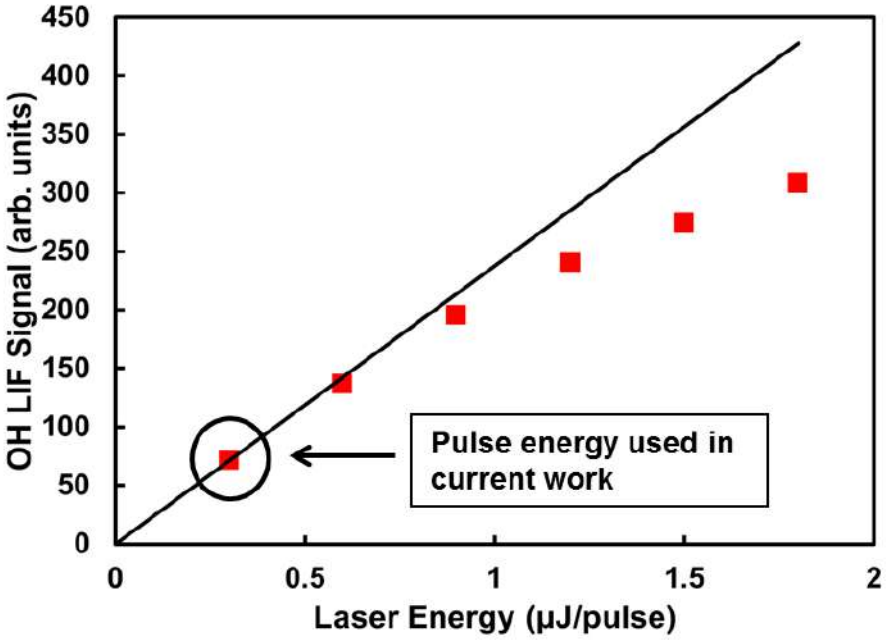

Fluorescence Signal

- Even though the fluorescence is emitted isotropically, only a portion of the light will be collected by the optical system
- The collected fluorescence signal (S_f) is a function of the total number (or rate) of fluorescence transitions, the collection efficiency of the optical system, the energy of the photons being excited and the size of the probe volume
- The exact expression depends on the desired units: photons, photons/sec, or photon power collected:

$$S_f[\text{photons collected}] = F\frac{\Omega}{4\pi}\eta LA \qquad \textbf{(134a)}$$

$$S_f[\text{photons/sec collected}] = F_R\frac{\Omega}{4\pi}\eta LA \qquad \textbf{(134b)}$$

$$S_f[\text{photon power collected}] = F_R\frac{\Omega}{4\pi}\eta LA(hf) \qquad \textbf{(134c)}$$

where Ω is the collection solid angle, L is the length of interaction volume, A is the cross sectional area of the beam, η is the collection efficiency of the optics, and hf is the photon energy

Fluorescence Signal

- For low-irradiance conditions ("linear regime"), the fluorescence signal [photons collected] is written as

$$S_f[\text{photons collected}] = \frac{\Omega}{4\pi}\eta V_c W_{12} n_1^0 \frac{A_{21}}{A_{21}+Q_{21}} t_l \qquad \textbf{(135)}$$

where the collection volume, $V_c = LA$.

- To further simplify this and write the fluorescence signal as a function of laser pulse energy (and other terms) we need to know a bit about the absorption lineshape (see Eq. 107) and how the laser interacts with the lineshape. We will look at this in the next lecture

Laser Diagnostics in Turbulent Combustion Research

Jeffrey A. Sutton

Department of Mechanical and Aerospace Engineering
Ohio State University

Princeton-Combustion Institute Summer School on Combustion, 2019

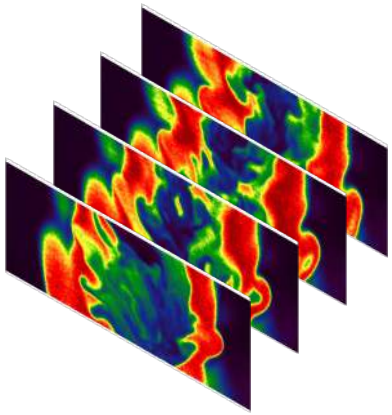

Lecture 10 – LIF Signal Factors and Applications

Overview and Outline of Lecture

Goal: Provide an Overview of the Specific Factors that Affect Laser-Induced Fluorescence Signal

- Discussion of Absorption Line Broadening
- Population Distributions (a little statistical thermodynamics)
- Collisional Quenching Dynamics
- Choosing the "Correct" Transition – i.e., the Sensitivity of the Fluorescence Signal to Environmental Factors
- Overview of LIF Examples in Turbulent Reacting Flows

Absorption Lineshapes

- So far, everything that we did in lecture 8 and 9 would lead to so-called “stick spectra”.
- When light is absorbed (and emitted), it occurs over a finite bandwidth. The transitions between energy levels in molecules are not infinitely thin (i.e., monochromatic), rather they have a finite thickness in frequency space, which is referred to as a “linewidth”
- There are many line broadening mechanisms. We will discuss three: (1) Natural or Lifetime broadening, (2) Collisional broadening, and (3) Doppler broadening. The first two are “homogeneous” and the last one is “inhomogeneous
- “Homogeneous” refers to the fact that all molecules subjected to the laser will broaden in the same way. “Inhomogeneous” implies that each molecule can have a different response

Natural Broadening

- Natural/Lifetime broadening occurs due to the Heisenberg uncertainty principle. Energy is not precisely defined and thus the frequency ($f = E/h$) of absorption and emission lines are broadened (think of it as a time averaged bandwidth due to probability of positioning at any point in time).

- The width is due to the finite excited-state lifetime of a molecule (i.e., the fluorescence lifetime). If the process has a short lifetime, it will have a very large energy uncertainty and thus broad emission and vice versa.

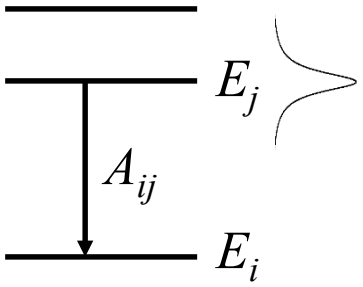

- The linewidth (FWHM) is determined from $\Delta E \Delta t \geq h/2\pi$ which leads to $\Delta f \approx A_{ij}/2\pi$ or $\Delta\nu_N \approx A_{ij}/2\pi c$

- The lineshape function is described by a Lorentzian

$$\varphi_N(\nu) = \frac{\Delta\nu_N}{2\pi} \frac{1}{(\nu - \nu_o)^2 - (\Delta\nu_N/2)^2} \qquad \textbf{(136)}$$

- This process is very small compared to other processes ($\Delta f \leq 1$ MHz or $\Delta\nu_N \leq 3 \times 10^{-5}$ cm^{-1}).

Collisional Broadening

- Collisional broadening results from collisions with other molecules. The frequent interruption of the interaction with the radiative field (absorption or emission) by collisions results in a broadened transition. Collisions impulsively change the phase of the coherence with the light and thus change the response of the molecule to the frequency of light

- The collisional-broadened lineshape function also is given by a Lorentzian distribution such that the integral over all frequencies is unity

$$\varphi_c(\nu) = \frac{\Delta\nu_c}{2\pi} \frac{1}{(\nu-\nu_o)^2 - (\Delta\nu_c/2)^2} \qquad \textbf{(137)}$$

- The collision-broadened width $\Delta\nu_c$ is a function of local composition and usually is cast in the form of an empirical relationship

$$\Delta\nu_c = \sum_i (P_i 2\gamma_i) \qquad \textbf{(138)}$$

where p_i is the partial pressure of species i and $2\gamma_i$ is the collision width per unit pressure induced by species i and given by

$$2\gamma_i = c_1 \left(\frac{T_{ref}}{T}\right)^m \qquad \textbf{(139)}$$

Collisional Broadening

- In Eq. (139), T_{ref} is a reference temperature and both c_1 and m are constants that are determined experimentally.
- As a comparison to natural broadening, $\Delta f \approx 10$ GHz or $\Delta \nu_N \approx 0.3$ cm^{-1} at atmospheric conditions
- Thus, for flows at atmospheric pressure or temperature, the natural linewidth is negligible compared to the collisional broadening
- Its noted that in addition to broadening of the transitions, collisions cause the transitions to shift in frequency space. The collision-induced shift also is a function of species composition and is determined from empirical relationships

Doppler Broadening

- Doppler broadening is due to the fact that molecules have kinetic energy, which is distributed randomly. Microscopically, the thermal motion of the molecules results in the Doppler effect (recall lecture 5). In simplistic terms, the radiative emission from a molecule traveling toward an observer will appear at a higher frequency than that traveling away from an observer, which appears at lower frequency.

- At low densities, the velocities are given by a Maxwell-Boltzmann distribution; that is the fraction of molecules with velocity v is given by

$$f(v) = \left(\frac{m}{2\pi kT} \right)^{3/2} e^{\frac{-mv^2}{2k_B T}} \qquad \textbf{(140)}$$

  where m is the particle mass and k_B is the Boltzmann constant.

- It is clear that the temperature governs the velocity distribution and hence the frequency distribution

Doppler Broadening

- The Doppler lineshape function is given by a Gaussian distribution:

$$\varphi_D(\nu) = \frac{2\sqrt{\ln 2}}{\Delta\nu_D\sqrt{\pi}} \exp\left[-4\sqrt{\ln 2}\frac{(\nu-\nu_o)^2}{\Delta\nu_D^2}\right] \qquad \textbf{(141)}$$

where ν_o is the center frequency of the absorption/emission transition and $\Delta\nu_D$ is the FWHM of the Gaussian distribution given by

$$\begin{aligned} \Delta\nu_D &= \sqrt{\frac{8kT\nu_o^2\ln 2}{mc^2}} \\ &= 7.16\times 10^{-7}\nu_o\sqrt{\frac{T}{MW}} \end{aligned} \qquad \textbf{(142)}$$

with MW as the molecular weight of the species

Voigt Profile

- When both Doppler and collisional broadening are of the same order, both effects must be considered.
- The two lineshapes can be convolved to determine the actual absorption and emission lineshapes. The convolution of the two distributions results in a Voigt Profile given by

$$Y(\nu) = \frac{2}{\Delta\nu_D}\sqrt{\frac{\ln 2}{\pi}}V(a,x) \qquad \textbf{(143)}$$

where $V(a,x)$ is the Voigt function given by

$$V(a,x) = \frac{a}{\pi}\int_{-\infty}^{\infty}\frac{e^{-y^2}}{a^2+(x-y)^2}\,dy \qquad \textbf{(144)}$$

and a and x are defined as

$$a = \sqrt{\ln 2}\frac{\Delta\nu_c}{\Delta\nu_D} \qquad \textbf{(145a)}$$

$$x = 2\sqrt{\ln 2}\frac{(\nu-\nu_o)}{\Delta\nu_D} \qquad \textbf{(145b)}$$

Voigt Profile

- A comparison of the Doppler-broadened, collision-broadened, and Voigt lineshapes is shown below for T = 1000K for a = 0.5, 1.0, and 2.0
- When a < 1, Doppler broadening dominates and the Voigt profile assumes a Gaussian shape.
- As a increases (due to increasing pressure or decreasing temperature), collisional effects dominate and the lineshape becomes Lorentzian
- At P = 1 atm, the profile is Lorentzian at low T and Gaussian at high T

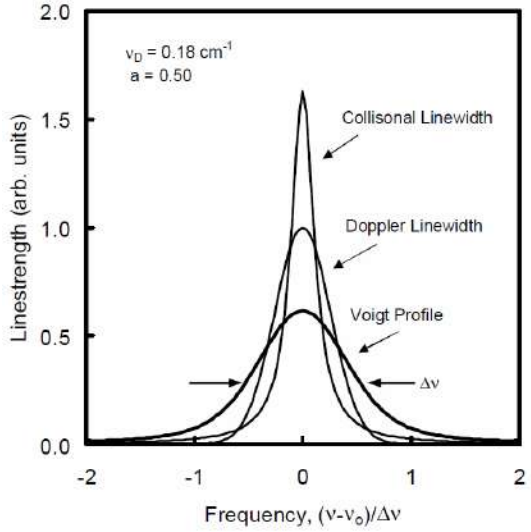

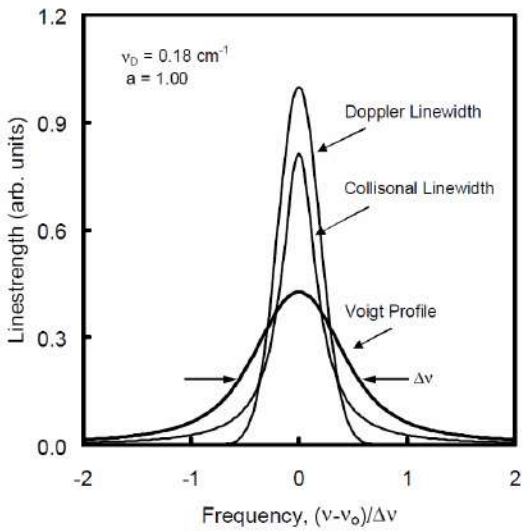

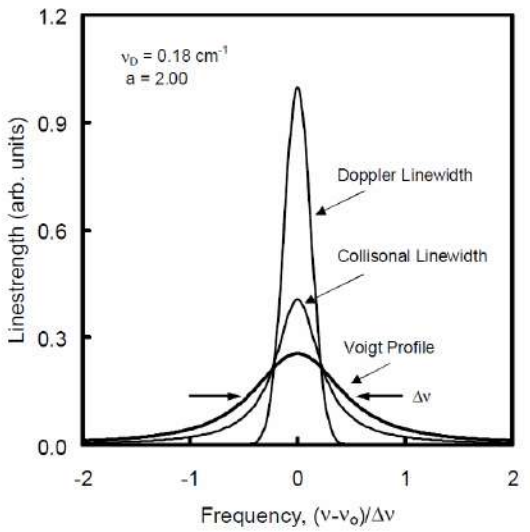

Spectral Overlap Integral

- We will now consider the interaction between the laser lineshape and the absorption lineshape
- We can define the spectral irradiance according to that of *Partridge and Laurendeau* (1995) as:

$$I_\nu(\nu) = I_\nu^o L'(\nu) \qquad \textbf{(146)}$$

where I_ν^0 is the normalized spectral irradiance and $L'(\nu)$ is the dimensionless spectral distribution function defined as

$$\int_\nu L'(\nu)\, d\nu = \Delta\nu_{laser} \qquad \textbf{(147)}$$

and $\Delta\nu_{laser}$ is the FWHM of the laser spectral irradiance distribution function or the "laser linewidth"

- I_ν^0 is related to the laser irradiance I through the relation

$$I = \int_\nu I_\nu(\nu)\, d\nu = \int_\nu I_\nu^o L'(\nu)\, d\nu = I_\nu^o \Delta\nu_{laser} \qquad \textbf{(148)}$$

Spectral Overlap Integral

- Defining the dimensionless overlap integral as

$$\Gamma = \int_{\nu} L'(\nu) Y(\nu)\, d\nu \qquad \textbf{(149)}$$

and substituting Eq. (146) into Eq. (107) yields an expression for the rate coefficient for stimulated absorption that is straightforward to deal with

$$W_{12} = B_{12} I_{\nu}^{o} \Gamma \qquad \textbf{(150)}$$

- Note that I_{ν}^{0} is easily calculated from physical quantities, $I_{\nu}^{0} = E_L/(A\Delta\nu_{laser} t_l)$, where E_L is the laser pulse energy, $\Delta\nu_{laser}$ is the laser linewidth, A is the laser beam cross-sectional area, and t_l is the laser pulse width

- The dimensionless overlap integral can be interpreted as the ratio of the total photon absorption rate in the actual broadband (and shifted) system to that which would exist in the monochromatic limit.

Spectral Overlap Integral

- Γ varies from 0 to 1, with Γ = 1 occurring for the monochromatic limit (i.e., monochromatic laser interacting with monochromatic absorption feature)
- If $\Delta\nu_{laser}$ << *absorption linewidth* ($\Delta\nu_a$), *then* $\Gamma \rightarrow \Delta\nu_{laser}/\Delta\nu_a$
- For broadband excitation ($\Delta\nu_{laser}$ >> $\Delta\nu_a$), $\Gamma \rightarrow 1$
- Understanding the interaction between the laser and the absorption linewidth is critical for quantitative measurements.

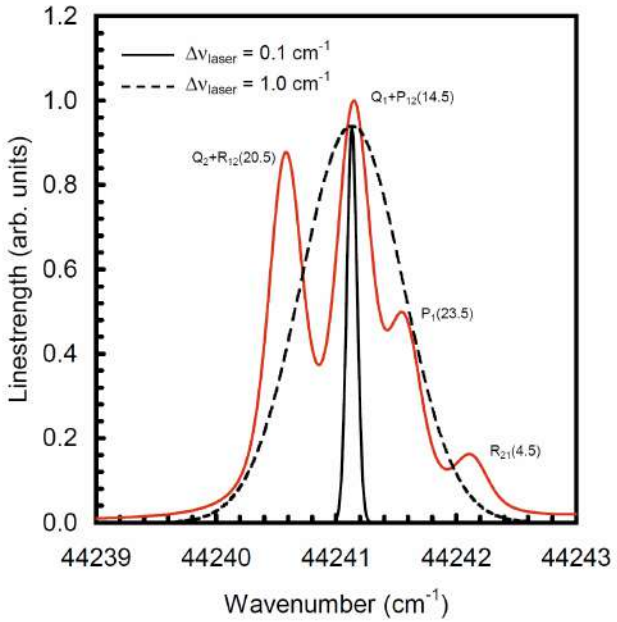

Boltzmann Fraction

- At any temperature the molecule does not occupy all energy levels; the internal energy is distributed or “partitioned” amongst various energy modes (electronic, vibrational, rotational)
- As we saw in Lecture 9, the fluorescence rate or number of fluorescence transitions is proportional to the number density of the directly pumped lower level (n_1^0), so it is important to know how the molecule is distributed over all of the possible energy states. This is quite important as one normally tunes their laser to “one” transition and measures fluorescence signal – how to relate n_1^0 to n_1 ?
- Referring back to Eq. (140), we know that for sufficiently low density (such that collisions equilibrate), the kinetic energy can be described by a Maxwell-Boltzmann distribution (kinetic energy is quantized)
- Along with kinetic energy, the internal modes (electronic, vibrational, rotational) also are quantized.

Boltzmann Fraction

- At low temperatures, all molecules lie within the ground electronic state, but occupy some range of rotational and vibrational levels
- Similar to kinetic energy, as temperature increases, the distribution increases and more and more rotational/vibrational levels are populated
- In addition, as temperature increases, some rotational levels become depopulated and at sufficiently high temperatures, higher electronic states can be populated without the influence of the laser (although we neglect this in our two-level model).
- The distribution amongst the various energy modes is described by the Boltzmann equation

$$f_{B,i} = \frac{n_i}{n} = \frac{g_i e^{-E_i/k_B T}}{\sum_i g_i e^{-E_i/k_B T}} \qquad \textbf{(150)}$$

where n_i is the number density in the i^{th} energy state, E_i; n is the total number density; k_B is the Boltzmann constant; T is the temperature, and g_i is the degeneracy of state i

Boltzmann Fraction

- The denominator is termed the partition function and is denoted Q. Based on the assumption that the translational, electronic, vibrational, and rotational energy modes are equilibrated, $Q = Q_{elec}Q_{vib}Q_{rot}$ (translational energy is not quantized so it is not considered here).

- In this manner, we can consider the distribution of the population over the rotational levels within a given vibrational state individually. Subsequently, we can consider the distribution of the population over the vibrational levels within a given electronic state…OR

$$f_{B,i} = f_{elec} f_{vib} f_{rot} \qquad \textbf{(151)}$$

where

$$f_{elec} = \frac{g_m \, \mathrm{e}^{-E_m/k_B T}}{Q_{elec}} \qquad f_{vib} = \frac{\mathrm{e}^{-E_\upsilon/k_B T}}{Q_{vib}} \qquad f_{rot} = \frac{(2J+1)\,\mathrm{e}^{-E_J/k_B T}}{Q_{rot}}$$

Boltzmann Fraction

- The electronic partition function is given by

$$Q_{elec} = \sum_{m} g_m e^{-E_m/k_B T} \qquad \textbf{(152)}$$

where m is the principle quantum number.

- ΔE_m often is measured. E_1 = 0 by convention in atoms. In diatomics, $E_1 \neq 0$ as it may be defined by the bottom of the classical vibrational energy well (to allow for dissociation)
- If E_1 = 0 then $Q_{elec} = g_m$; if $E_1 \neq 0$ then $Q_{elec} = g_m exp(D_e/k_B T)$
- The fraction of molecules in a particular electronic transition is then

$$f_{elec} = \frac{g_m \, \mathrm{e}^{-E_m/k_B T}}{Q_{elec}} \approx \frac{g_m}{g_m} \approx 1$$

if $E_1 = 0$ (simple harmonic model for vibrational state)

Boltzmann Fraction

- The vibrational partition function is given by

$$Q_{vib} = \sum_{\upsilon} e^{-E_\upsilon / k_B T} \qquad \textbf{(153)}$$

where the vibrational energy can be modeled with a simple harmonic oscillator (Eq. 78) or a more complex function such as Eq. (80)

$$E_\upsilon = \underbrace{(\upsilon + 1/2)\hbar\omega_e}_{\text{harmonic}} + \underbrace{\ldots}_{\text{anharmonic terms}}$$

- The vibrational partition function can be written for a harmonic oscillator as

$$Q_{vib} = \frac{e^{-\hbar\omega/2k_B T}}{1 - e^{-\hbar\omega/k_B T}} \qquad \textbf{(154)}$$

- The fraction of molecules in a particular vibrational energy level is

$$f_{vib} = \frac{\mathrm{e}^{-E_\upsilon/k_B T}}{Q_{vib}} = e^{-\upsilon\hbar\omega/k_B T}(1 - e^{-\hbar\omega/k_B T}) \qquad \textbf{(155)}$$

Boltzmann Fraction

- The rotational partition function is given by

$$Q_{rot} = \sum_J (2J+1) e^{-E_J/k_B T} \qquad \textbf{(156)}$$

where the rotational energy can be modeled as that from a rigid rotator, with or without centrifugal distortion, as Eq. (92)

$$E_{rot} = B_e J(J+1) + \underbrace{D_e J^2 (J+1)^2}_{\text{centrifugal distortion}}$$

- Ignoring the centrifugal distortion for a moment, the rotational partition function is written as

$$Q_{rot} = \sum_J (2J+1) e^{-hcB_v J(J+1)/k_B T} \qquad \textbf{(157)}$$

where B_v is a spectroscopic constant given by $B_v = h/8\pi^2 cI$ and I is the moment of inertia of the molecule

Boltzmann Fraction

- Since the value of $k_B T/hcB_v = T/\theta_{rot}$ (θ_{rot} is the rotational temperature) typically is large, the summation in Eq. (157) can be replaced with integration to yield

$$Q_{rot} = \frac{k_B T}{hcB_v} = \frac{8\pi^2 k_B T I}{h^2} \quad \textbf{(159)}$$

- The fraction of molecules in a particular rotational energy level is

$$f_{rot} = \frac{(2J+1)\,\mathrm{e}^{-E_J/k_B T}}{Q_{rot}} = \frac{hcB_v}{k_B T}(2J+1)e^{-hcB_v J(J+1)/k_B T} \quad \textbf{(160)}$$

- Now we can write the fraction of molecules in a particular rotational/vibrational energy level as

$$\frac{n_i}{n} = f_B(T) = f_{vib} f_{rot} = \frac{hcB_v}{k_B T}(2J+1)e^{-hcB_v J(J+1)/k_B T} e^{-\upsilon h\omega/2\pi k_B T}(1-e^{-h\omega/2\pi k_B T}) \quad \textbf{(161)}$$

Boltzmann Fraction

- For example, let's consider the OH molecule using the $R_1(8)$ line of the (1,0) vibrational band of the $A^2\Sigma^+ \leftarrow X^2\Pi$ system
- At 600K, 99.99% of the molecules are in the v' = 0 vibrational band, while at 2000K, 93% of the molecules are in the v' = 0 vibrational band
- At 600K, 2.1% of the molecules are in the N = 8 (J = 8.5) rotational band, while at 2000K, 8% of the molecules are in the N = 8 (J = 8.5) rotational band

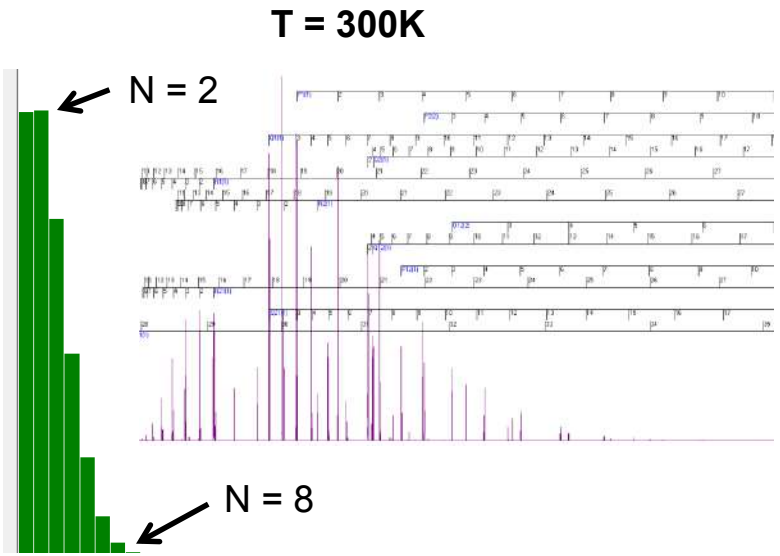

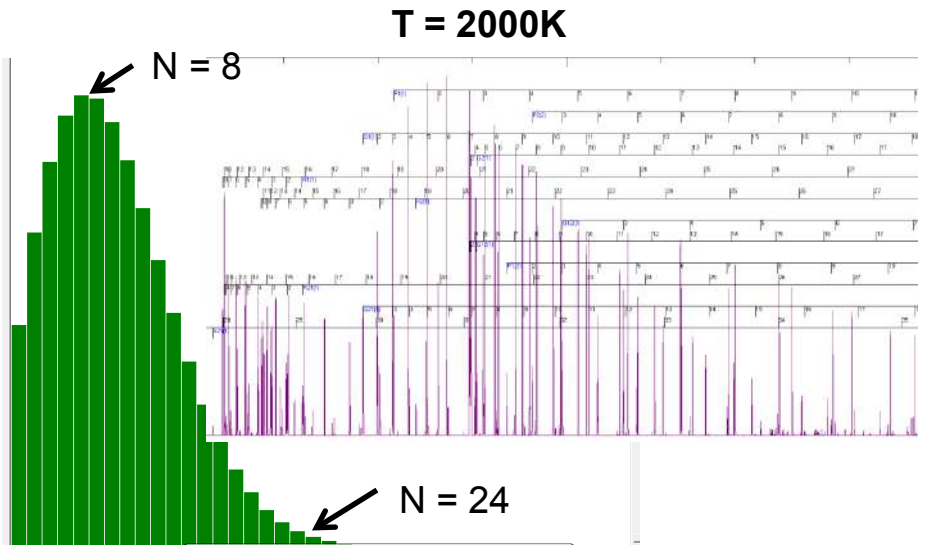

Collisional Dynamics

- If one wants a quantitative interpretation of the LIF signal, knowledge of both spectroscopy AND collisional dynamics that occur during the excitation process are needed.
- We already discussed the fact that collisions between the excited molecule and other species can cause line broadening (and shifting) of the absorption transition.
- In addition, collisions can cause non-radiative energy transfer between energy levels of the absorber, leading to a depopulation of the excited state and loss of fluorescence signal
- These non-radiative energy transfer mechanisms are rotational and vibrational energy transfer (RET and VET) and electronic energy transfer, known as “collisional quenching”

Collisional Dynamics

- Electronic energy transfer or "quenching" is the simplest of the collision-induced depopulation processes. This process describes the case where some fraction of the laser-excited absorber is de-excited due to collisions The quenching rate between two species can be written as

$$Q_{21} = n\sigma(X_j, T)v_i \qquad \textbf{(162)}$$

where $\sigma(X_j,T)$ is the electronic quenching cross section, which is a function of all colliding species j and the local temperature, T; X_j is the mole fraction of species j; and v_i is the mean molecular speed of species i given by

$$v_i = \sqrt{\frac{8kT}{\pi m_i}} \qquad \textbf{(163)}$$

- The total electronic quenching cross section is given by

$$\sigma(X_j, T) = \sum_j X_j(1 + m_i/m_j)^{1/2}\sigma_j(T) \qquad \textbf{(164)}$$

where m_j and $\sigma_j(T)$ are the molecular mass and temperature-dependent quenching cross section of colliding species j, respectively. Cross sections are found within the literature with varying degrees of accuracy

Collisional Dynamics

- RET and VET become increasingly important as laser irradiance increases and can be a significant depopulation mechanism in the high-irradiance limit
- The relative importance of RET and VET are species specific
- RET rates have been found to be unaffected by the specific vibrational state and thus, the same RET rates can be used over any vibrational state
- RET and VET rates are usually calculated in an analogous manner to that of electronic quenching. RET and VET cross sections can be found within the literature
- In general, in the low-irradiance limit and for typical flame conditions, RET and VET may be omitted without significant error (again the degree is species specific)

Back to Fluorescence Signal

- Last lecture we ended with this…

$$S_f[\text{photons collected}] = \frac{\Omega}{4\pi}\eta V_c W_{12} n_1^0 \frac{A_{21}}{A_{21}+Q_{21}} t_l \qquad \textbf{(135)}$$

- Since then, we have examined processes that help us manipulate the $W_{12}n_1^0$ term. In addition, we can state that the collection solid angle and the system collection efficiency must be determined for each experiment and thus can be lumped into a single constant, C_{opt}

- In this manner, the fluorescence equation can now be written as

$$S_f = C_{opt} n_i I_\nu^0 \sum_i^N f_B \Gamma B_{12} \frac{A_{21}}{A_{21}+Q_{21}} t_l \qquad \textbf{(165)}$$

  where the summation accounts for all possible excitation transitions in the vicinity of the laser center frequency.

- Quantitative measurements typically are made by referencing LIF signals to signals acquired at known conditions. Although other calibration methods (such as Rayleigh scattering or absorption) are used.

Some Examples: OH

- Perhaps the most utilized molecule is OH.
- OH is excited in the UV (typically near 282 for (1,0) or 306 nm for (0,0))
- OH is rapidly formed during in the high-temperature regions and is destroyed by slow three-body reactions. Thus, it is a good marker of the combustion products and turbulent transport
- OH PLIF produces high signals due to the abundance of OH (~2000 ppm)
- Primarily used for visualization, but it actually is one of the easier species to place on a quantitative basis.

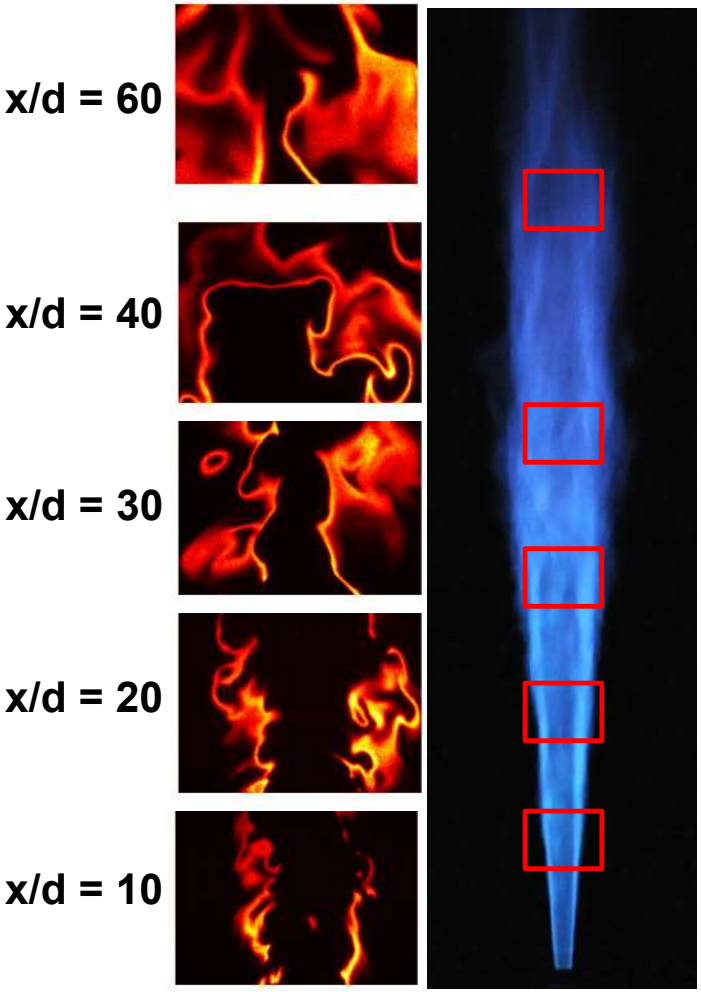

Some Examples: OH

- Upon examining Eq. (165), the most challenging aspect of quantitative measurements in the need for temperature. This appears in f_B, Γ, and Q_{21}
- However, it turns out for OH that through a judicious selection of the rotational line, the measured fluorescence signal can be directly proportional to mole fraction or concentration.
- Measurements have shown that the quenching rate is temperature independent for T > 1300K and that the choice of an N = 8 rotational line results in a total Boltzmann fraction that varies by less than 4% over the temperature range of 1300 to 2000 K

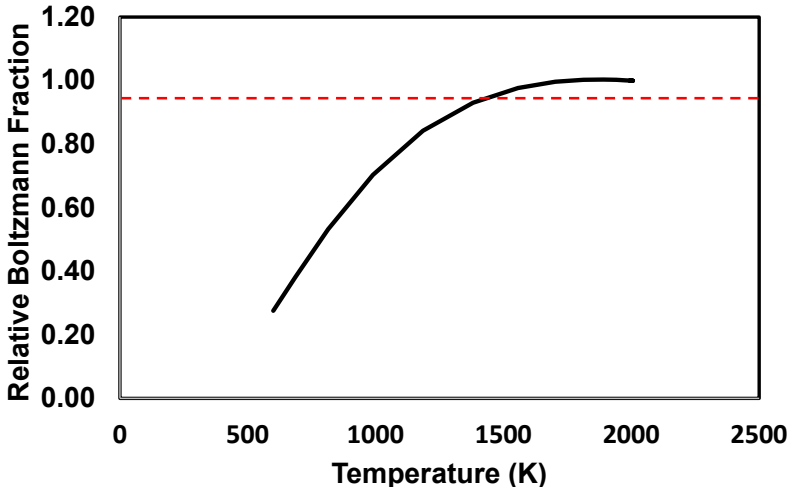

Some Examples: CH

- CH has been used to visualize the location of the primary reaction zone.
- CH is excited in the UV/vis (near 390 nm for B-X, 413 nm for A-X, or 314 nm for C-X)
- CH occurs within the final stages of fuel decomposition, but is unstable and short-lived
- This creates a spatially thin distribution that marks a region of high reactivity
- In premixed flames, CH can be used to identify the flame front; in nonpremixed flames, CH is used to identify the stoichiometric surface.
- Under turbulent flame conditions it is used purely for visualization

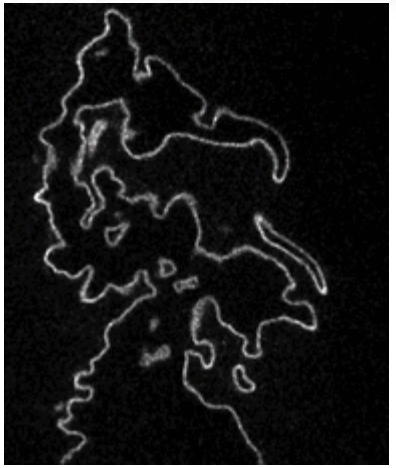

Hammack et al., 2018

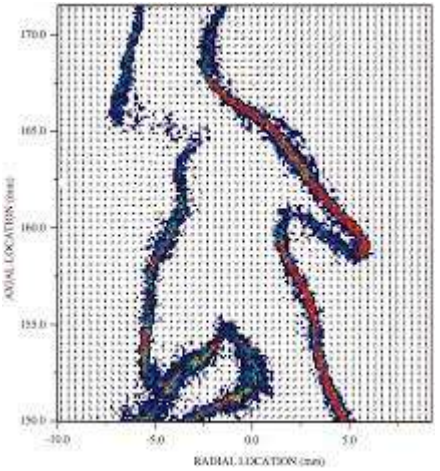

Carter et al., 1998

Some Examples: NO

- Nitrogen oxides (NOx) are pollutants that are heavily regulated. The formation and destruction pathways under turbulent flame and engine conditions are not completely understood and thus *in situ* measurements are invaluable
- NO is excited in the UV (near 226 nm for A-X)
- Quantitative imaging of NO concentrations with LIF have been attempted for many years. It poses a challenge due to low signal levels (ppm level NO and significant quenching) and difficulty in quantification
- Beyond these few species, there other examples with CO, CH_2O, HCN, CN, O_2, …

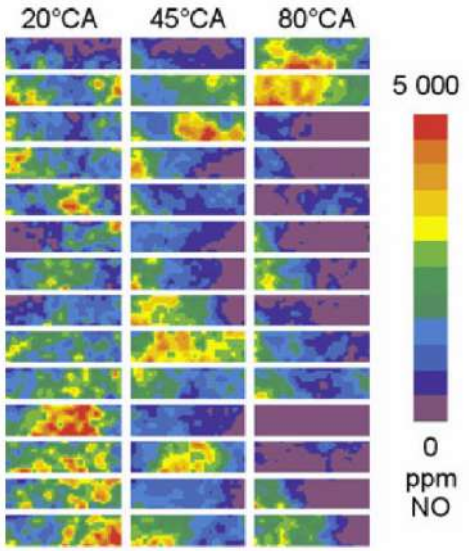

Bessler et al., 2007

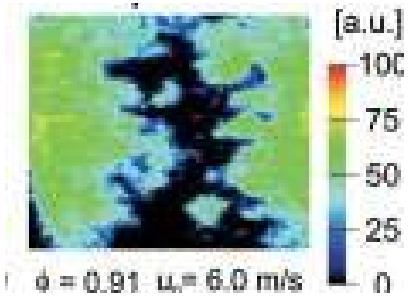

Herrmann and Boulouchos 2005

Some Examples: Reaction Rate Imaging

- Measurements of reaction rates in turbulent flames have proven challenging, if not untenable
- A specific interest is to measure heat release rate. There is no direct way to measure this, but there have been a few proposed proxies.
- The first suggested approach involved imaging of HCO. However, the signal is very weak. Instead of this approach, one could measure the over lap of $[CH_2O]x[OH]$ since $CH_2O + OH \rightarrow HCO+H_2O$
- Additional approaches such as [CO] x [OH] have been suggested to examine the forward reaction rate of $CO + OH \rightarrow CO_2+H$

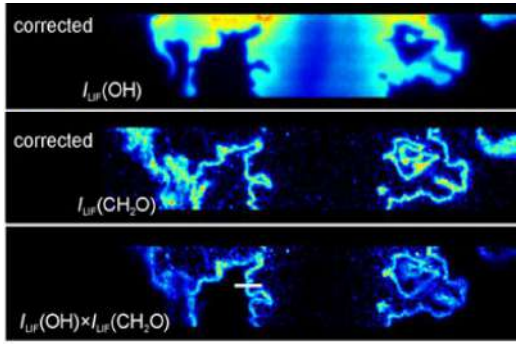

Röder et al., 2012

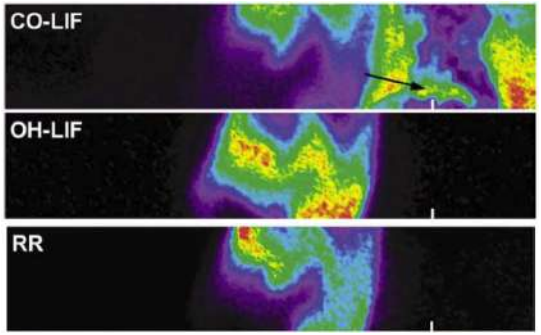

Frank et al., 2005

Laser Diagnostics in Turbulent Combustion Research

Jeffrey A. Sutton

Department of Mechanical and Aerospace Engineering
Ohio State University

Princeton-Combustion Institute Summer School on Combustion, 2019

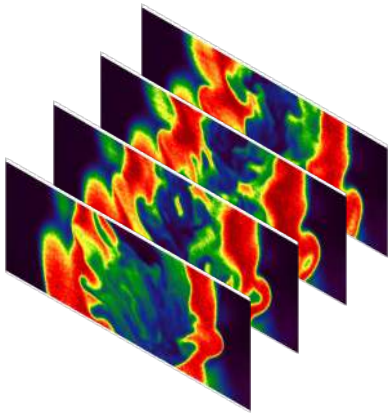

Lecture 11 – Spontaneous Rayleigh and Raman Scattering

Overview and Outline of Lecture

Goal: Provide an Overview of Rayleigh and Raman Scattering with a Focus on Rayleigh Scattering

- Background of Rayleigh and Raman Scattering
- Development of Rayleigh Scattering Equations
- Experimental Considerations
- Applications of Rayleigh Scattering in Reacting Flows

Scattering Processes

- Contrary to a resonant process like LIF, spontaneous scattering processes can be performed with any laser wavelength (I will show why in this lecture)
- There are many potential scattering processes to consider:

  Rayleigh scattering – elastic scattering of a photon due to density (random, thermal) fluctuations

  Raman scattering – inelastic scattering of a photon due to vibrational/rotational transitions in the bonds between neighboring atoms

  Brillouin scattering – inelastic scattering of a photon due to density (correlated, periodic acoustic) fluctuations (“phonons”)

  Thomson scattering – elastic scattering of a photon by a free charged particle

  Compton scattering – inelastic scattering of a photon by a free charged particle

- In combustion, we typically only consider Rayleigh* and Raman scattering

Electric Dipole – "Classical" Model

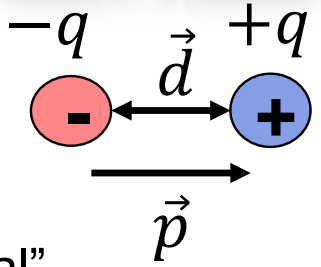

- In Lecture 9 we introduced the electric dipole, primarily as a means to quickly move into the dipole operator and transition dipole moment (quantum mechanics) to examine absorption
- For Rayleigh and Raman scattering, we can use this "classical" formulism to develop the necessary theory and equations (you also can develop the Rayleigh/Raman signal response with quantum mechanics formulations as well)
- That is, the electrons in atoms or molecules (or generally small particles) radiate like dipoles (or dipole antennas) when forced to oscillate by an applied electric field
- The treatment of the scattering process as an emitting dipole is very accurate for monatomic gases such as He or Ar because they are spherical with no internal degrees of freedom
- For molecules, this approximation weakens due to changes in vibrational and rotational states during scattering (however, we can 'correct' for these)

Electric Dipole – "Classical" Model

- In Lecture 9 we referred to a "static dipole"; however, for the case of the interaction of the electric field with a small particle, it is better to consider an electric dipole that is oscillating in time

- If we do not consider any spatial variation in Eq. (15), the time-dependent expression for the incident electric field (modeled as harmonic oscillator) is

$$\vec{E}(t) = \vec{E}_o \cos(\omega t) \qquad \textbf{(166)}$$

- When the electric field interacts with the molecule the electrons and nuclei move in opposite directions in accordance with Coulomb's law. Previously, I referred to this as "perturbing" the electron cloud". Therefore, there is a time-dependent charge

$$q(t) = q_o \cos(\omega t) \qquad \textbf{(167)}$$

- …and thus, the incident electric field produces an oscillating dipole moment in the molecule (again, we discussed this earlier), written as

$$\vec{p}(t) = \vec{p}_o \cos(\omega t); \quad \vec{p}_o = q_o \cdot \vec{d} \qquad \textbf{(168)}$$

Electric Dipole – "Classical" Model

- Once an oscillating dipole is generated, an oscillating electric field propagates away from the dipole as

$$\vec{E}_s(r,\phi) = \frac{\vec{p}_o \sin(\phi)\omega^2}{4\pi\varepsilon_o r c^2}\cos\left[\omega(t - r/c)\right]\hat{\phi} \qquad \textbf{(169)}$$

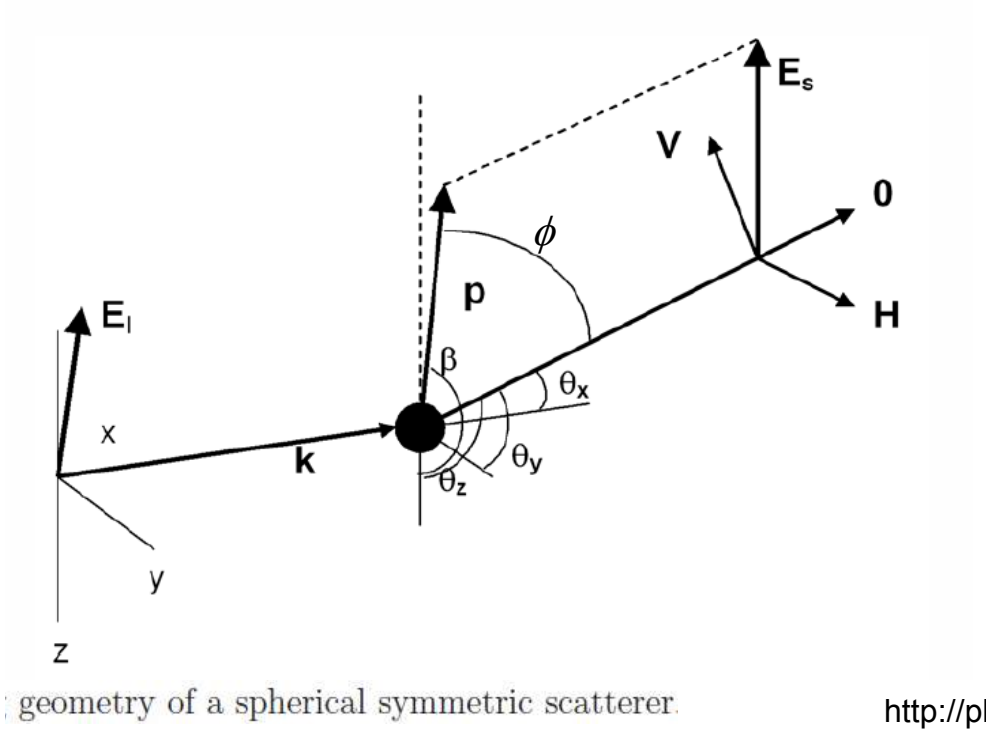

geometry of a spherical symmetric scatterer.

Static dipole

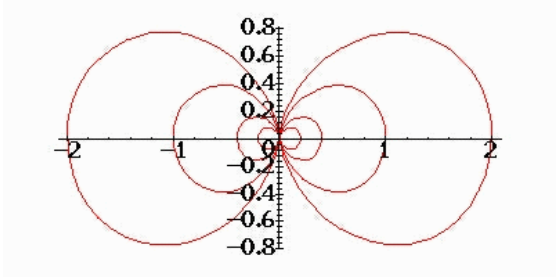

Oscillating dipole

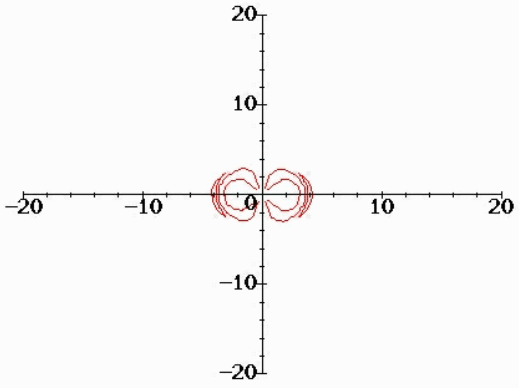

http://physics.usask.ca/~hirose/ep225/radiation.htm

Electric Dipole – "Classical" Model

- For a spherically symmetric molecule, $\vec{p}$ is induced in the same direction as the incident field polarization and thus the dipole moment is linearly proportional to the incident electric field, written as

$$\vec{p} = \alpha \vec{E} \qquad \textbf{(170)}$$

where α is the polarizability which describes the relative tendency of a charge distribution (i.e., electron cloud of a molecule) to be displaced by the external electric field

- If you recall from Lecture 3, we introduced the polarization vector

$$\vec{P} = \varepsilon_o \chi \vec{E} \qquad \textbf{(22)}$$

where the susceptibility (χ) is a material parameter representing the ability of the dipoles to respond to the 'polarizing' electric field

Electric Dipole – "Classical" Model

- The (average) susceptibility is related to the polarizability of individual atoms/molecules through the Clausius-Mossotti relation:

$$\alpha = \frac{3\varepsilon_o}{N}\frac{\chi}{3+\chi} \qquad \textbf{(171)}$$

  where N is the number of molecules per unit volume contributing to the polarization

- Why do we have two parameters that seem to do the same thing?

- The *local electric field* can differ significantly from the *overall applied field*. In some ways, measurement of the susceptibility describes the applied electric field and measurement of the polarizability describes the applied electric field minus the effect produced by the dipole

- Because of the oscillating nature of the electric field, the dipole moment also can be written as

$$\vec{p}(t) = \vec{p}_o \cos(\omega t) = \alpha \vec{E}_o \cos(\omega t) \qquad \textbf{(172)}$$

Electric Dipole – "Classical" Model

- Let's assume that in addition to translation of the molecule, there is some internal motion (electronic, vibrational, or rotational) that modulates the induced oscillating dipole. This can cause additional frequencies to appear
- We can write the polarizability as the combination of a static term (α_o) and an oscillating term α_1 with a characteristic molecular frequency of ω_m

$$\alpha = \alpha_o + \alpha_1 \cos(\omega_m t) \qquad \textbf{(173)}$$

- The modulation at ω_m causes the dipole moment to oscillate at frequencies other than ω, which is characteristic of the incident electric field.
- The induced dipole moment can now be written as

$$\vec{p} = \alpha \vec{E} = [\alpha_o + \alpha_1 \cos(\omega_m t)] * \vec{E}_o \cos(\omega t) \qquad \textbf{(174)}$$

- …and with some manipulation….

$$\vec{p} = \underbrace{\alpha_o \vec{E}_o \cos(\omega t)}_{\text{Rayleigh}} + \frac{\underbrace{\alpha_1 \vec{E}_o \cos(\omega - \omega_m)t}_{\text{Stokes}} + \underbrace{\alpha_1 \vec{E}_o \cos(\omega + \omega_m)t}_{\text{anti-Stokes}}}{2} \qquad \textbf{(175)}$$

Electric Dipole – "Classical" Model

- The oscillating portion of the polarizability (α_1) can be related to the physical molecule by recognizing that the ability to perturb the electron cloud depends on the relative position of the individual atoms. Thus, polarizability is a function of the instantaneous positions of the atoms.

- Since energy levels are quantized, individual atoms correspond to specific rotational/vibrational modes. Focusing just on vibration for the moment, the displacement (dQ) of atoms about some equilibrium position due to their vibrational mode is expressed as

$$dQ = Q_o \cos(\omega_{vib} t) \qquad \textbf{(176)}$$

  where Q_o is the amplitude of vibration about the equilibrium position and ω_{vib} is the vibrational frequency of the molecule

- The displacement from the equilibrium position is fairly small, so a Taylor expansion can be used to write the polarizability as

$$\alpha = \alpha_o + \frac{\partial \alpha}{\partial Q} \partial Q \qquad \textbf{(177)}$$

Electric Dipole – "Classical" Model

- Substituting Eq. (176) in (177) yields

$$\alpha = \alpha_o + \frac{\partial \alpha}{\partial Q} Q_o \cos(\omega_{vib} t) \qquad \textbf{(178)}$$

$$\vec{p} = \underbrace{\alpha_o \vec{E}_o \cos(\omega t)}_{\text{Rayleigh}} + \frac{\partial \alpha}{\partial Q} \frac{Q_o \vec{E}_o}{2} \underbrace{\left[\cos(\omega - \omega_{vib})t}_{\text{Stokes}} + \underbrace{\cos(\omega + \omega_{vib})t\right]}_{\text{anti-Stokes}} \qquad \textbf{(179)}$$

- So, if the polarizability does not change with vibration (i.e., $\partial\alpha/\partial Q$=0), then there is no vibrational Raman effect. Thus, we can summarize…
- **Rayleigh scattering:** If the induced polarization does NOT couple with polarization oscillations due to vibration, then the vibrational state of the molecule is unperturbed – scattered photon is at same energy (frequency) as original photon – "elastic" scattering
- **Raman scattering**: If the induced polarization couples to a vibrational state, this corresponds to "vibrational excitation". The scattered photon is at a different energy (frequency) as original photon (+/- frequency of molecular vibration) – "inelastic" scattering

Energy Diagram and "Classical" Explanation

- Going back to Eq. (169), the electric field induced by the dipole is proportional to the dipole moment. This means that the propagating electric field (which we will tie to emission) oscillates at multiple frequencies, i.e., "scattered light" is generated at multiple frequencies (or wavelengths). **How does this work?**

1) The incident electric field (laser) induces an oscillating dipole moment, i.e., the relative positions between the electrons and nucleus are moved
2) This means that the molecular system is in a different energy state – called a "virtual state"
3) The energy level of the virtual state is higher than that of the vibrational quanta, but it is less than that than required to move to an excited electronic state (i.e., it is not equal to any particular electronic quantum energy). Therefore, the molecule stays in its ground electronic state
4) Only about 1 out of 10^4 non-resonant photons transition to the 'virtual state' as the majority transmit through the medium

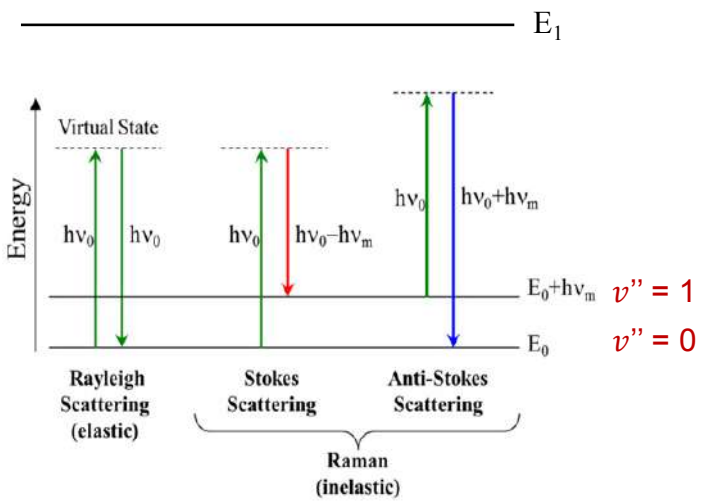

Energy Diagram and "Classical" Explanation

6) Of these photons, the majority simply return to the initial vibrational state. However, they are "re-directed" from the molecule in a different direction (i.e., "spontaneous"). During this interaction, no energy exchange has taken place, so the photon is emitted at the same frequency.

7) In a gas, there is a large number of molecules and the molecular motion leads to microscopic density fluctuations (non-uniform distribution of scatter sources). These fluctuations randomize the phase of the scattered light and leads to incoherent light in all but forward direction. However, interference between each scattering source removes coherence effects and the total scattered intensity is proportional to the number of scattering sources.

8) If there were not density fluctuations (uniform), then the scattering from each isolated oscillator cancels out in all but the forward direction. Thus, density fluctuations are responsible for Rayleigh scattering.

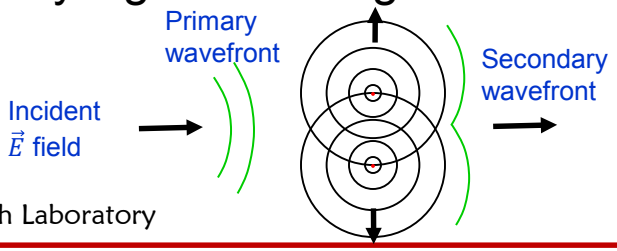

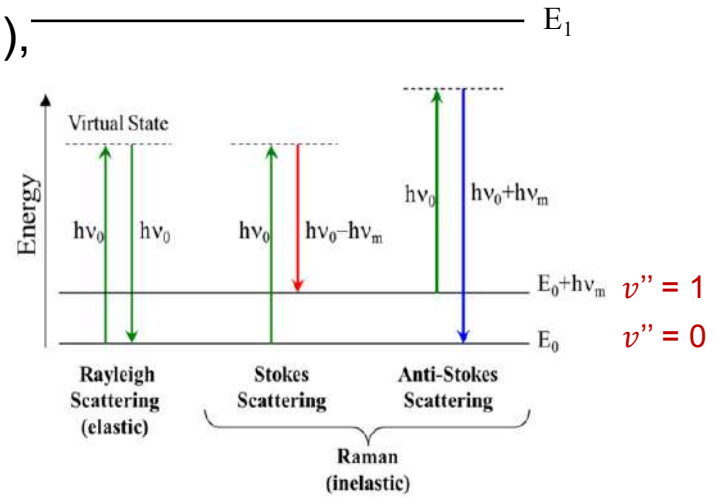

Energy Diagram and "Classical" Explanation

9) Ok, back to the 'virtual state'…During the interaction between the incident electric field and the molecule, an amount of energy equal to the vibrational mode may be transferred from a photon to the molecule. The remaining photon energy is now less than the energy of the incident photon.

10) Conservation of energy requires that the emitted photon has energy of $h(\nu - \nu_{vib})$ and thus the photon returns from the virtual state to a higher vibrational level, which is frequency-shifted (inelastically scattered) radiation. This is Stokes Raman scattering.

11) Now, if a molecule is in an excited vibrational state (i.e., v" = 1), a photon can gain energy from the molecule during the interaction and result in an emitted photon with energy of $h(\nu + \nu_{vib})$. This is anti-Stokes scattering.

12) Both Stokes and anti-Stokes scattering occur simultaneously since there is a large number of molecules, but Stokes is more probabilistic (since it is more likely that a molecule is in the ground state) and thus, intensity of the Stokes scattering is higher.

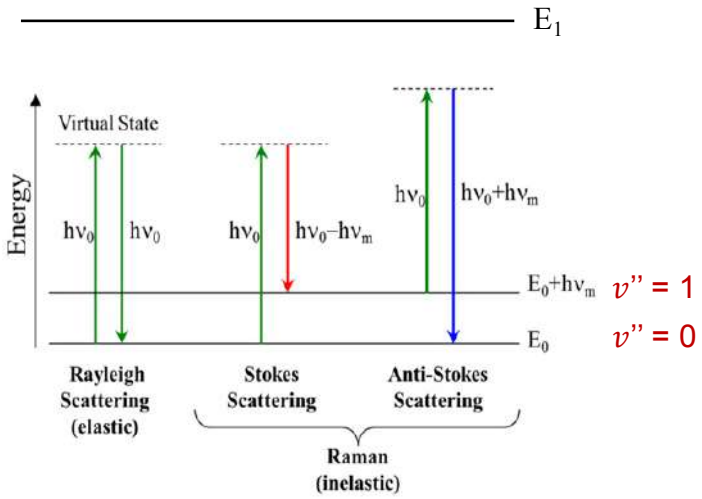

Is This LIF?

- Are scattering processes different from LIF processes?
- They both involve the absorption and emission of a photon (sort of…)
- Fluorescence emission can be at the same wavelength or shifted – so is it elastic and inelastic?
- Actually, LIF can be considered a type of scattering (some people will disagree with you on this!)

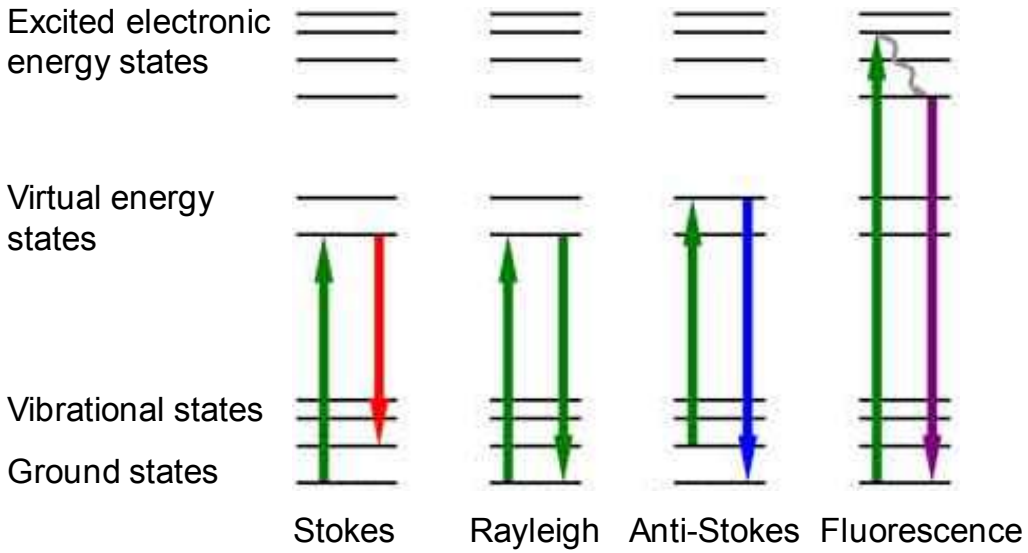

Is This LIF?

- The primary distinction is the mechanism giving rise to the signal
- **Fluorescence** involves the complete absorption of a photon to excite the molecule to a higher energy state with considerable changes to the electronic configuration (this is why incident energy ≥ energy gap for excitation of valence electrons). This is a resonant process.
- **Rayleigh/Raman** involves the use of any energy for excitation to the virtual energy state. For Raman, any energy can be absorbed for exciting to a higher vibrational mode. Hence Rayleigh/Raman is a non-resonant process. Photon emission (whether $\Delta\nu = 0$ or $\Delta\nu - \nu_{vib}$) is at a constant offset from excitation frequency.
- Lifetime in the 'virtual state' is ~10^{-14} seconds for Rayleigh/Raman, while lifetime in the excited electronic state is ~ 10^{-8} seconds for LIF due to transfer amongst various rotational/vibrational levels

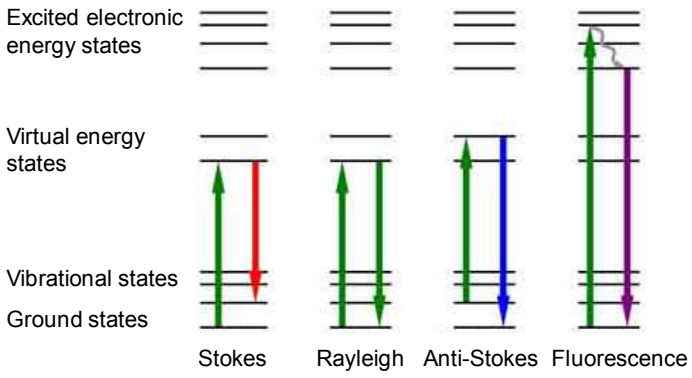

Rayleigh and Raman Scattering

- We will discuss two types of spontaneous scattering processes: (i) Rayleigh scattering and (ii) Raman scattering

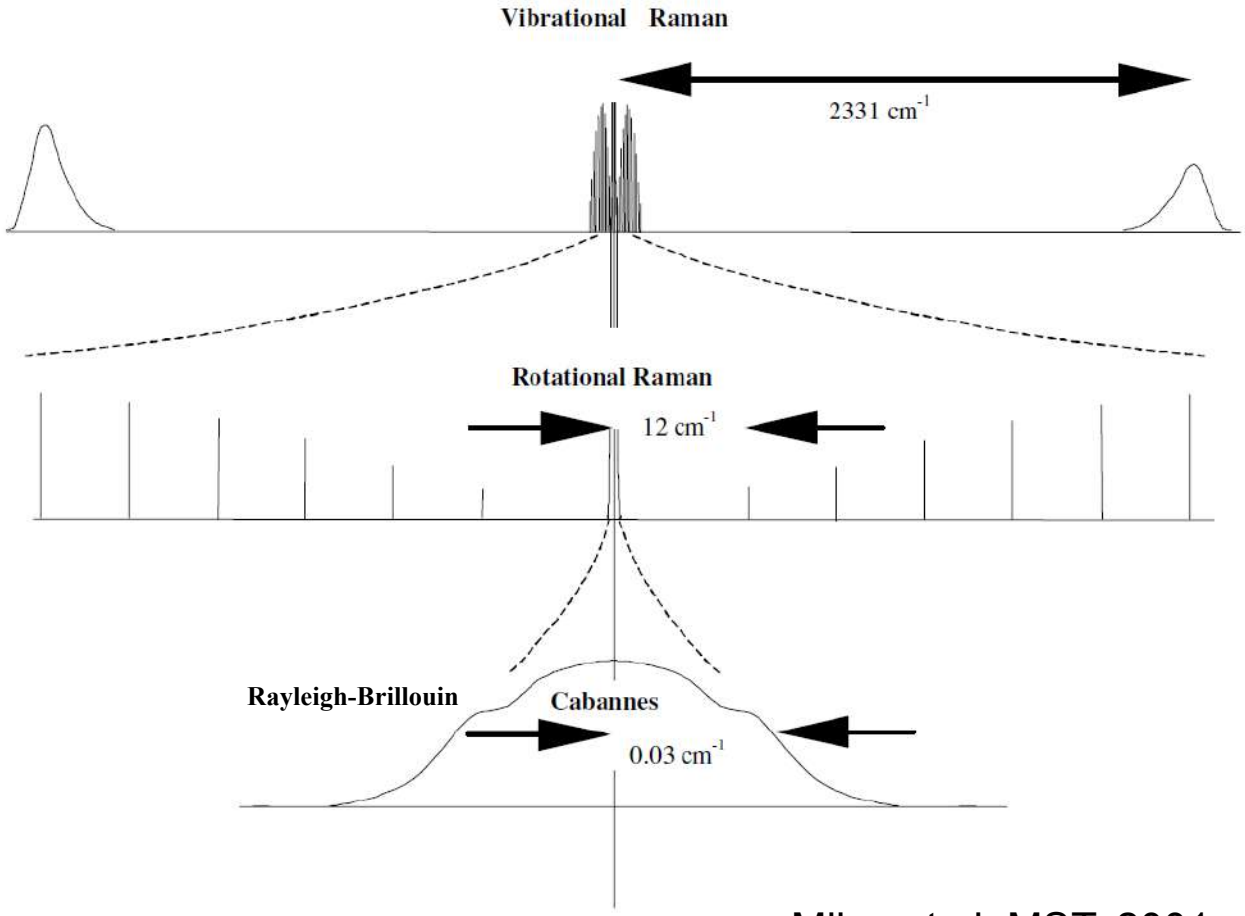

Miles et al, MST, 2001

Rayleigh Scattering

$$\vec{p} = \underbrace{\alpha_o \vec{E}_o \cos(\omega t)}_{\text{Rayleigh}} + \frac{\partial \alpha}{\partial Q}\frac{Q_o \vec{E}_o}{2}\left[\cos(\omega - \omega_{vib})t + \cos(\omega + \omega_{vib})t\right] \quad \textbf{(179)}$$

- Let's start with just the elastic portion of the dipole moment right now such that $\vec{p}_o = \alpha_o \vec{E}_o$
- Recall from Lecture 3, Poynting's vector gives the "intensity" of the electric field. Thus, the time-averaged intensity of Rayleigh-scattered light from a single oscillating dipole is

$$I_s = \left\langle \vec{S} \right\rangle = \left\langle \frac{1}{\mu_o}\vec{E}_s \times \vec{B}_s \right\rangle = \left\langle \frac{1}{\mu_o}\vec{E}_s \times \left(\frac{1}{c}\hat{r} \times \vec{E}_s\right)\right\rangle = c\left(\frac{1}{2}\varepsilon_o \left|\vec{E}_s\right|^2\right)$$

$$I_s = \frac{\vec{p}_o{}^2 \omega^4 \sin^2(\phi)}{32\pi^2 \varepsilon_o r^2 c^3} \quad \textbf{(180)}$$

Rayleigh Scattering

- The time-averaged power scattered from one oscillating dipole can be obtained by integrating the scattered intensity over a spherical surface containing the dipole

$$\langle P \rangle = \frac{|\vec{p}_o|^2 \omega^4}{12\pi\varepsilon_o c^3} = \frac{(\alpha E_o)^2 \omega^4}{12\pi\varepsilon_o c^3} \qquad \textbf{(181)}$$

- This can be written in terms of the incident intensity ($I_I = c\varepsilon_o E_o^2/2$) as

$$\langle P \rangle = \frac{8\pi^3\alpha^2}{3\varepsilon_o^2\lambda^4} I_I \qquad \textbf{(182)}$$

- It is common to define a scattering cross section as $\langle P \rangle / I_I$:

$$\sigma_{ss} = \frac{8\pi^3\alpha^2}{3\varepsilon_o^2\lambda^4} \qquad \textbf{(183)}$$

- To remove some of the geometric dependence, a differential scattering cross section is defined as

$$I_s = \frac{\partial\sigma_{ss}}{\partial\Omega}\frac{1}{r^2} I_I \qquad \textbf{(184)}$$

Rayleigh Scattering

- Thus, the differential cross section is

$$\frac{\partial \sigma_{ss}}{\partial \Omega} = \frac{\pi^2 \alpha^2 \sin^2(\phi)}{\varepsilon_o{}^2 \lambda^4} \qquad \textbf{(185)}$$

- Equations (183) and (185) are simplified by relating the polarizability to the refractive index through the Lorentz-Lorenz equation (N is number density)

$$\alpha = \frac{3\varepsilon_0}{N}\frac{n^2-1}{n^2+2} \qquad \textbf{(186)}$$

such that

$$\sigma_{ss} = \frac{24\pi^3}{\lambda^4 N^2}\left(\frac{n^2-1}{n^2+2}\right)^2 \qquad \textbf{(187)}$$

and

$$\frac{\partial \sigma_{ss}}{\partial \Omega} = \frac{9\pi^2}{N^2\lambda^4}\left(\frac{n^2-1}{n^2+2}\right)^2 \sin^2(\phi) \qquad \textbf{(188)}$$

Rayleigh Scattering

- The $[(n^2\text{-}1)/(n^2\text{+}2)]^2$ term can be simplified by taking a Taylor expansion around $(n^2\text{-}1)^2$ to yield ($n \approx 1$ for a gas)

$$\left(\frac{n^2-1}{n^2+2}\right)^2 \cong \frac{4(n-1)^2}{9} \qquad \textbf{(189)}$$

- This gives

$$\sigma_{ss} \cong \frac{32\pi^3}{3\lambda^4}\left(\frac{n-1}{N}\right)^2 \qquad \textbf{(190)}$$

and

$$\frac{\partial \sigma_{ss}}{\partial \Omega} \cong \frac{4\pi^2}{\lambda^4}\left(\frac{n-1}{N}\right)^2 \sin^2\phi \qquad \textbf{(191)}$$

- Although this model is for a simple symmetric scatterer, it does offer some physical insights.
- First, we see the well known wavelength dependence (λ^{-4}) in the cross section. This possibly suggests the use of high-energy UV sources.
- Also, for an observation angle of zero degrees, the cross section is zero.

Rayleigh Scattering – Real Molecules

- Ok…so now there is one significant complication. Real molecules are not symmetric (some are close). In this manner, the induced dipole does not have lie in the same direction as the applied electric field and thus $\vec{p}$ and $\vec{E}$ can point in different directions
- The random orientation of the molecule with respect to the applied electric field (and with respect to the observation direction), requires that the scattering model be extended and averaged over all molecular orientations
- Thus, Eq. (170) becomes

$$\vec{p} = \vec{\alpha}\vec{E} \qquad \textbf{(192)}$$

where $\vec{\alpha}$ is a 3 x 3 symmetric matrix and is termed the polarizability tensor

- Since it is symmetric, there are 6 unique components of α_{ij} leading to

$$p_x = \alpha_{xy}E_{I_y} + \alpha_{xz}E_{I_z}$$

$$p_y = \alpha_{yy}E_{I_y} + \alpha_{yz}E_{I_z} \qquad \textbf{(193)}$$

$$p_z = \alpha_{zy}E_{I_y} + \alpha_{zz}E_{I_z}$$

Rayleigh Scattering – Real Molecules

- In Eq. (193) is it assumed that the electric field is propagating in the "x-direction" according to the figure to right and that the electric field can be broken into its two polarization components

$$E_{I_y} = E_I \sin\beta \qquad \text{and} \qquad E_{I_z} = E_I \cos\beta \qquad \textbf{(194)}$$

  where β is the angle between the incident field polarization and the z-axis

- As you can probably guess, dealing with all of the components of the dipole moment orientation, both polarizations of the electric field and all possible observation angles can create some tedious math. For a complete general derivation, see Miles et al., *Meas. Sci. Tech*., 2001

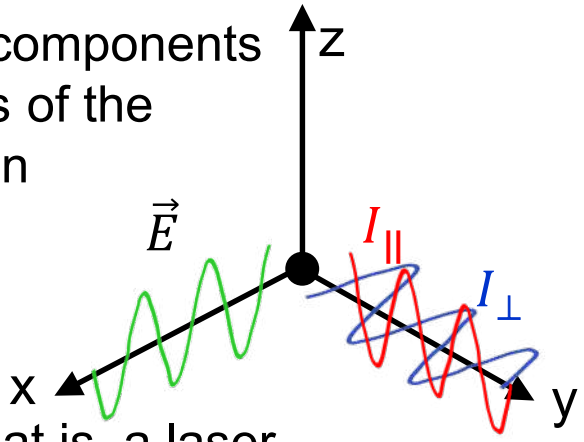

- For our purposes here, we will consider the most common case that is performed in experiments. That is, a laser propagating in the x direction, with 'vertical polarization' (polarization only in the z direction) and light collection at 90° (along the y direction). For this case, there will be two polarization components of scattered intensity, denoted $I_\perp$ and $I_{||}$.

Rayleigh Scattering – Real Molecules

- For this case the dipole moment components reduce to

$$p_z = \alpha_{zz} E_{Iz} \qquad \textbf{(195a)}$$

$$p_x = \alpha_{xz} E_{Iz} \qquad \textbf{(195b)}$$

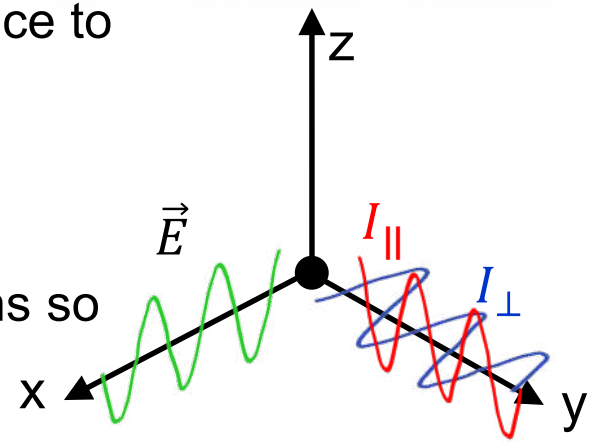

- In general, the molecules have random orientations so the polarizability elements must be averaged over all different orientations. This can be cast as the mean polarizability (a) and the anisotropy (γ)

$$a^2 = \frac{1}{9}(\alpha_{xx} + \alpha_{yy} + \alpha_{zz})^2 \qquad \textbf{(196)}$$

$$\gamma^2 = \frac{1}{2}\left[(\alpha_{xx} - \alpha_{yy})^2 + (\alpha_{yy} - \alpha_{zz})^2 + (\alpha_{zz} - \alpha_{xx})^2 + 6(\alpha_{xy}^2 + \alpha_{yz}^2 + \alpha_{zx}^2)\right] \qquad \textbf{(197)}$$

- For our case, the orientation averages are

$$\left\langle \alpha_{zz}^2 \right\rangle = \frac{45a^2 + 4\gamma^2}{45} \qquad \left\langle \alpha_{xz}^2 \right\rangle = \frac{\gamma^2}{15} \qquad \textbf{(198)}$$

Rayleigh Scattering – Real Molecules

- This leads to averages of the components of the dipole moments as

$$\left\langle p_z^2 \right\rangle = \frac{2}{\varepsilon_o c}\left(\frac{45a^2 + 4\gamma^2}{45}\right) I_I \qquad \textbf{(199a)}$$

$$\left\langle p_x^2 \right\rangle = \frac{2}{\varepsilon_o c}\left(\frac{\gamma^2}{15}\right) I_I \qquad \textbf{(199b)}$$

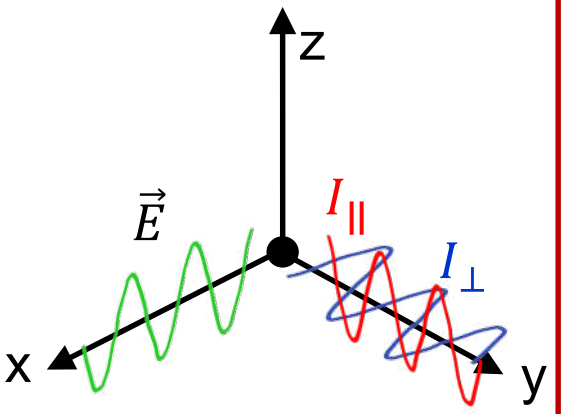

- Going back to Eq. (180), the scattered intensity (Watts/steradian) for each polarization is written (for collection at 90°) as:

$$I_{\parallel}'' = \frac{\omega^4}{32\pi^2 \varepsilon_o c^3}\left\langle p_z^2 \right\rangle = \frac{\pi^2}{\varepsilon_o^2 \lambda^4}\left(\frac{45a^2 + 4\gamma^2}{45}\right) I_I \qquad \textbf{(200a)}$$

$$I_{\perp}'' = \frac{\omega^4}{32\pi^2 \varepsilon_o c^3}\left\langle p_x^2 \right\rangle = \frac{\pi^2}{\varepsilon_o^2 \lambda^4}\left(\frac{\gamma^2}{15}\right) I_I \qquad \textbf{(200b)}$$

Rayleigh Scattering – Real Molecules

- Since the total scattered intensity is equal to $I_S'' = I_{||}'' + I_{\perp}''$

$$I_S'' = \frac{\pi^2}{\varepsilon_o^2 \lambda^4}\left(\frac{45a^2 + 7\gamma^2}{45}\right) I_I \qquad \textbf{(201)}$$

- The differential scattering cross section is now calculated from I_S''/I_I:

$$\frac{\partial \sigma_V}{\partial \Omega} = \frac{\pi^2}{\varepsilon_o^2 \lambda^4}\left(\frac{45a^2 + 7\gamma^2}{45}\right) \qquad \textbf{(202)}$$

- The effect of polarization on the scattering cross section is usually written in terms of a depolarization ratio $\rho = I_{\perp}''/I_{||}''$, which is the ratio of the intensities scattered perpendicular rand parallel to the polarized light source. For linear and diatomic molecules, the depolarization ratio is

$$\rho_p = \frac{3\gamma^2}{45a^2 + 4\gamma^2} \qquad \textbf{(203)}$$

Rayleigh Scattering – Real Molecules

- Substituting Eq. (203) into Eq. (202), using the Lorentz-Lorenz equation (Eq. 186), and assuming $n \approx 1$ yields

$$\frac{\partial \sigma_V}{\partial \Omega} \cong \frac{4\pi^2}{\lambda^4}\left(\frac{n-1}{N}\right)^2 \cancel{\sin^2\phi}^{\,1} \frac{3}{3-4\rho_p} \qquad \textbf{(204)}$$

  which is the same as that for the spherically symmetric scatterer with the depolarization correction term added

- Eq. (201) was for a single scattering source (molecule). As we discussed earlier, because the molecular motion randomizes the scattered electric fields from each molecule, coherence effects cancel and the total scattering is the sum of the scattering from each molecule.

- Thus, if we consider a probe volume V with number density N, the total scattered intensity (per steradian) is

$$I''_{S,total} = NV \frac{\partial \sigma_V}{\partial \Omega} I_I \qquad \textbf{(205)}$$

Rayleigh Scattering – Real Molecules

- Experimentally, we have some finite collection volume which is a function of our optical setup with a collection efficiency of η. Thus, we can write

$$I_{RAY} = I_I \eta N V \Omega \frac{\partial \sigma_V}{\partial \Omega} \qquad \textbf{(206)}$$

- Now it is noted that each species has a different differential scattering cross section. We will write our differential scattering cross section in the probe volume as a weighted molar average of all of the individual differential scattering cross section of the molecules in the probe volume:

$$\left(\frac{\partial \sigma}{\partial \Omega}\right)_{mix} = \sum_i X_i \left(\frac{\partial \sigma}{\partial \Omega}\right)_i \qquad \textbf{(207)}$$

where X_i is the mole fraction of species i

- Our final expression looks like

$$I_{RAY} = C E_I \frac{p}{kT} \left(\frac{\partial \sigma}{\partial \Omega}\right)_{mix} \qquad \textbf{(206)}$$

Applications of Rayleigh Scattering

- So from Eq. (206) we can see that Rayleigh scattering is NOT species specific. The collected signal is a function of N and the species mixture
- There are two primary applications of Rayleigh scattering in thermal/fluid sciences: (i) mixing measurements under non-reacting conditions and (ii) temperature measurements under reacting conditions
- Let's go back to Eq. (206) and assume that we have isobaric and isothermal conditions (perhaps this is the mixing stage before combustion occurs or well upstream in a lifted flame)
- Let's assume the constant C and the incident intensity do not vary (if I_I varies, that is not a major problem as we usually make simultaneous "energy correction" measurements). Also, we can assume a binary mixture consisting of species "1" and "2". If we normalize Eq. (206) by a measurement in a reference gas of known conditions, i.e., pure "1":

$$\frac{I_{RAY}}{I_1} = \left(\frac{\partial\sigma}{\partial\Omega}\right)_{mix} \Bigg/ \left(\frac{\partial\sigma}{\partial\Omega}\right)_1 \qquad \textbf{(207)}$$

Applications of Rayleigh Scattering

- Which can be written as

$$\frac{I_{RAY}}{I_1} = \left[X_1 \left(\frac{\partial \sigma}{\partial \Omega} \right)_1 + (1 - X_1) \left(\frac{\partial \sigma}{\partial \Omega} \right)_2 \right] \Bigg/ \left(\frac{\partial \sigma}{\partial \Omega} \right)_1 \qquad \textbf{(208)}$$

- After some simple manipulation

$$X_1 = \frac{\dfrac{I_{RAY}}{I_1} - \dfrac{\sigma_2'}{\sigma_1'}}{\left(1 - \dfrac{\sigma_2'}{\sigma_1'} \right)} = \frac{\left(I_{RAY} / I_2 \right) - 1}{\left(\sigma_1' / \sigma_2' \right) - 1} \qquad \textbf{(209)}$$

- With the mole fraction, the mass fraction ($Y_i = X_i W_i / W_{mix}$) and mixture fraction [$\xi = (\beta - \beta_{ox}) / (\beta_{fuel} - \beta_{ox})$; β is a conserved scalar] are easily obtained:

$$\xi = \frac{X_{fuel} W_{fuel}}{X_{fuel} W_{fuel} + \left(1 - X_{fuel} \right) W_{air}}; \quad X_{fuel} = \frac{\left(I_{RAY} / I_{air} \right) - 1}{\left(\sigma_{air}' / \sigma_{fuel}' \right) - 1} \qquad \textbf{(210)}$$

Applications of Rayleigh Scattering

- What does a typical setup look like?

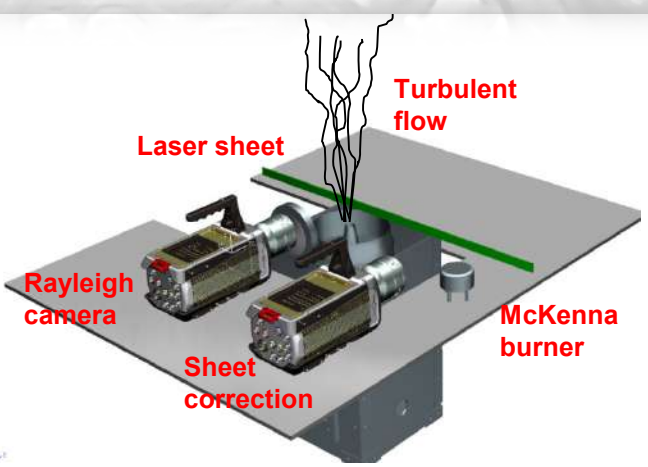

- Consider an example of a turbulent propane jet issuing into an air coflow

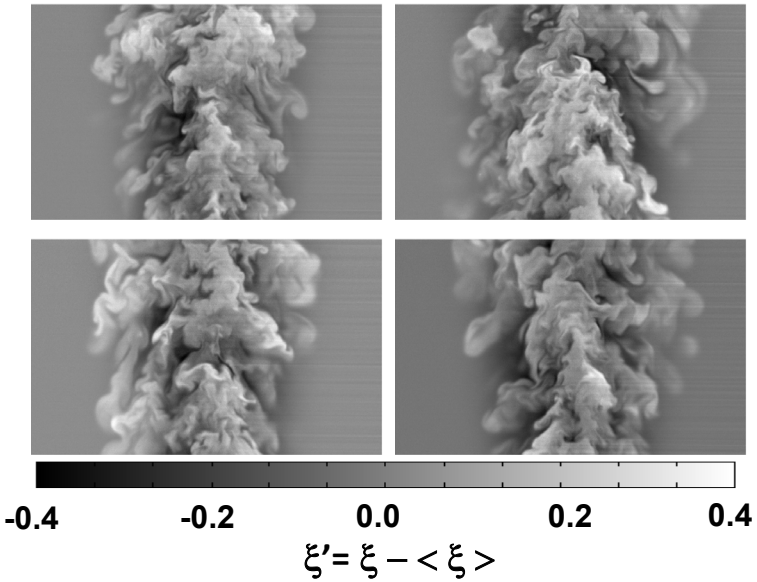

Fuel Concentration/Mixing in Diesel Engine Simulator

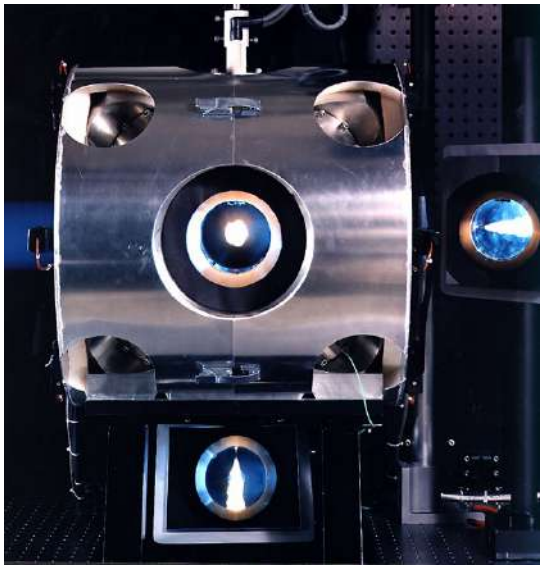

courtesy of L. Pickett

Well-defined ambient conditions:

- 300 to 1300 K
- up to 350 bar
- 0-21% O_2 (EGR)

Injector

- single or multi-hole injectors
- diesel, gasoline, jet

Full optical access

- 100 mm on a side

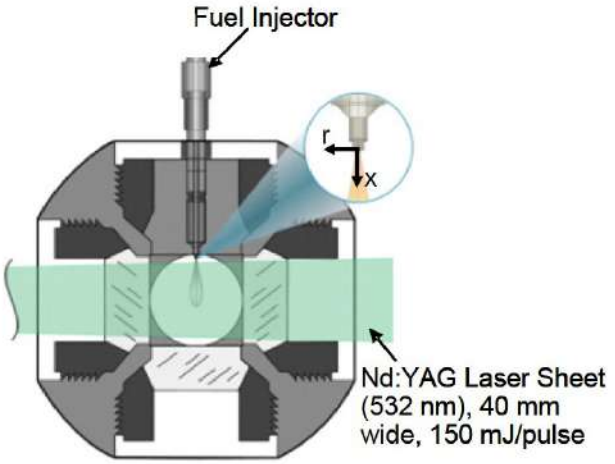

Idicheria and Pickett, 2007

C_7H_{16} into 1000K N_2 at 40 atm

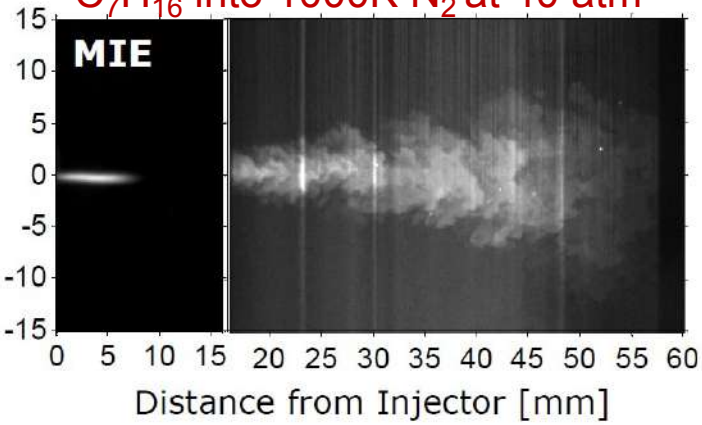

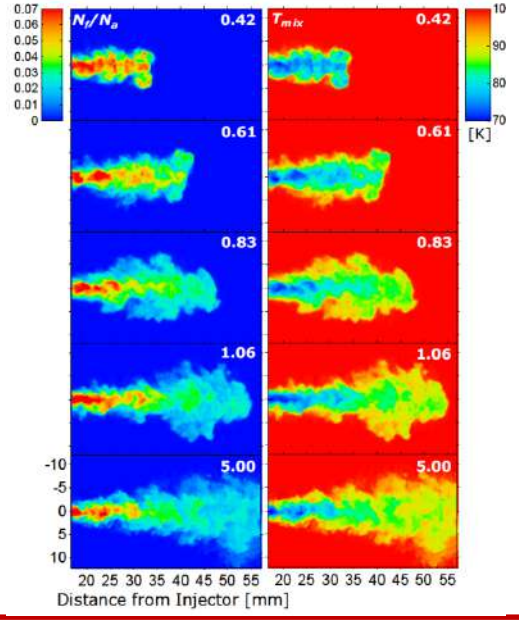

Rayleigh Scattering Thermometry

- What happens if composition varies? The mixture-averaged scattering cross section will be very different under "lean" and "rich" conditions. How do we measure temperature?

- Consider the expression for temperature

$$T = T_{ref} \frac{I_{ref}}{I_{RAY}} \frac{\sigma'_{mix}}{\sigma'_{ref}} \qquad \textbf{(212)}$$

where I_{ref} is the measured Rayleigh scattered intensity at a reference condition of known temperature (T_{ref}) and species (yielding σ'_{ref})

- In lean premixed flames, the major species is N_2, thus it is common to determine temperature as

$$T \approx T_{ref} \frac{I_{ref}}{I_{RAY}} \frac{\sigma'_{N2}}{\sigma'_{ref}} \qquad \textbf{(213)}$$

- If the reference condition is pure N_2, then $T \approx T_{ref} I_{ref} / I_{RAY}$. Care should be taken with this approach as the deviation of σ'_{mix} from σ'_{N2} can lead to sizeable error under certain circumstances

Rayleigh Scattering Thermometry

- Let's go back to Eq. (106) again and this time we will consider an isobaric process only

$$I_{RAY} \propto \frac{1}{T}\left(\frac{\partial\sigma}{\partial\Omega}\right)_{mix} \qquad \textbf{(211)}$$

- We have to think about the mixture-averaged differential scattering cross section
- Scattering cross sections for some select gases (532 nm, STP):

O_2	$5.08 \cdot 10^{-28}$ cm^2/sr
N_2	$6.13 \cdot 10^{-28}$ cm^2/sr
H_2	$1.34 \cdot 10^{-28}$ cm^2/sr
CO	$7.87 \cdot 10^{-28}$ cm^2/sr
CO_2	$13.8 \cdot 10^{-28}$ cm^2/sr
H_2O	$4.43 \cdot 10^{-28}$ cm^2/sr
C_3H_8	$79.8 \cdot 10^{-28}$ cm^2/sr

Rayleigh Scattering Thermometry

- Another approach is to correlate the mixture-averaged scattering cross section with temperature (or measured intensity) and determine the cross section (and temperature) iteratively. For higher hydrocarbons like propane, the cross section varies such that the of $\sigma'_{mix} = \sigma'_{N2}$ assumption becomes too weak and this approach must be taken.

- It is not possible to determine the of σ'_{mix}-$temperature$ relationship *in situ*, so typically a "state relation" is determined from laminar flame simulations using detailed chemistry. The inherent assumption here is that the thermo-chemical state that exists under laminar flame conditions is the same as that which occurs instantaneously within turbulent flames

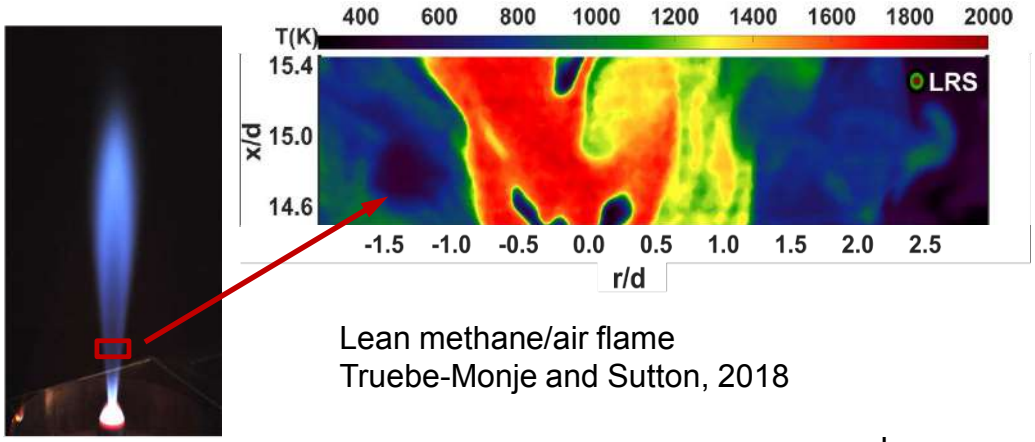

Lean methane/air flame
Truebe-Monje and Sutton, 2018

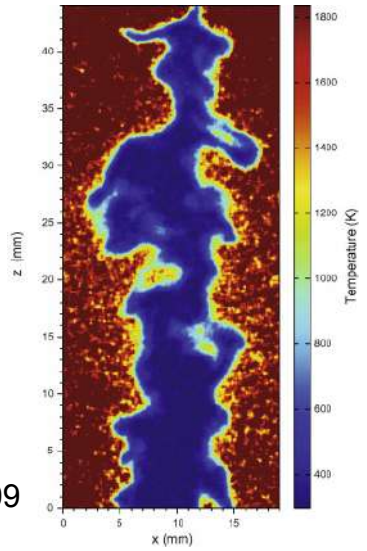

Lean propane/air flame
Yuen and Gülder, CNF, 2009

Rayleigh Scattering Thermometry

- What about non-premixed flames? This is challenging as (in general) σ'_{mix} varies throughout the entire domain from fuel to products to oxidizer
- However, it is possible to consider a 'specialized' set of jet flames with a particular fuel such that the differential scattering cross section does not vary significantly throughout the domain
- The most common is the DLR CHN flames (fuel: 22.1% CH_4/33.2%H_2/ 44.7%N_2 by volume). This flame was developed such that the differential scattering cross section is ± 3% across flame (*i.e., from fuel to products to air*)

(1) $$I_{Ray} = CI_I \, P/kT \, \sigma'_{mix}$$

(2) $$T = T_{ref} \frac{I_{ref}}{I_{Ray}} \frac{\sigma'_{mix}}{\sigma'_{ref}}$$

(3) $$T = T_{ref} \frac{I_{ref}}{I_{Ray}}$$

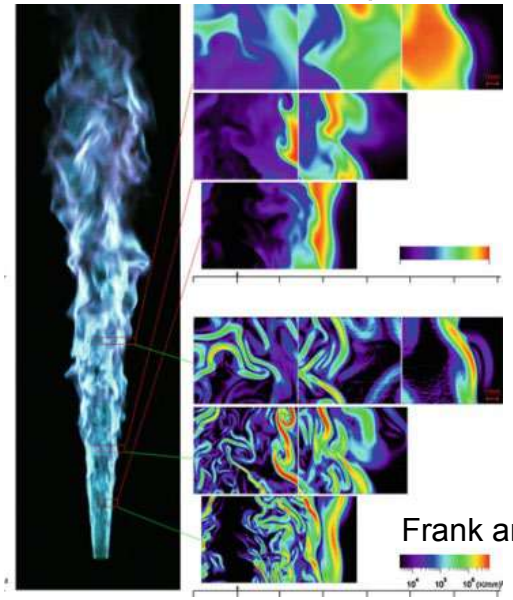

Frank and Kaiser, 2010

Pros/Cons of Rayleigh Scattering

Pros	Cons
• Implementation is straightforward	• Not species specific
• Non-resonant process (any laser)	• Outside of "controlled" setting, signal interpretation may be difficult
• "Instantaneous" 2D image and topology	• Scattering is at same wavelength as laser – interference from windows, surfaces, particulate, etc
• Can yield temperature or concentration	
• Good sensitivity and resolution is possible	

Possible solutions for this in next lecture

Laser Diagnostics in Turbulent Combustion Research

Jeffrey A. Sutton

Department of Mechanical and Aerospace Engineering
Ohio State University

Princeton-Combustion Institute Summer School on Combustion, 2019

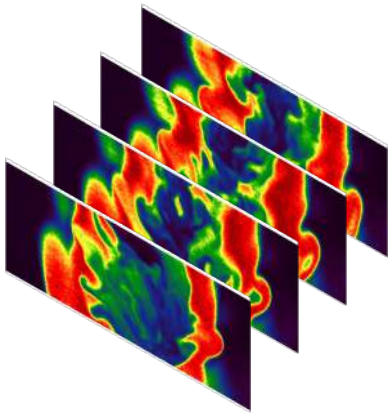

Lecture 12 – Filtered Rayleigh Scattering

Overview and Outline of Lecture

Goal: Provide an Overview of Filtered Rayleigh Scattering and Possible Applications

- Limitations of Rayleigh Scattering
- Filtered Rayleigh Scattering Theory (FRS)
- Experimental Considerations
- Applications of FRS in Reacting Flows

Limitations of Rayleigh Scattering

- How does a laser light show work? You need a laser and particles in the air (dust, fog, smoke, humidity, rain, snow, etc.). Light effectively scatters off of these particles yielding wonderful images.
  We know from our lectures on PIV that Mie/Tyndall scattering describes this effect

http://www.lighting-geek.com

- As we saw in the last lecture, Rayleigh scattering also occurs at the same frequency as the incident electric field, i.e., the wavelength of the scattered light is nominally the same as the wavelength of the laser (we haven't talked about lineshapes or Doppler shift)

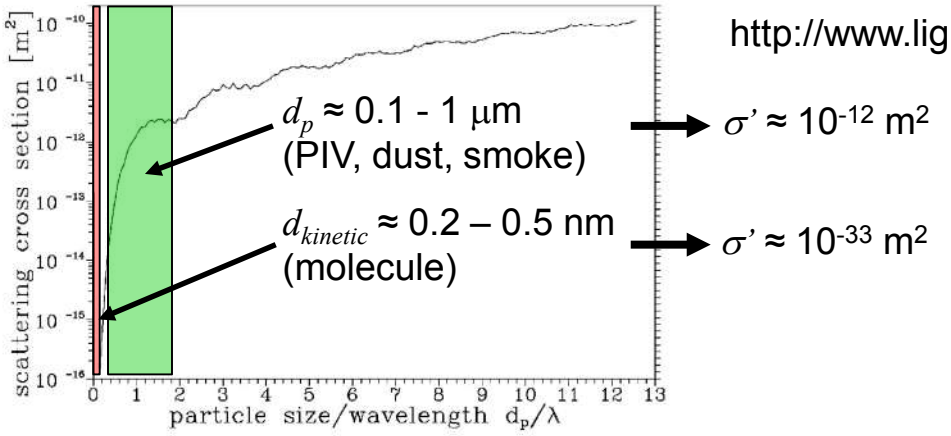

Limitations of Rayleigh Scattering

- Rayleigh scattering is greatly limited in the presence of particles.
- As an example, consider the attempt of Rayleigh thermometry in a sooting flame (remember soot is fairly small!). We can see that the Rayleigh signal is overwhelmed by the particle scattering
- As an extension, you can imagine that Rayleigh scattering and PIV are not possible simultaneously (hint: you only see particle scattering in PIV images – no gas-phase scattering!)
- Rayleigh scattering also is overwhelmed by surface scattering. Thus, measurement in confined combustors (windows and walls) are challenging

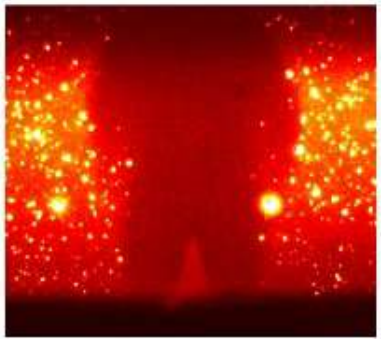

http://www.forbrf.lth.se/english/research/measurement-methods/rayleigh-and-filtered-rayleigh-scattering/

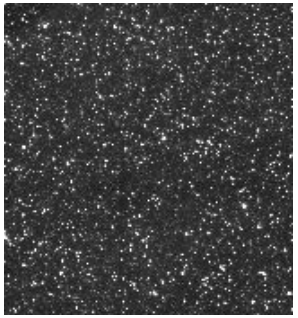

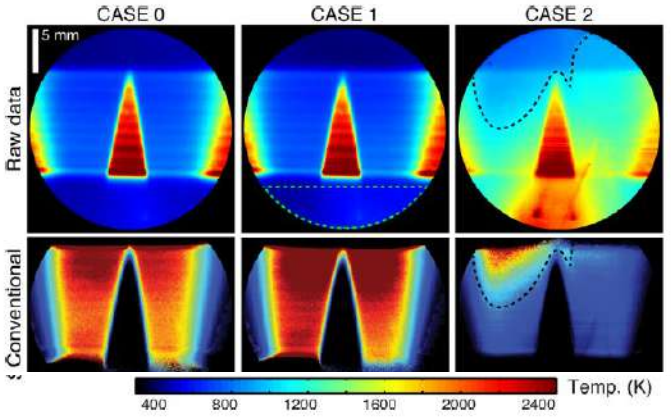

Adapted from Fig. 3: Kistensson et al., PCI, 2015

Spectroscopy of Rayleigh Scattering

- So far, we have simply referred to the emitted intensity as “having the same frequency” as the incident electric field.
- We saw in a previous lecture that there is no such thing as pure monochromatic light, so you probably expect that the emitted Rayleigh-scattered light has a bandwidth that is at least as “wide” as the laser.
- For broadband laser sources, this would be your observation if you measured the bandwidth of the scattered light, but what if you had a spectrally narrow laser source?

  What would the lineshape of the scattered intensity look like if you had really good frequency resolution around the center frequency of the laser?

Spectroscopy of Rayleigh Scattering

- First, we need to refine our terminology – if we send a laser into a neutral gas medium and collect light, we will collect three (actually four) distinct sources: (i) vibrational Raman, (ii) pure rotational Raman scattering (rotation of the molecule modulates the scattered light adding new frequencies), and (iii) the Cabannes line
- The Cabannes lineshape can contain two components itself: (i) the central Gross or Landau-Placzek line and (ii) shifted Brillouin-Mandel'shtam scattering doublets
- Let's start with the case of low bulk density (low pressure or high temperature)
- The random, uncorrelated thermal motion of the molecules leads to a Doppler linewidth that is a Gaussian distribution centered around the mean velocity of the flow

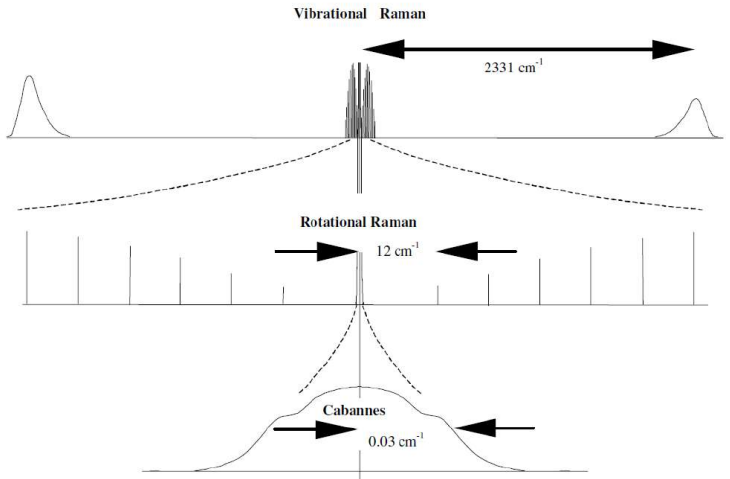

Miles et al, MST, 2001

Spectroscopy of Rayleigh Scattering

- The formulation is very similar to what we saw when discussing LIF:

$$\varphi_D(\nu) = \frac{2\sqrt{\ln 2}}{\Delta\nu_D\sqrt{\pi}}\exp\left[-4\sqrt{\ln 2}\frac{(\nu-\nu_o)^2}{\Delta\nu_D^2}\right] \qquad \textbf{(214)}$$

$$\Delta\nu_D = \frac{2}{\lambda}\sin(\theta/2)\sqrt{\frac{8kT\ln 2}{m}}$$

- Note, the observation angle (θ) plays a role in the perceived width
- The scattering profile only reflects the motion of the molecules
- This is the Knudsen regime in gas kinetics

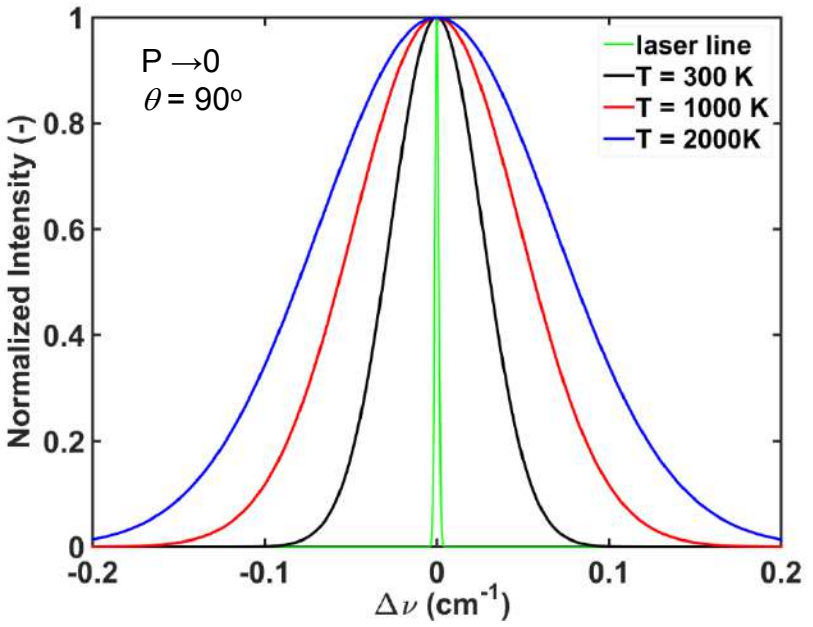

Spectroscopy of Rayleigh Scattering

- Now as pressure increases, we need to discuss what actually is happening in the probe volume
- If scattering is observed at angle θ (say from the thermal density fluctuations), then the observed scattering and the incident laser light (at wavelength λ_l) formed an interference pattern with a grating frequency satisfying Bragg's condition:

$$\lambda_s = \frac{\lambda_l}{2}\frac{1}{\sin(\theta/2)} \qquad \textbf{(215)}$$

- At the same time, the microscopic (thermal) density fluctuations (due to molecular motion) create acoustic disturbances that travel through the medium and propagate in all directions
- The acoustic disturbances create additional microscopic scale density fluctuations, but these are transported at the speed of sound
- As number density increases, the mean free path (ℓ) decreases and when $\ell < \lambda_s$, Bragg's condition can be satisfied and the density fluctuations (due to acoustic perturbations) contribute to the total scattering

Spectroscopy of Rayleigh Scattering

- Since the density fluctuations are moving at the speed of sound, they undergo a Doppler shift and the scattering is observed at frequency shifts:

$$\Delta f = \pm \frac{2fa}{c} \sin(\theta/2) \qquad \textbf{(216)}$$

where f is the frequency of the incident light and a is the speed of sound

- These acoustic sidebands are known as Brillouin-Mandel'shtam or Brillouin scattering
- In addition, there is a central peak due to the non-propagating density fluctuations (Gross line)
- When $\ell << \lambda_s$ this is the hydrodynamic regime in gas kinetics and all three bands will be described by a Lorentzian lineshape

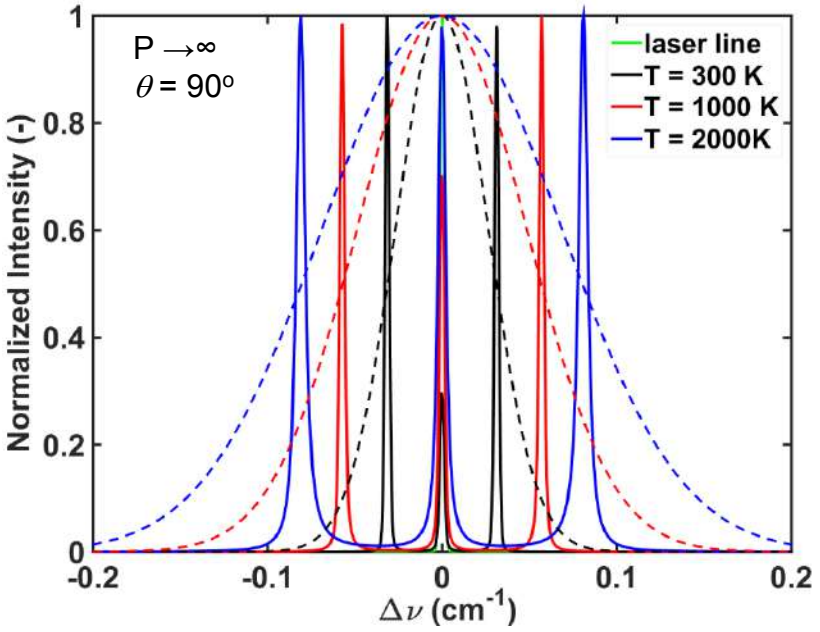

“Rayleigh-Brillouin” Lineshape

N_2

T = 300 K

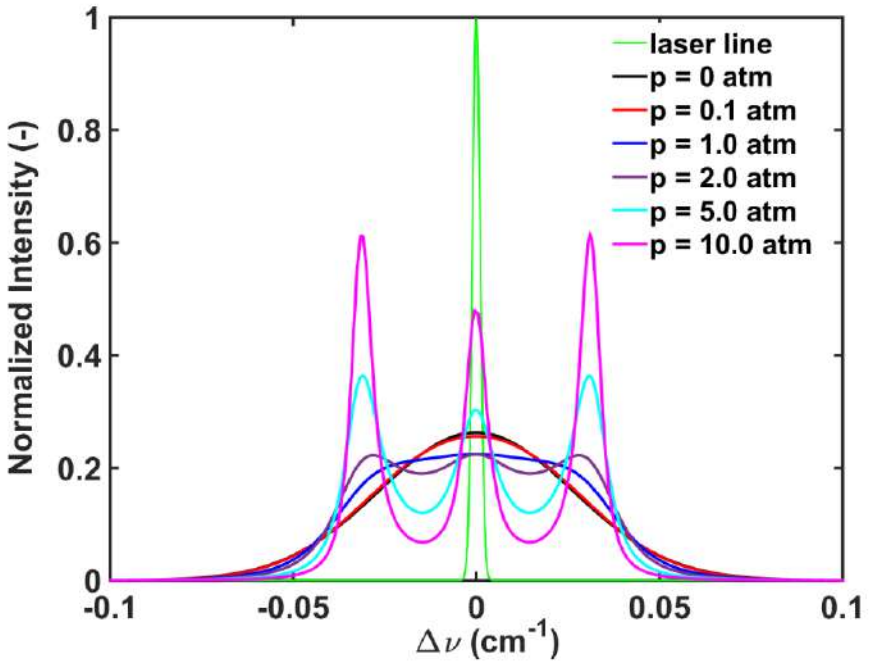

P = 10 atm

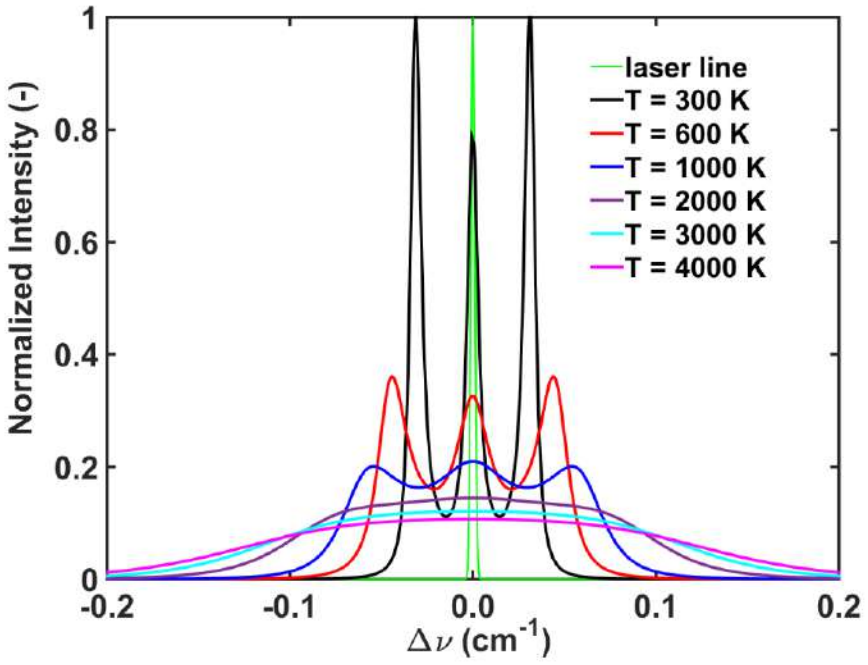

"Rayleigh-Brillouin" Lineshape

- In order to compare the relative importance of the random thermal motion as compared to the correlated acoustic motion, a quantity called the y-parameter is defined as the ratio of the characteristic scattering wavelength to the mean free path

$$y = \frac{1}{2\pi\ell}\frac{\lambda_l}{2\sin(\theta/2)} \cong \frac{Nk_BT}{k\mu v_o} \cong \frac{N}{k\mu}\left(\frac{mk_BT}{2}\right)^{1/2} \qquad \textbf{(217)}$$

- If y >>1: hydrodynamic regime; if y << 1: Knudsen regime and acoustic effects are neglected. Otherwise, both processes are important and the lineshape must be modeled (more on this later)

- For example, T = 300, p = 1 atm yields $y \approx 0.75$ which means acoustic effects do need to be taken into account. Combustion conditions yield low values of y, but they are still not quite fully Guassian profiles.

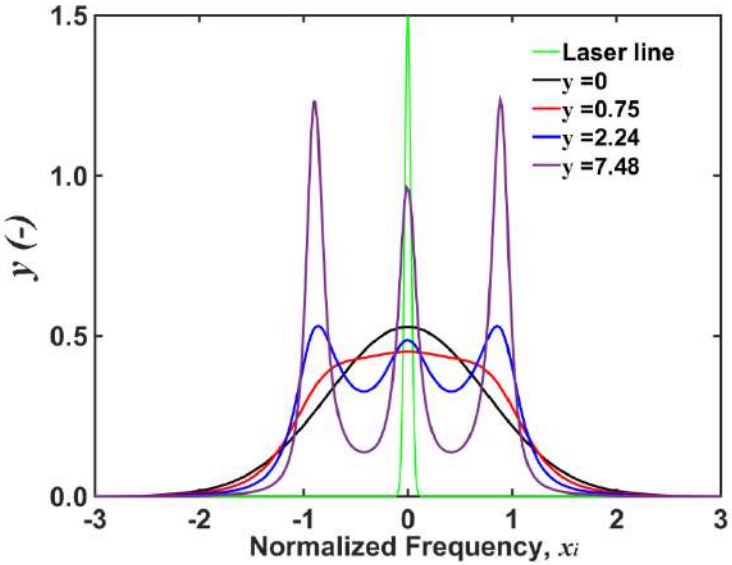

Filtered Rayleigh Scattering

- What about the particle or surface scattering? Solid/liquid particles have very little thermal motion (due to proximity of molecules). Thus, the scattered lineshape is almost exactly the same as the laser lineshape.
- Thus, there are significant spectral differences between light scattering from solid/liquid particles (or surfaces) and gases
- Let's assume we have a very narrow spectral laser with linewidth ($\Delta\nu_L << \Delta\nu_{RBS}$)
- We can couple the camera to an atomic or molecular vapor cell (used as filter).
- Absorption transition of iodine is $\Delta\nu_L < \Delta\nu_{\mathbf{iodine}} < \Delta\nu_{RBS}$
- Light scattered from particles (or surface) has linewidth of $\Delta\nu_L$ and is blocked.
- A portion of the gas-phase signal is collected

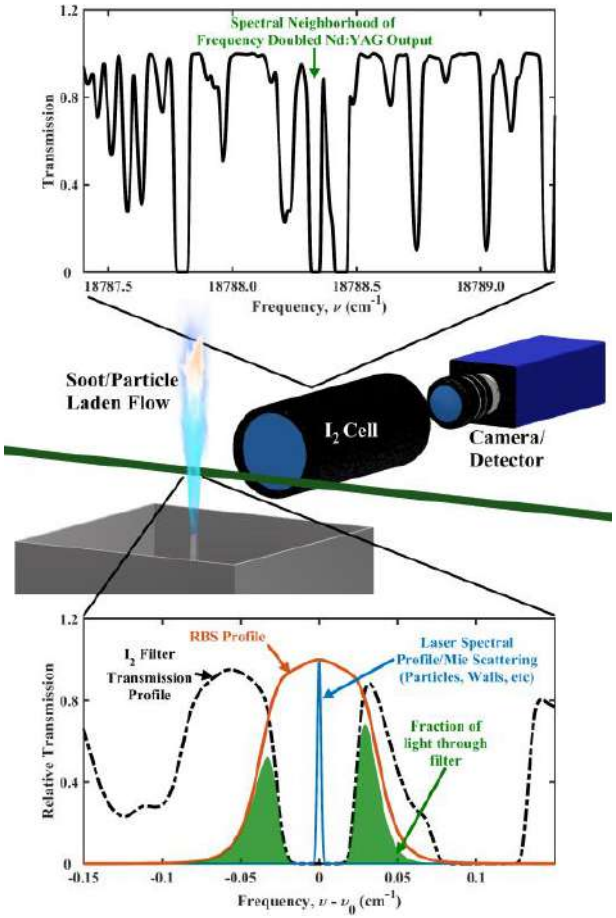

Filtered Rayleigh Scattering

- The equation for FRS is a modification of that developed for Rayleigh scattering (or LRS). For a single species it is written as

$$I_{FRS,i} = CI_I N\psi_i \qquad \textbf{(216)}$$

where ψ is an FRS specific variable expressed as

$$\psi_i = \sigma_i' \int_\nu R_i(P,T,V,\theta,\nu)\cdot\tau(\nu) \qquad \textbf{(217)}$$

and R_i is the RBS spectral lineshape, and $\tau(\nu)$ is the filter species transmission profile

- It is noted that contrary to traditional LRS, the FRS signal is highly dependent on the overlap between the filter species transmission profile and the RBS spectrum for any given species, which is temperature dependent.
- Quantitative interpretation of the measured FRS signal requires knowledge of the RBS lineshape of each species (more on this in a minute)

A Comparison of LRS and FRS

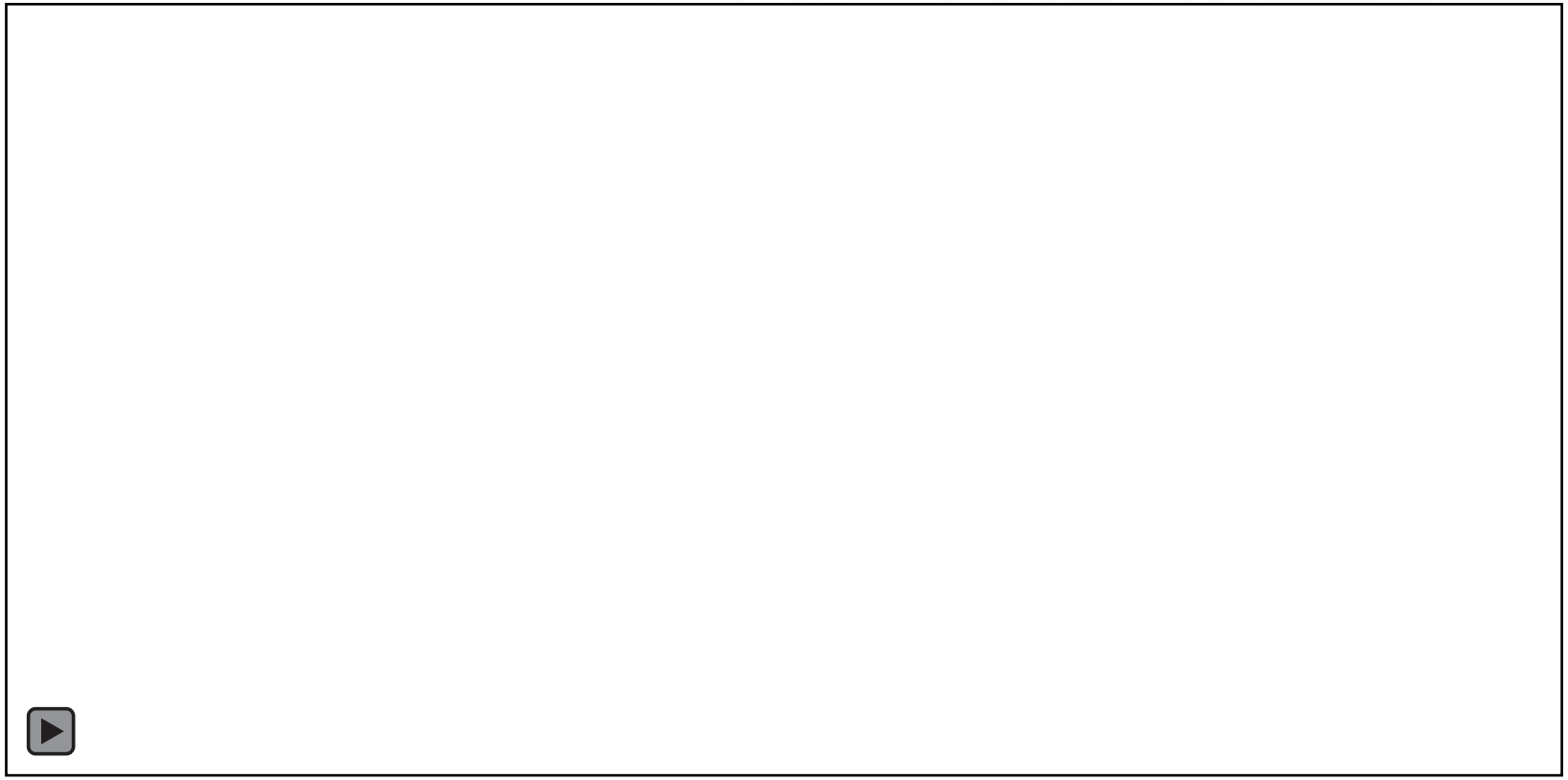

- LRS has a 1/T signal dependence
- FRS has a 1/T signal dependence + a dependence on the RBS spectra and its transmission through the I_2 cell (species and temperature dependent).

Filtered Rayleigh Scattering

- For a mixture, the FRS equation should be expressed as follows:

$$I_{FRS} = CI_I \eta N \sigma'_{mix} \int_{\nu} R_{mix}(P,T,V,\theta,\nu) \cdot \tau(\nu) \qquad \textbf{(218)}$$

- However, a kinetic description (modeling) of the RBS spectrum from gas mixtures is very complex because there is a need for transport coefficients describing inter-species transport that are not known.
- In lieu of knowing R_{mix}, it is common simply to express the measured FRS signal as:

$$I_{FRS,i} = CI_I N \sum_i X_i \psi_i \qquad \textbf{(219)}$$

- Recent measurements in my group have shown that this appears to be valid for the kinetic regime
- This allows us to move forward with an approach for thermometry in the presence of strong scatterers and other interference

Filtered Rayleigh Scattering

- Similar to LRS, normalizing the measurements by a reference condition at known conditions, the temperature can be cast as

$$T = T_{ref} \frac{I_{ref}}{I_{FRS}} \frac{\sum_i \sigma'_i \int_\nu R_i(P,T,V,\theta,\nu)\cdot\tau(\nu)}{\sigma'_{ref} \int_\nu R_{ref}(P,T,V,\theta,\nu)\cdot\tau(\nu)} \qquad \textbf{(220)}$$

- This shows that in order to determine temperature from measured FRS signals, (i) the RBS spectral profiles for the species must be known and (ii) the spectral filter characteristics must be known
- Each species has a different RBS lineshape that changes as a function of temperature. Since these cannot be measured *in situ*, their overlap with the filter species profile (I_2 shown here – dashed line) must be modeled. We will discuss this later in the lecture.

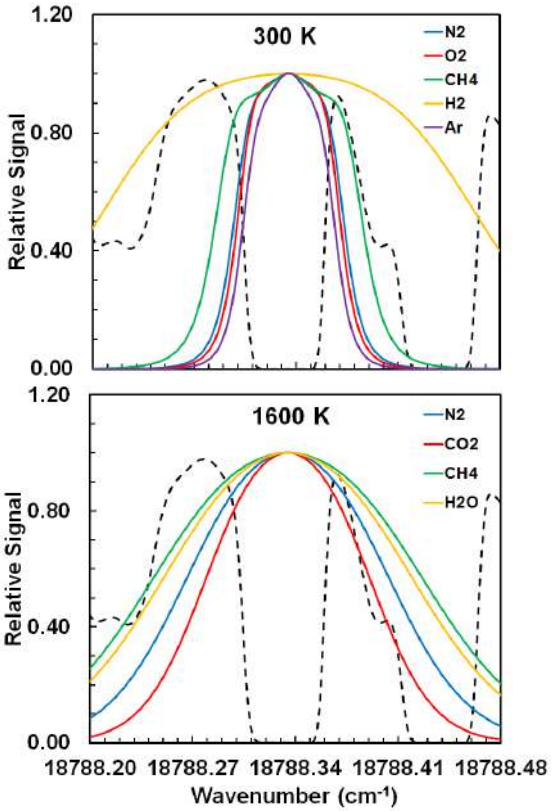

Experimental Considerations

- There are three primary areas to consider experimentally:

  (1) laser/filter cell combination

  (2) RBS and filter species model(s)

  (3) data reduction/accounting for variable species

- It is not difficult to achieve a narrow spectral bandwidth in a laser at a number of spectral frequencies.
- The difficulty is having a high-energy pulsed laser with narrow spectral output overlap with a atomic or molecular species that shows considerable absorption at discrete locations (i.e., a “broadband” absorber is not good)

Experimental Considerations

- Miles et al. (2001) discusses possible candidates (many of which also have been used in the LIDAR community) including:

(i) molecular iodine at 532 nm (2nd harmonic of Nd:YAG)
(ii) mercury vapor at 254 nm (3rd harmonic of Ti:Sa or Alexandrite)
(iii) barium at 554 nm (dye laser output)
(iv) lead vapor at 283 nm (frequency-doubled dye laser output)
(v) potassium vapor at 770 nm (Ti:Sa, Alexandrite, dye laser)
(vi) iron vapor at 248 nm (excimer, frequency-doubled dye laser output)
(vii) rubidium vapor at 780 nm (Ti:Sa, Alexandrite, dye laser)
(viii) cesium vapor at 389 nm (frequency-doubled dye laser)

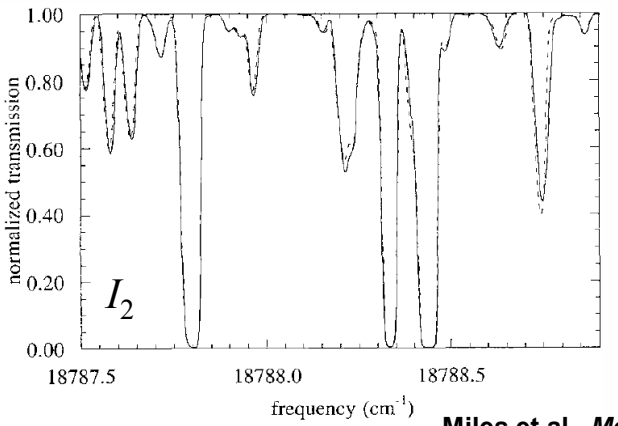

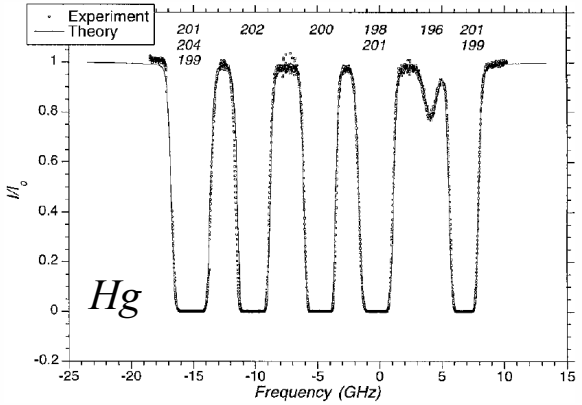

Miles et al., *Meas. Sci. Tech.*, 2001

Models - Filter

- For traditional LRS, the complete spectrally dispersed Cabannes line is collected and no model is needed to relate the scattering signal (of a single species) to number density
- For FRS, accurate models describing the filter species transmission spectra and the RBS spectra are needed to relate the collected signal to number density
- For I_2, the most common model to calculate the spectral transmission is the code developed by Forkey and co-workers (Forkey et al., *Appl. Opt.*, 1997). It calculates the absorption spectra of the $B({}^3_0\Pi_{0^+u}) \leftarrow X({}^1_0\Sigma_g{}^+)$ electronic transition of iodine. The code has been expanded to account for non-resonant background effects and has been validated experimentally to a certain extent.
- For Hg, model results have been presented by practitioners. The models are not as widespread and have not had the same type of validation as I_2. However Hg, being an atomic species, has simpler spectroscopy

Models - RBS

- In the kinetic regime ($0.3 \lesssim y \lesssim 3.0$), neither a Gaussian nor a set of Lorentzian functions can be used to describe the RBS lineshape
- In general this would require the solution to the Boltzmann equation to describe the scattered light – this requires knowledge of collisional cross sections between molecules, which are not known in general
- The most common set of models describing RBS spectra of individual species are the Tenti S6 and S7 models
- These models describe scattering profiles based on solutions to the linearized Boltzmann equation (Wang Chang-Uhlenbeck approximation)
- For S6 (or S7) models, calculation of the RBS spectra required knowledge of the temperature-dependent transport coefficients, including the dynamic or shear viscosity, thermal conductivity, internal specific heat capacity, and *bulk viscosity*
- For many combustion-relevant species, this information is sparse

Models - RBS

- The accurate modeling of the RBS spectral lineshape is important in many other fields such as LIDAR-based measurements for atmospheric measurements.
- This application has prompted many high-resolution measurements from gases such as N_2, O_2, CO_2, and air. As one example:

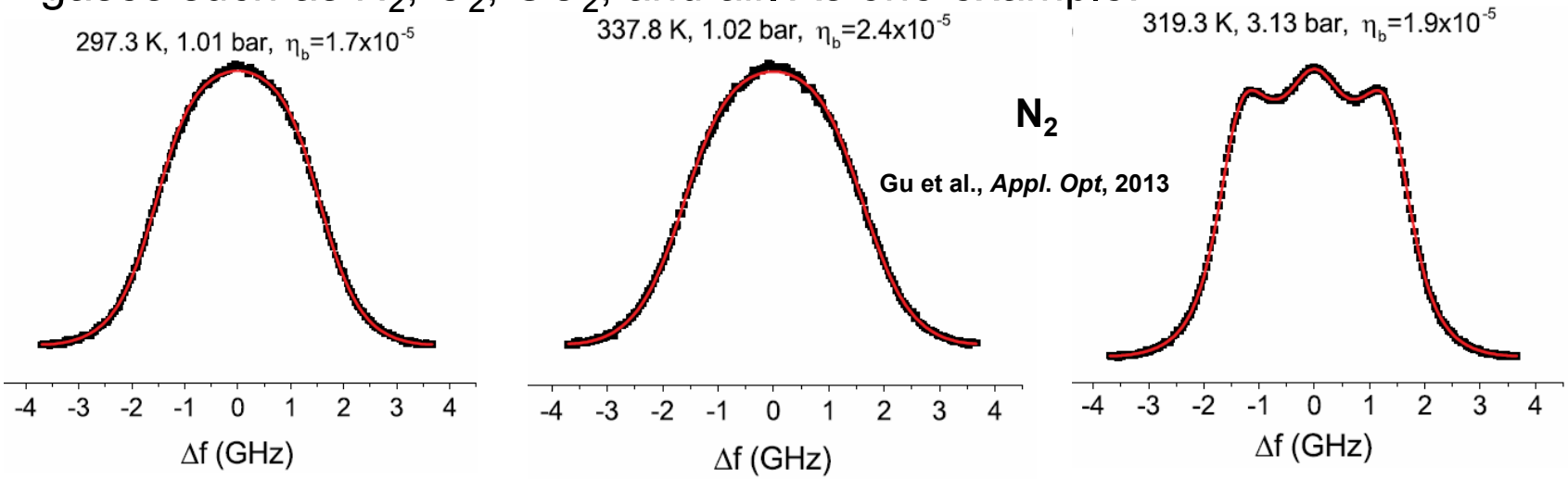

- In general, there is good agreement between measurements and the S6 model at lower temperatures and pressures; S6 performs the best
- There are fewer measurements for combustion-specific species (i.e., fuels, products, intermediates)

Further Assessment of Tenti S6

Heated Flows

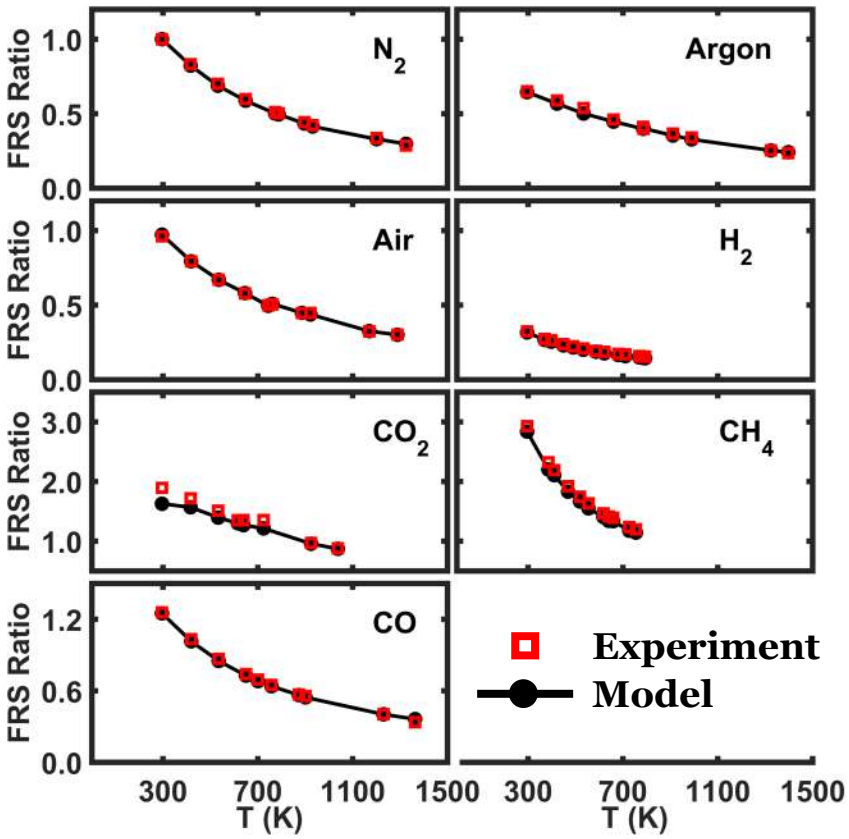

Near-Adiabatic Hencken Flames

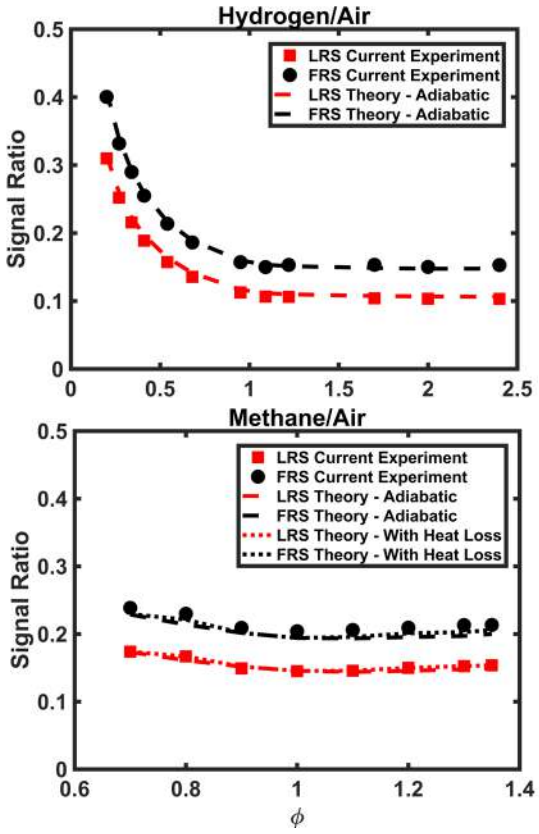

- Overall, there is good agreement between experiments and model

Limitations to FRS

- FRS has a lot of potential benefits in more complex environments (flows with particles, sooting flames, flame-wall interactions, etc.)
- Beyond demonstration, why has FRS not been widely implemented?
- The major limitation with FRS (e.g., in flows with particles) has been the ability to properly suppress the unwanted interference

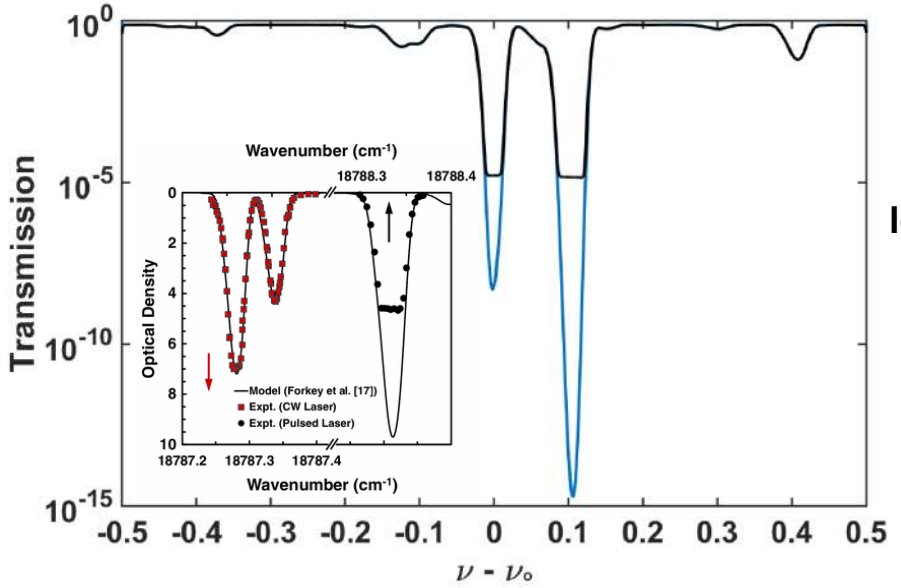

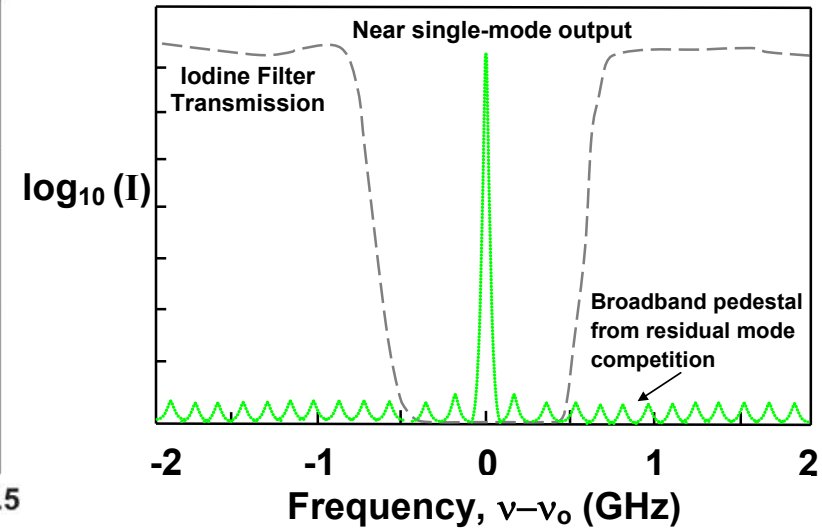

Applications: Sooting Flames

- One of the first applications of FRS in flames by Leipertz and co-workers in a weakly sooting premixed CH_4/air flame:

  Hoffmann et al., **Two-dimensional temperature determination in sooting flames by filtered Rayleigh scattering,** *Opt. Lett.*, 1996

  Hoffman and Leipertz, **Temperature field measurements in a sooting flame by filtered rayleigh scattering (FRS),** *Proc. Combust. Inst*, 1996

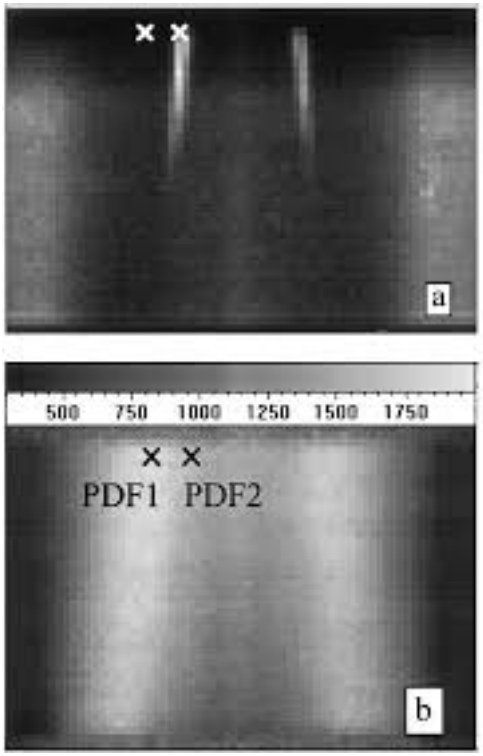

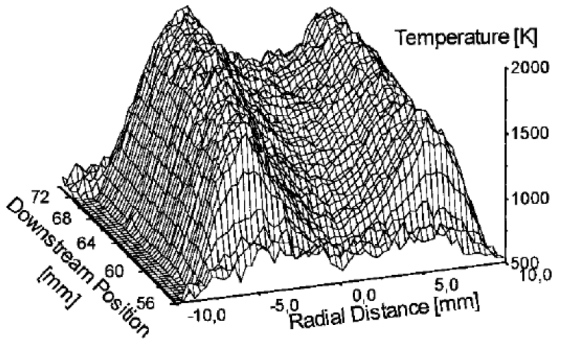

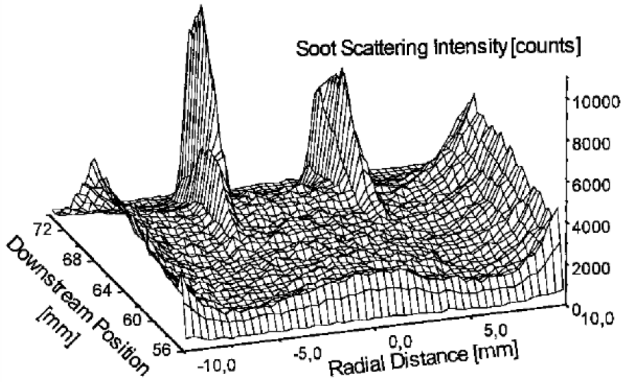

Applications: Sooting Flames

- Later measurements were performed using the combination of a 254-nm source (tripled Alexandrite) and a mercury vapor filter

  Zetterberg et al., **Two-Dimensional Temperature Measurements in Flames Using Filtered Rayleigh Scattering at 254 nm,** *Appl. Spectroscopy,* 2008

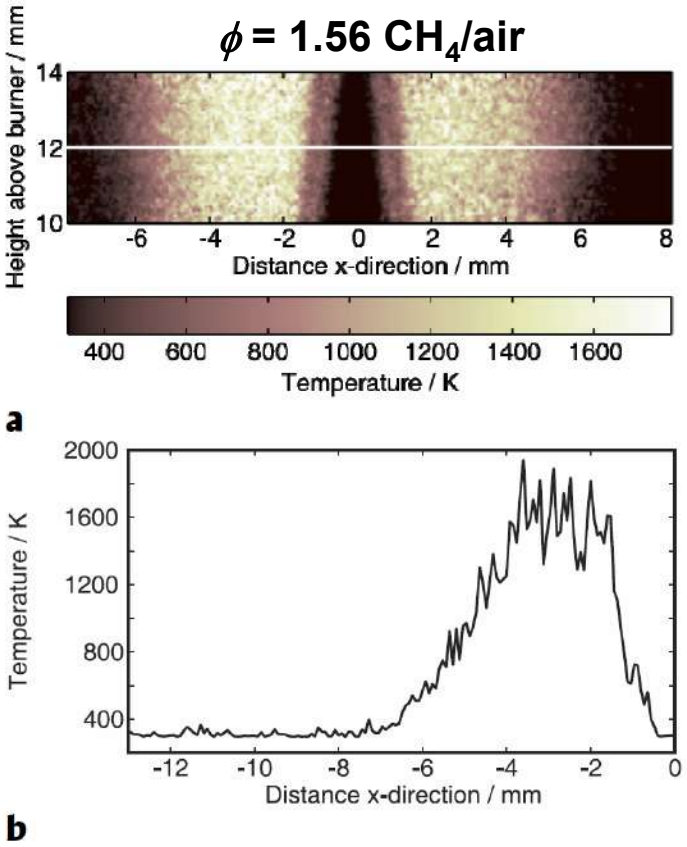

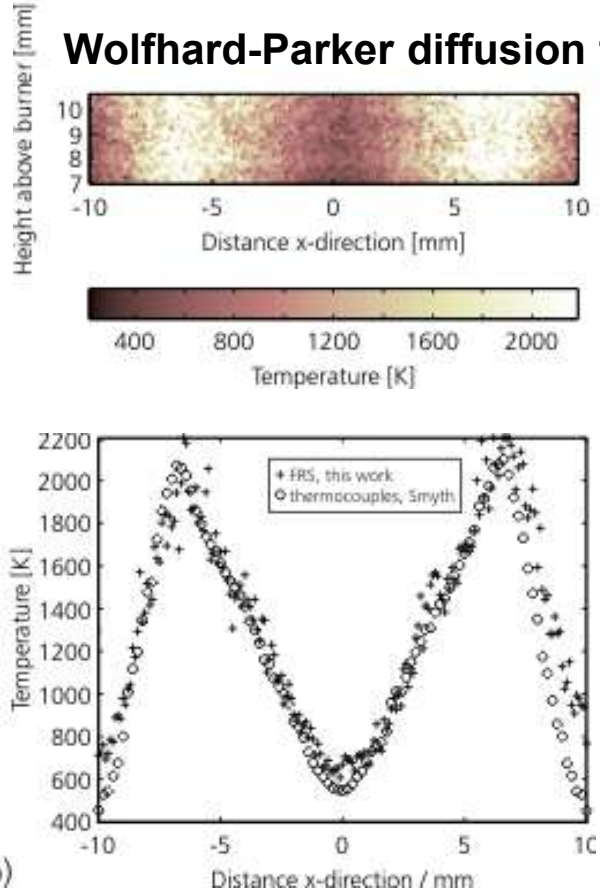

Applications: Near Surfaces

- Geometric or “surface scattering” renders Rayleigh scattering (and many other thermometry approaches) useless near surfaces such as walls and windows
- Near-surface measurements are critical for heat transfer studies

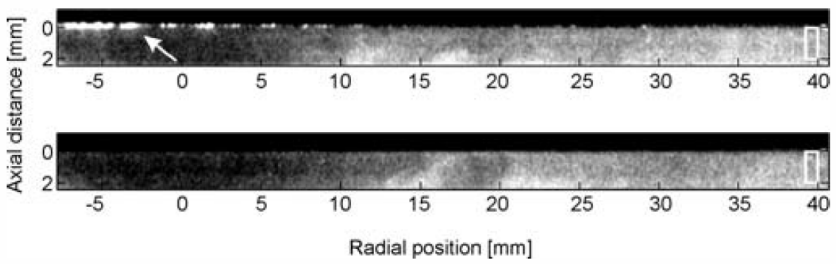

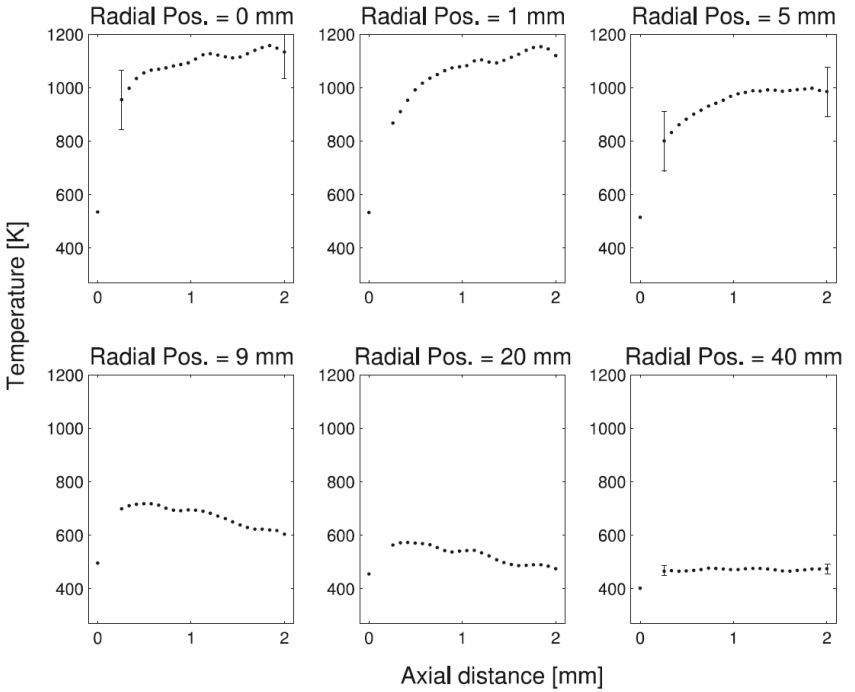

Measurements were performed within 250 μm of surface

Brübach et al., **Determination of surface normal temperature gradients using thermographic phosphors and filtered Rayleigh scattering,** *Appl. Phys. B,* 2006

Applications: Near Surfaces

- Geometric or “surface scattering” renders Rayleigh scattering (and many other thermometry approaches) useless near surfaces such as walls and windows
- Near-surface measurements are critical for heat transfer studies

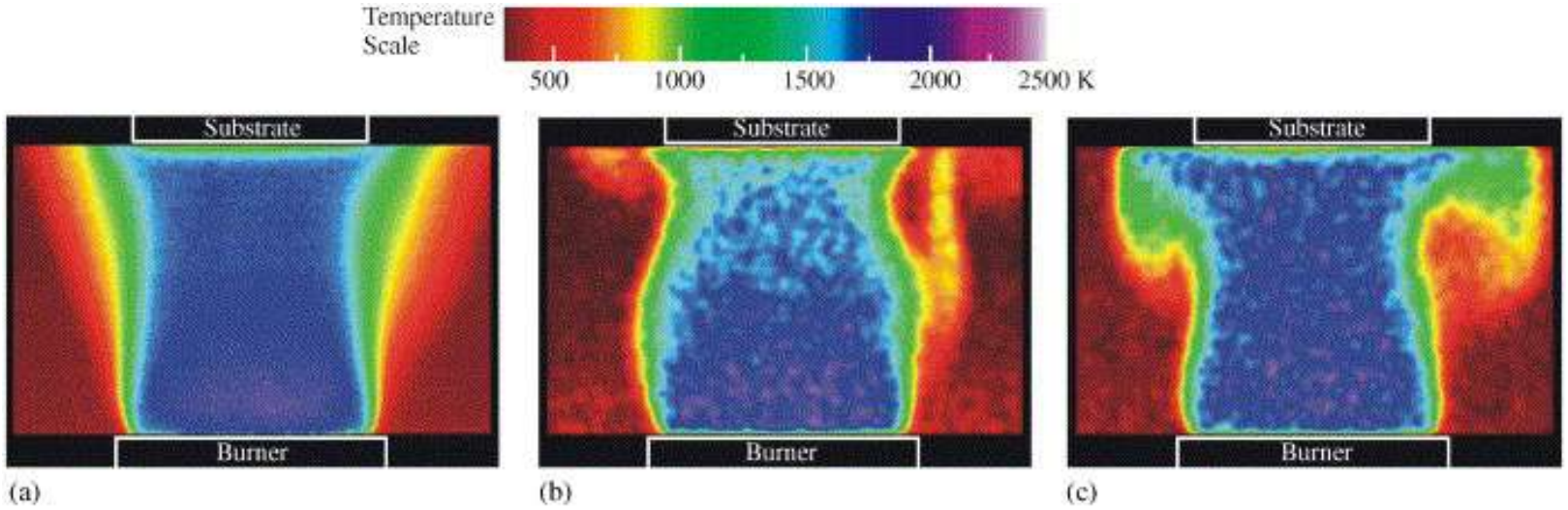

Bogusko and Elliott, Property measurement utilizing atomic/molecular filter-based diagnostics, *Prog. Aero. Sci,* 2005

Applications: Flows w/ Particulate

- 2D temperature distributions in a HDMSO loaded propane/air flame intended for combustion chemical vapor deposition processes

  Müller et al., **Two-dimensional temperature measurements in particle loaded technical flames by filtered Rayleigh scattering,** *Appl. Optics,* 2014

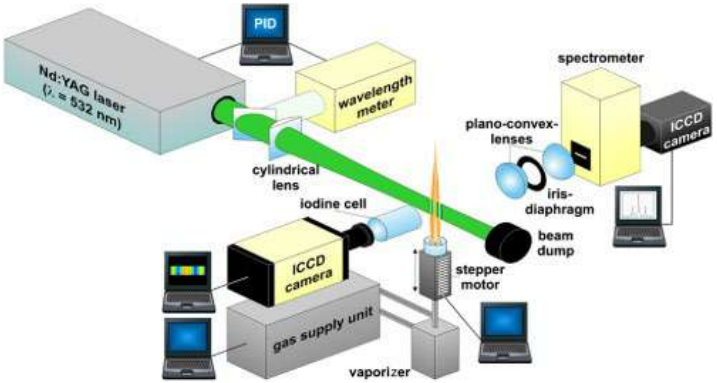

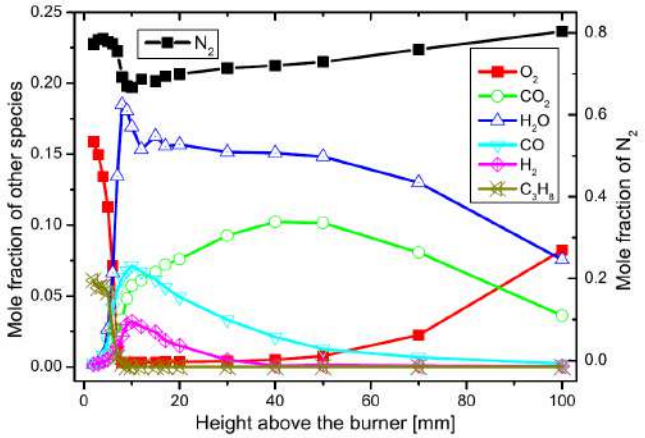

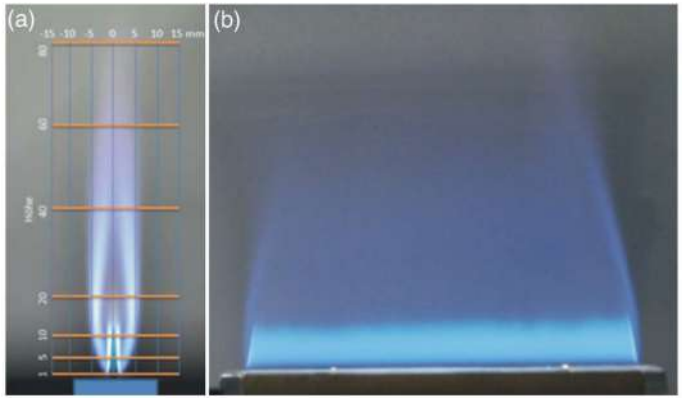

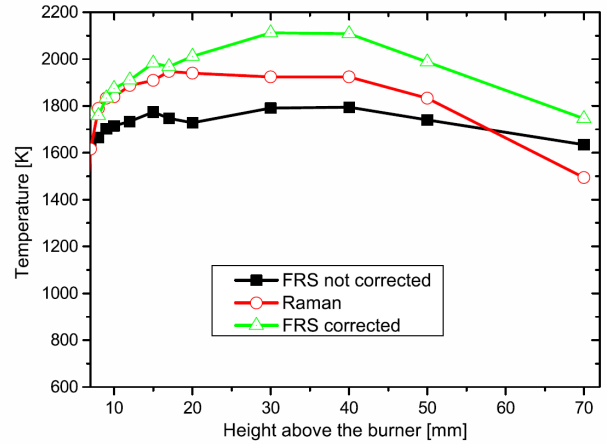

Applications: w/ PIV

- A significant strength of FRS is the potential for simultaneous temperature/velocity measurements using FRS/PIV

  Most and Leipertz, **Simultaneous two-dimensional flow velocity and gas temperature measurements by use of a combined particle image velocimetry and filtered Rayleigh scattering technique,** *Appl. Opt.,* 2001

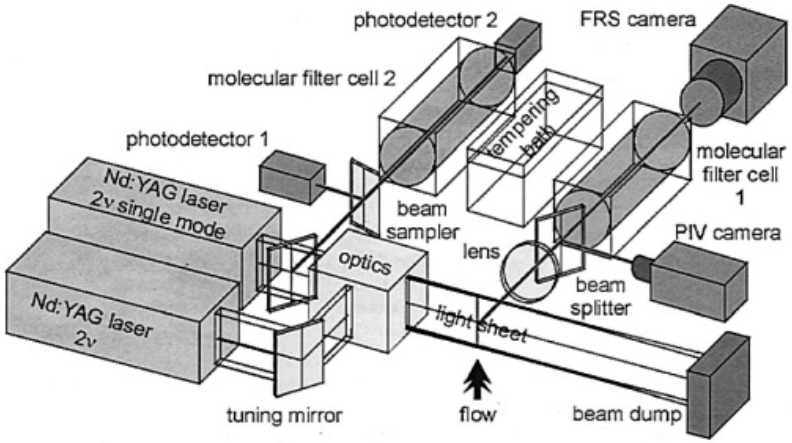

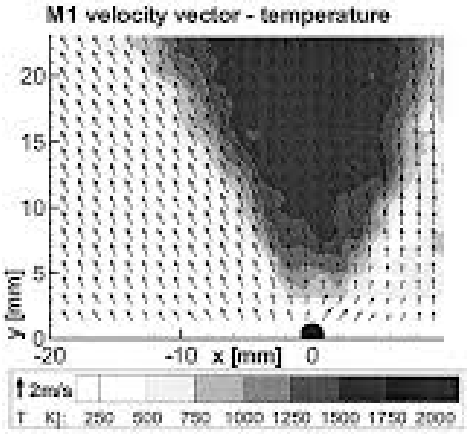

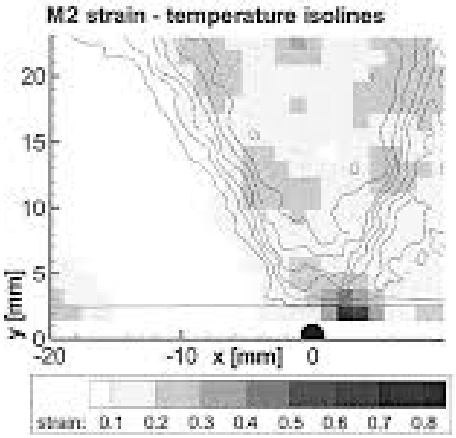

Applications: w/ PIV

- A significant strength of FRS is the potential for simultaneous temperature/velocity measurements using FRS/PIV

  Most et al, **Direct determination of the turbulent flux by simultaneous application of filtered Rayleigh scattering thermometry and particle imaging velocimetry ,** *Proc. Combust. Inst.,* 2002

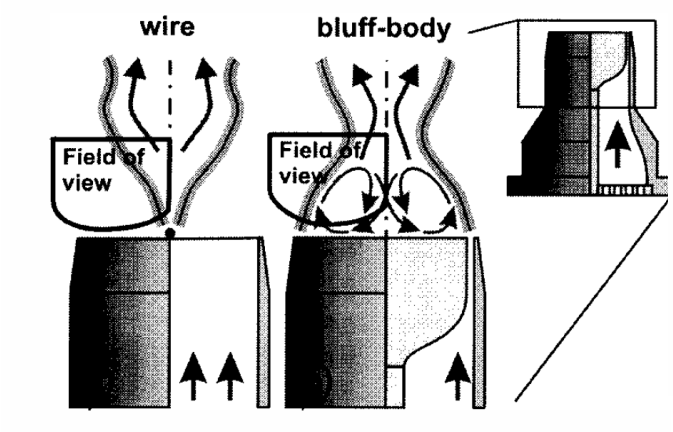

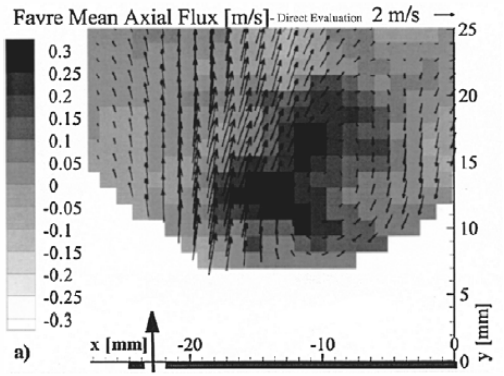

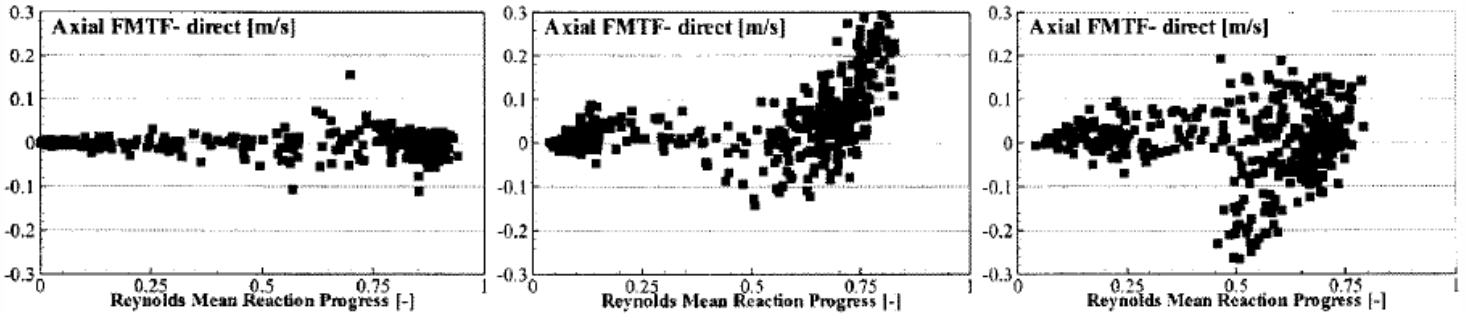

Applications: Nonpremixed Flames

- Nonpremixed flames are much more difficult because of the large change in species (cross sections, RBS profiles, etc) throughout the domain

Kearney et al, **Temperature imaging in nonpremixed flames by joint filtered Rayleigh and Raman scattering,** *Appl. Opt.,* 2005

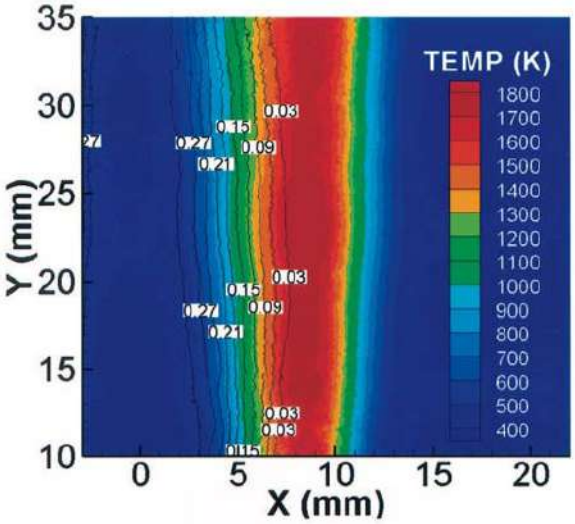

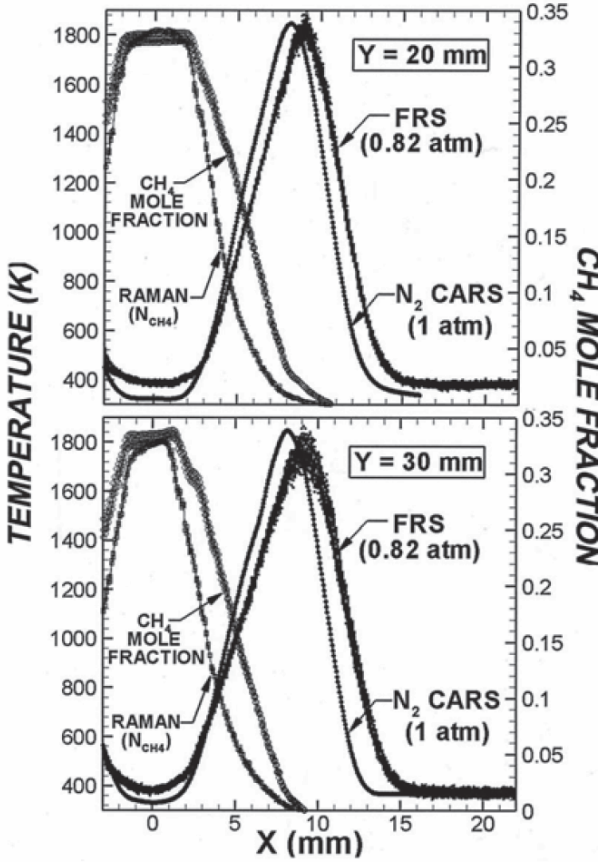

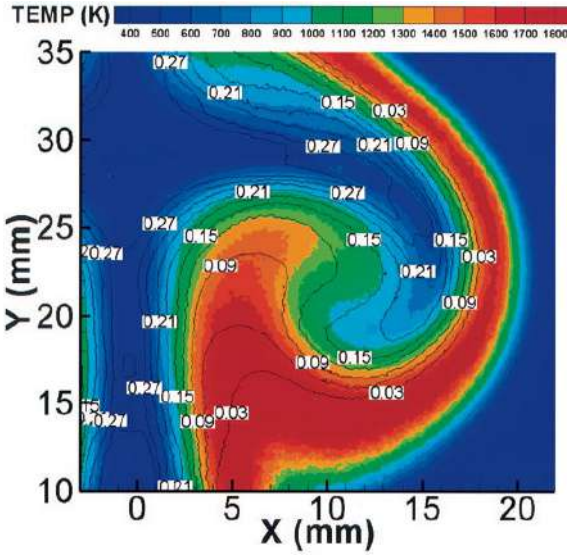

Applications: Nonpremixed Flames

- Nonpremixed flames are much more difficult because of the large change in species (cross sections, RBS profiles, etc) throughout the domain
- In my group we have taken a different approach. We have designed specific fuel blend such that the FRS parameter (ψ) does not vary throughout the flow field

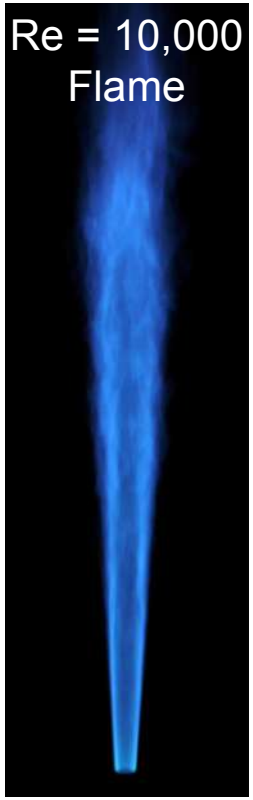

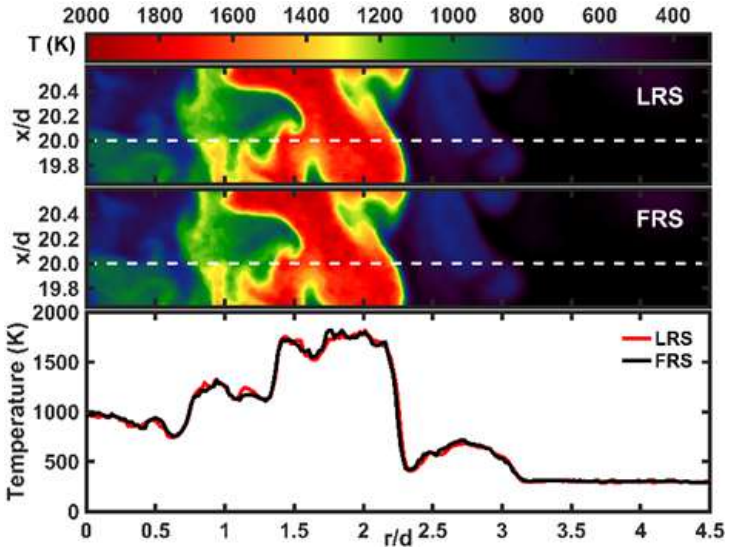

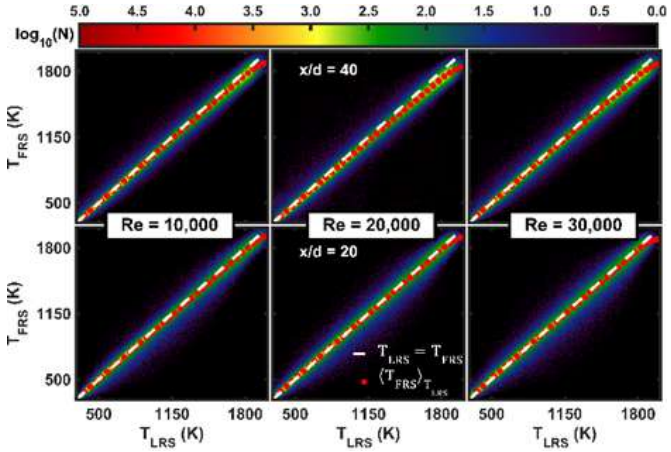

Applications: Sprays

- FRS also has the potential for extension to multi-phase flows
- The challenge lies with developing accurate RBS models for complex polyatomic species at high pressures

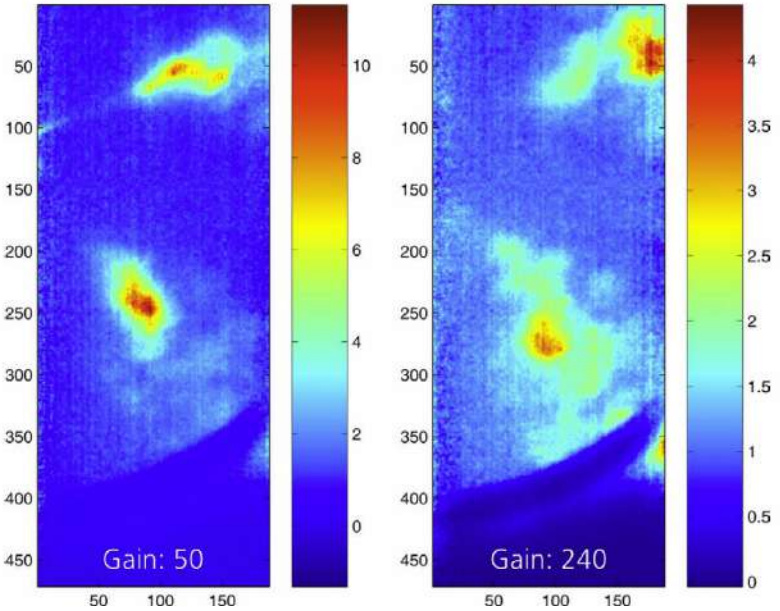

Zetterberg et al., "**Development of Filtered Rayleigh Scattering for Real World Temperature and Fuel/Air Ratio Imaging",** THIRD EUROPEAN COMBUSTION MEETING ECM 2007

Fuel distribution measured with FRS in the cylinder of a diesel engine at -7 and -6 crank angel degree respectively. P = 5 atm, isooctane

Applications: Sprays

- FRS also has the potential for extension to multi-phase flows
- The challenge lies with developing accurate RBS models for complex polyatomic species at high pressures

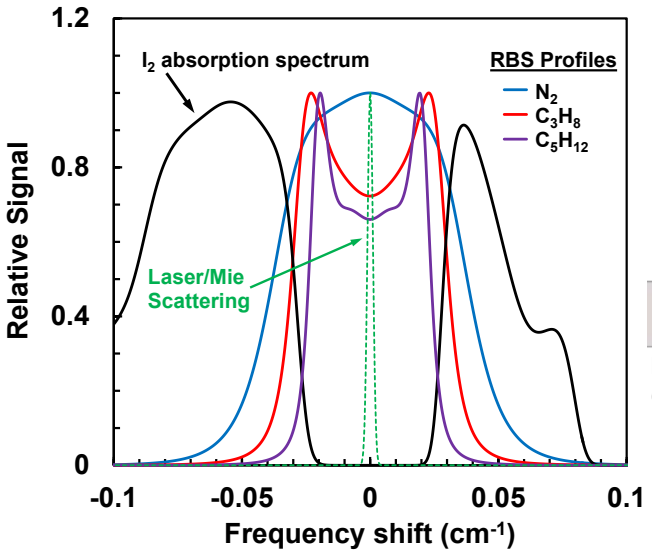

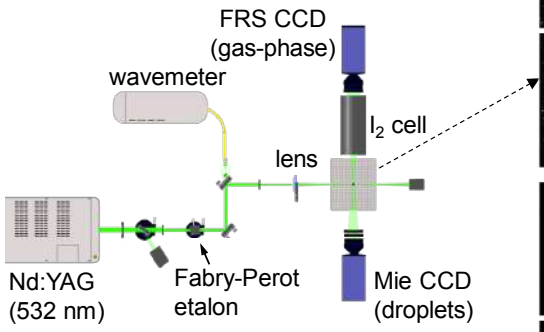

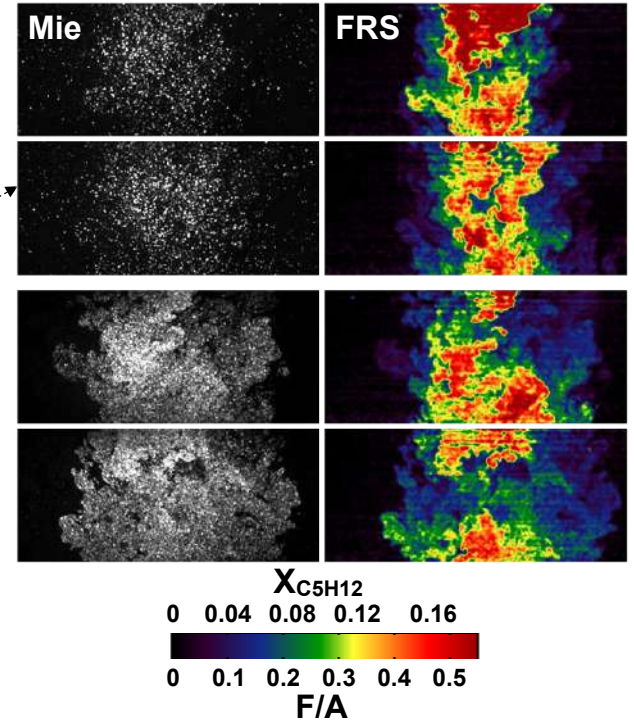

Allison et al., **Quantitative Fuel Vapor/Air Mixing Imaging in Droplet/Gas Regions of an Evaporating Spray Flow Using Filtered Rayleigh Scattering,** *Opt. Lett.*, 2015

Laser Diagnostics in Turbulent Combustion Research

Jeffrey A. Sutton

Department of Mechanical and Aerospace Engineering
Ohio State University

Princeton-Combustion Institute Summer School on Combustion, 2019

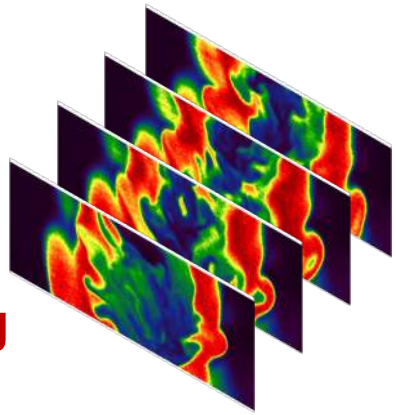

Lecture 13 – Spontaneous Raman Scattering

Overview and Outline of Lecture

Goal: Provide an Overview of Raman Scattering and Applications in Turbulent Flames

- Species Measurements in Flames
- Rotational vs Vibrational Raman Scattering
- Raman Scattering Theory (Extension of Rayleigh)
- Experimental Considerations and Data Analysis
- Applications of FRS in Reacting Flows

Raman Scattering: History

- The inelastic scattering of photons was first predicted theoretically in 1923 by Adolf Smekal in 1923 (largely forgotten)

- C.V. Raman (and student K.S. Krishnan) discovered the effect in solids, liquids, and gases in 1928
- Landsberg and Mandelstam independently discovered the same effect in crystals around the same time
- Raman's experiment consisted of "monochromatic light" from a mercury arc lamp whose radiation passed through water and transparent blocks of ice before reaching a spectrometer
- Raman received the Nobel Prize in 1930 for pioneering work on the scattering of light

Raman Scattering Overview

- We saw in Lecture 11 that Rayleigh scattering (let's just focus on the Cabannes line) is not species specific – it gives information on the number density and only that is directly measurable if the species are known
- Raman scattering offers a method to measure individual species in combustion environments.
- Because of the "weak" signal levels, the technique only is useful for "major species", i.e., hydrocarbon fuel, CO, CO_2, H_2O, O_2, N_2, H_2, (C_2H_2, and possibly other hydrocarbons)
- This measurement of major species compliments measurement techniques such as LIF which can measure minor species (OH, NO, CH, etc.), but cannot easily measure species such as H_2, N_2, CO_2, H_2O, etc.
- In addition, Raman scattering often is combined with Rayleigh scattering. The Raman scattering allows a determination of the mixture-averaged Rayleigh scattering cross section and the temperature measurement allows quantification of the Raman signal into concentration!

Species Measurements

- In combustion, species measurements are critical. We already discussed LIF for minor species measurements (there are many other approaches)
- For major species, there are additional approaches including CARS (we briefly discussed this in Lecture 2)
- Conventional CARS (say ns or ps lasers) measurements do not have enough bandwidth to cover "all" major species simultaneously (the full width of species of interest may be ~ 4000 cm^{-1}). One or two species (e.g., O_2 and N_2) may be excited. The primary utility of CARS was/is traditionally that of a highly accurate thermometry approach
- New ultrafast (fs) approaches have the potential for covering a very broad spectral region. For example, researchers at Sandia have demonstrated single-shot fs-CARS measurements with > 4200 cm^{-1} bandwidth

Bohlin, A. and C. J. Kliewer. Single-shot hyperspectral coherent Raman planar imaging in the range 0–4200 cm^{-1}. *Appl. Phys. Lett.* **2014,** *105* (16), 161111.

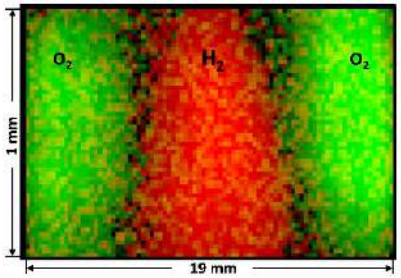

Species Measurements

- Subsequently, this approach has been used for 1D imaging of temperature and major species in the near-wall region of a CH_4/air flame

Bohlin, et. al. Multiparameter spatio-thermochemical probing of flame–wall interactions advanced with coherent Raman imaging. *Proc. Combust. Inst.* **2016,** *36,* 4557.

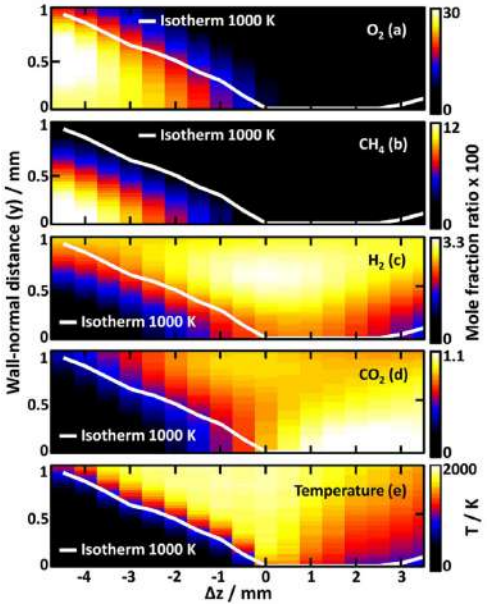

- So what is the importance of species measurements?
- Accurate species measurements are needed to understand the thermochemical state. Temperature and minor species cannot tell you the entire story.
- Furthermore, the measurement of "all" major species permits the measurement of the mixture fraction (ξ) in turbulent nonpremixed flames:

$$\xi = \frac{\beta - \beta_{ox}}{\beta_{fuel} - \beta_{ox}}; \qquad \beta = Y_{ce} \quad \rightarrow \qquad \textbf{(221)}$$

$$\xi = \frac{2\left(Y_C - Y_{C,ox}\right)/W_C + \left(Y_H - Y_{\mathrm{H},ox}\right)/2W_H - \left(Y_O - Y_{\mathrm{O},ox}\right)/W_O}{2\left(Y_{C,fuel} - Y_{C,ox}\right)/W_C + \left(Y_{H,fuel} - Y_{\mathrm{H},ox}\right)/2W_H - \left(Y_{O,fuel} - Y_{\mathrm{O},ox}\right)/W_O} \qquad \textbf{(222)}$$

Raman Scattering

- Let's go back to an intermediate result from Lecture 11

$$\vec{p} = \underbrace{\alpha_o \vec{E}_o \cos(\omega t)}_{\text{Rayleigh}} + \frac{\partial \alpha}{\partial Q}\frac{Q_o \vec{E}_o}{2}\underbrace{\left[\cos(\omega - \omega_{vib})t}_{\text{Stokes}} + \underbrace{\cos(\omega + \omega_{vib})t\right]}_{\text{anti-Stokes}} \qquad \textbf{(179)}$$

- The classical derivation predicts that the Stokes and anti-Stokes lines will have the same intensity. This usually is not the case
- The anti-Stokes lines will be weaker due to the ratio of populations in the ground state vs. excited vibrational level (remember Boltzmann fractions)
- The ratio of the intensities can be determined by examining the relative Boltzmann distributions and noting that the emitted intensity scales as ν^4:

$$\frac{I_{anti-Stokes}}{I_{Stokes}} = \frac{\left(\omega - \omega_{vib}\right)^4 e^{-\hbar\omega_{vib}/k_B T}}{\left(\omega + \omega_{vib}\right)^4} \qquad \textbf{(223)}$$

Rayleigh and Raman Scattering

- We will discuss two types of spontaneous scattering processes: (i) Rayleigh scattering and (ii) Raman scattering

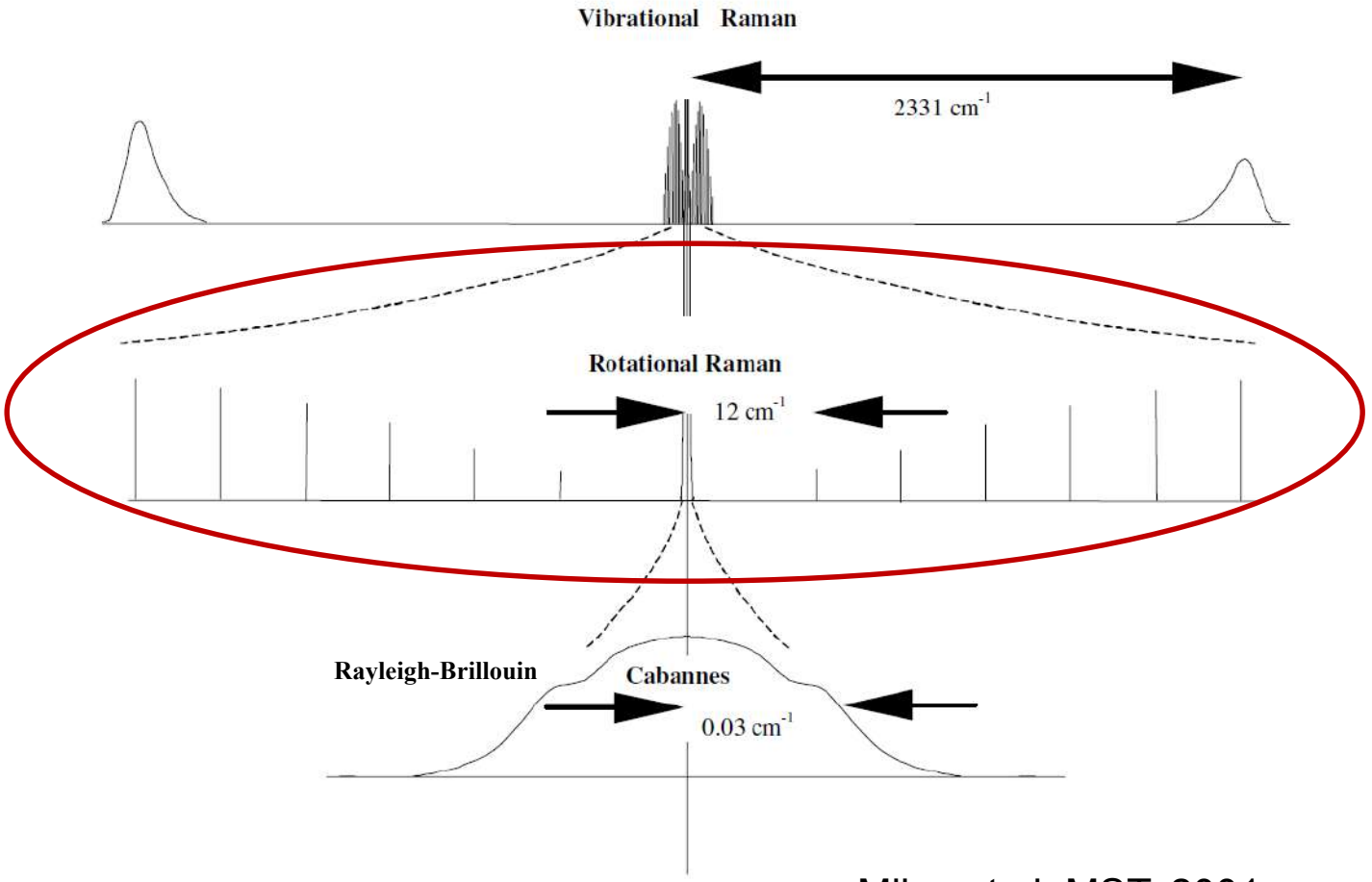

?

Miles et al, MST, 2001

Rotational Raman Scattering

- Recall from Lecture 11 that, in general, the induced dipole does not have lie in the same direction as the applied electric field and thus $\vec{p}$ and $\vec{E}$ can point in different directions
- This led to the polarizability tensor being written as a symmetric 3 x 3 matrix (vs. a scalar for a spherical scatterer)
- The polarizability tensor can be simplified by changing to a principle axis system **of the molecule** (i.e., "molecular coordinate system") through an orthogonal transformation (rotation of the x, y, and z axes) that diagonalizes $\vec{\alpha}$:

$$\vec{\alpha}' = \begin{pmatrix} \alpha_x & 0 & 0 \\ 0 & \alpha_y & 0 \\ 0 & 0 & \alpha_z \end{pmatrix} \qquad \textbf{(224)}$$

- For linear molecules we can now write $\alpha_{||} = \alpha_z$ and $\alpha_{\perp} = \alpha_x = \alpha_y$; where the polarizability (in the new reference frame) is parallel to z axis.
- Thus, $a = (\alpha_{||} + 2\alpha_{\perp})$ and $\gamma = (\alpha_{||} - \alpha_{\perp})$

Rotational Raman Scattering

- Also recall from Lecture 11 that we referred to the fact that some internal motion can modulate the induced oscillating dipole.
- Eqs. (173) – (175) are valid for rotational or vibrational motion
- When a molecule rotates, the polarizability presented to the incident electric field changes with rotation; that is, the electric field (and the resultant scattering) are in the original x-, y-, and z- axes, but the polarizability is in the "molecular coordinate system"
- Thus, the induced dipole and the scattered light are modulated by the rotation of the molecule (unless the molecule is a spherical top)
- This modulation results in rotational transitions (different than the vibrational transitions that we discussed in Lecture 11)
- To have observable rotational Raman spectra, the anisotropic portion of the polarizability tensor has to be non-zero, i.e., $\alpha_{\parallel} \neq \alpha_{\perp}$

Rotational Raman Scattering

- Now, it may be noted that if we go back and examine the Rayleigh scattering cross section (with 90^o observation) that the anisotropy factor arises from the emergence of the rotational Raman components

$$\frac{\partial \sigma_V}{\partial \Omega} = \frac{\pi^2}{\varepsilon_o^2 \lambda^4}\left(\frac{45a^2 + 7\gamma^2}{45}\right) \qquad \textbf{(202)}$$

symmetric — Anisotropy factor

- Thus, our Rayleigh scattering cross section that we calculated contains rotational Raman information! We could separate them out if we wanted…
- "Rayleigh scattering" = Gross line + Brillouin scattering + rotational Raman
- In Lecture 11 we stated that to have a vibrational Raman effect, the polarizability had to change with vibration. The same type of idea holds for rotational Raman.
- We can now state that to be Raman active, a molecule must have anisotropic polarizability

Rotational Raman Scattering

- We won't go through the derivation of the selection rules for rotational Raman scattering, but the result is $\Delta J = 0, \pm 2$ for linear molecules; that is, it is an effective two-photon process (a single photon places the molecule in a virtual state; a second photon is emitted)
- $\Delta J = 0$ is many times reported as Rayleigh scattering, but it is actually an unresolved Q branch (not discussed).
  Cabannes line = Gross line + Brillouin scattering + Q branch Raman.
  The $\Delta J = \pm 2$ are S branches
- Assuming a rigid rotator, $E_{rot} = BJ(J+1)$ and the transition frequencies are determined by

$$\nu = \nu_o \pm B(J+2)(J+3) - BJ(J+1) = \nu_o \pm B(4J+6) \qquad \textbf{(225)}$$

Nitrogen rotational Raman spectrum

Varghese et al. AIAA-1996-176-399(1)

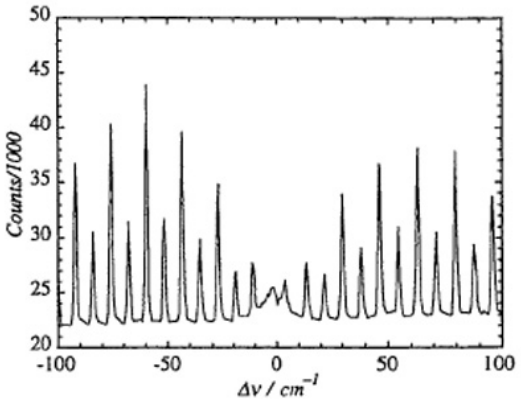

Ro-Vibrational Raman Scattering

- Since rotational transitions are “embedded” within vibrational levels, rotational structure is superimposed onto vibrational Raman spectra
- For diatomic molecules the selection rules are $\Delta\upsilon = \pm 1;\ \Delta J = 0, \pm 2$. The $\Delta J = -2, 0, 2$ rules result in O, Q, and S branches, respectively
- Recall from Lecture 8 (w/ slight modifications):

$$\tilde{E}_{vib} = (\upsilon + 1/2)\nu_e - (\upsilon + 1/2)^2 \nu_e x_e \qquad \textbf{(98')}$$

$$\nu = (\tilde{E}''_{vib,2} - \tilde{E}''_{vib,1}) + (\tilde{E}''_{rot,2} - \tilde{E}''_{rot,1}) \qquad \textbf{(99')}$$

- Thus, the transition frequencies are determined by adding the rotational positions (Eq. (225)) onto vibrational positions

$$\nu_Q = \nu_{laser} - \nu_e(1 - 2x_e) \qquad \textbf{(226a)}$$

$$\nu_S = \nu_{laser} - \nu_e(1 - 2x_e) - B(4J + 6) \qquad \textbf{(226b)}$$

$$\nu_O = \nu_{laser} - \nu_e(1 - 2x_e) + B(4J + 6) \qquad \textbf{(226c)}$$

Ro-Vibrational Raman Scattering

- Thus, the transition frequencies are determined by adding the rotational positions (Eq. (225)) onto vibrational positions

$$\nu_Q = \nu_{laser} - \nu_e(1-2x_e) \qquad \textbf{(226a)}$$

$$\nu_S = \nu_{laser} - \nu_e(1-2x_e) - B(4J+6) \qquad \textbf{(226b)}$$

$$\nu_O = \nu_{laser} - \nu_e(1-2x_e) + B(4J+6) \qquad \textbf{(226c)}$$

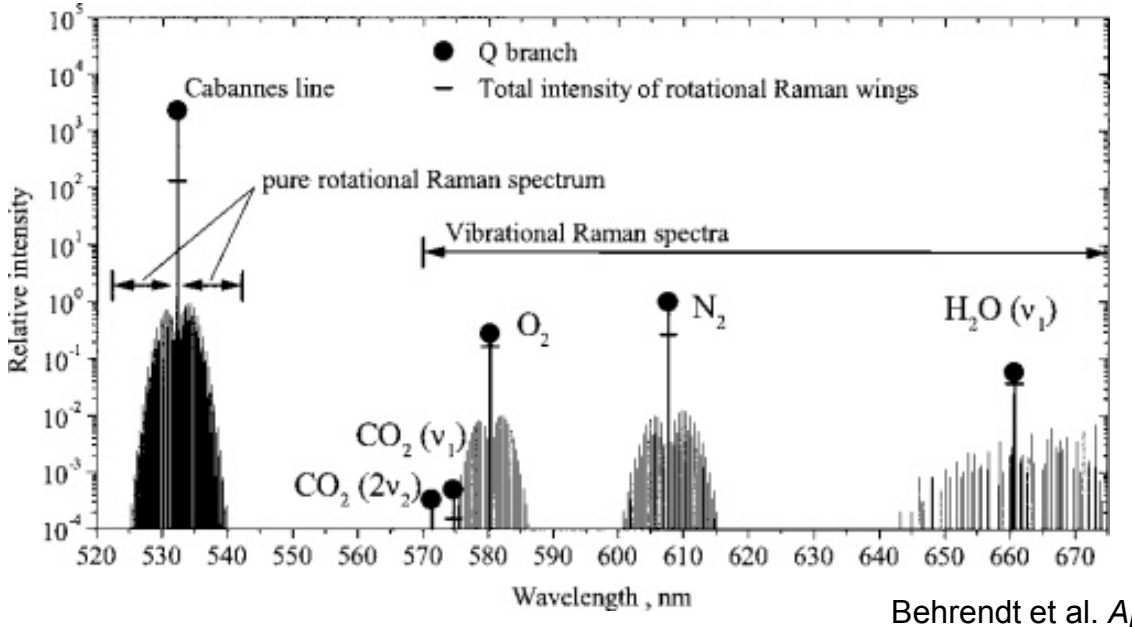

Behrendt et al. *Appl. Opt.*, 2002

Ro-Vibrational Raman Scattering

- The intensity expressions developed for Rayleigh scattering (Eqs. 200, 201) can be applied for the vibrational Raman effect
- In a similar manner to Eq. (177) we can write the polarizability expansion as

$$\alpha_{ij} = \alpha_{e,ij} + \left.\frac{\partial \alpha_{ij}}{\partial r}\right|_{r_e} (r - r_e) \qquad \textbf{(227)}$$

  where α_e is the polarizability at the equilibrium position, r is the internuclear distance and r_e is the internuclear distance at the equilibrium position
- It can be shown using vibrational spectroscopy results that

$$\alpha_{ij} = \left(\frac{h}{8c\pi^2(\nu_{vib})}\right)^{1/2} \left.\frac{\partial \alpha_{ij}}{\partial r}\right|_{r_e} \qquad \textbf{(228)}$$

- Combining Eqs. (228) and (201):

$$I''_{S,Ram} = \frac{h}{8c\varepsilon_o^2 \lambda^4 \nu_{vib}} \left(\frac{45(a')^2 + 7(\gamma')^2}{45}\right) I_I \qquad \textbf{(229)}$$

Ro-Vibrational Raman Scattering

- In Eq. (229) the single-primed quantities represent partial derivatives with respect to r and are defined as

$$(a')^2 = \frac{1}{9}\left(\alpha_x' + \alpha_y' + \alpha_z'\right)^2 \qquad \textbf{(230)}$$

$$(\gamma')^2 = \frac{1}{2}\left(\left(\alpha_x' - \alpha_y'\right)^2 + \left(\alpha_y' - \alpha_z'\right)^2 + \left(\alpha_z' - \alpha_x'\right)^2\right) \qquad \textbf{(231)}$$

- Eq. (229) was for a single scatterer. Similar to our formulation for Rayleigh, we can consider a volume V with number density No in the ground state:

$$I_{S,Ram,total}'' = I_{S,Ram}'' N_o V \qquad \textbf{(232)}$$

- We also have to note that we have to replace the population in the ground state with a weighted population relative to the total number density (recall the Boltzmann fraction from Lecture 10):

$$I_{S,Ram,total}'' = I_{S,Ram}'' \frac{N}{Q_{vib}} V \qquad \textbf{(233)}$$

Ro-Vibrational Raman Scattering

- So for our case of linear polarization (along z) with collection at 90° and for the case of Stokes scattering (for single species i):

$$I''_{S,Ram,i} = \frac{h(\nu_{laser} - \nu_{vib})^4}{8c\varepsilon_o^2 \nu_{vib}(1 - e^{-hc\nu_{vib}/k_B T})} \left(\frac{45(a')^2 + 7(\gamma')^2}{45} \right) N_i V I_I \quad \textbf{(234)}$$

- This implies that we can write a differential Raman scattering cross section for each species *i* as:

$$\frac{\partial \sigma_{Ram,i}}{\partial \Omega} = \frac{h(\nu_{laser} - \nu_{vib})^4}{8c\varepsilon_o^2 \nu_{vib}(1 - e^{-hc\nu_{vib}/k_B T})} \left(\frac{45(a')^2 + 7(\gamma')^2}{45} \right) \quad \textbf{(235a)}$$

- or

$$\frac{\partial \sigma_{Ram,i}}{\partial \Omega} = \frac{h(\nu_{laser} - \nu_{vib})^4}{2c\nu_{vib}(1 - e^{-hc\nu_{vib}/k_B T})} \left(\frac{(n-1)}{N} \right)^2 \frac{3}{3 - \rho_p} \quad \textbf{(235b)}$$

- Similar to Rayleigh, there is a ν^4 power dependence on the scattering cross section. We also see that since ν_{vib}, a' and γ' vary for each species, the scattering cross section is species specific.

Raman Shifts and Cross Sections

- Again noting that we collect signal over some finite collection volume:

$$I_{Ram,i} = I_I \eta N_i V \Omega \frac{\partial \sigma_{Ram,i}}{\partial \Omega} \qquad \textbf{(236)}$$

- Cross sections (at 532 nm) and Raman shifts for typical combustion species (Eckbreth, 1988):

Gas species	Rayleigh cross-section ($\times 10^{28}$ cm^2 ster^{-1})	Raman shift (cm^{-1})	Raman cross-section ($\times 10^{31}$ cm^2 ster^{-1})
Hydrogen	1.1	4160	9.4
Methane	11.6	2915	26.0
		3017	17.0
Ethylene	25.5	3020	19.0
		1623	7.6
Oxygen	4.4	1556	4.7
Nitrogen	5.1	2331	3.7
Argon	4.7	—	—
Helium	0.1	—	—
Air	5.1	—	—
Freon 22	59.5	—	—
Water vapour	3.8	3657	9.0
Carbon dioxide	11.9	1388	6.0
		1285	4.5
Carbon monoxide	6.8	2145	4.8
Nitric oxide	5.2	1877	2.0

Enables species-specific measurements!

Raman Measurements in Flames

- Sandia National Labs Combustion Research Facility - state-of-the art!!!

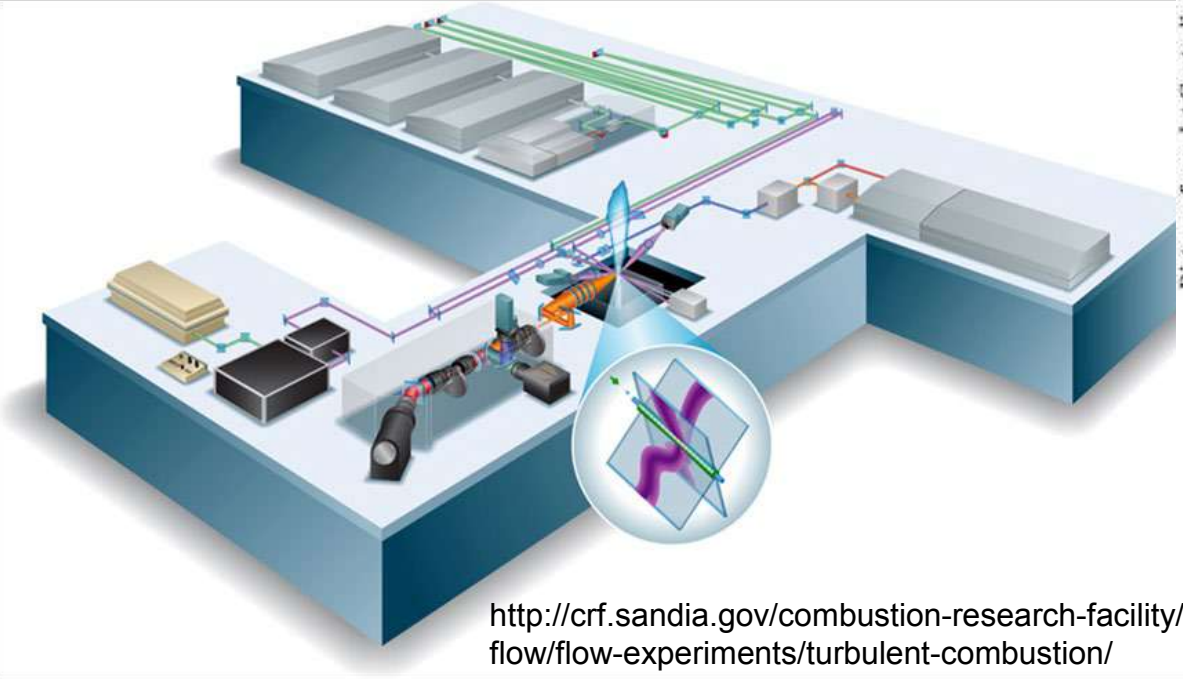

http://crf.sandia.gov/combustion-research-facility/reacting-flow/flow-experiments/turbulent-combustion/

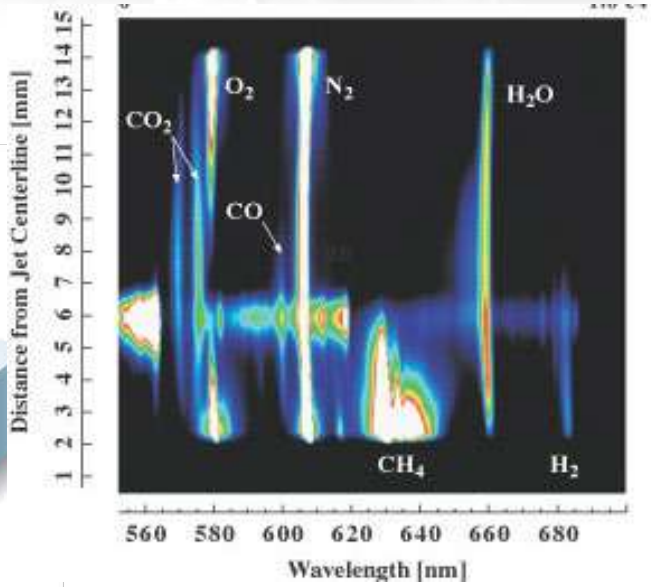

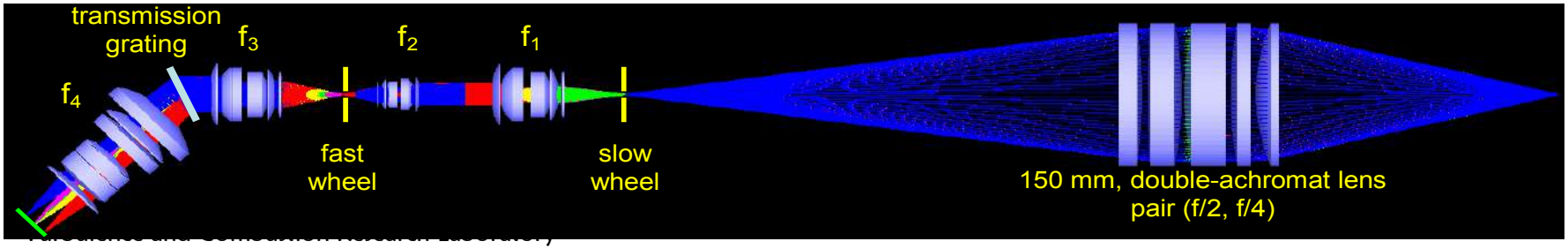

Experimental Setup and Detection

- Rayleigh/Raman scattering can be excited with any laser; for single-shot measurements in turbulent flames, high-energy pulsed lasers are used.
- The most common is the 2nd-harmonic (532 nm) output of a Q-switched Nd:YAG laser (or series of lasers)
- Since the laser is focused down to a point in space, dielectric breakdown occurs well before maximum pulse energies can be used
- It is common to employ a laser pulse stretcher to increase the effective pulse duration. In this manner the laser pulse power (which controls breakdown) decreases so higher pulse energies can be used

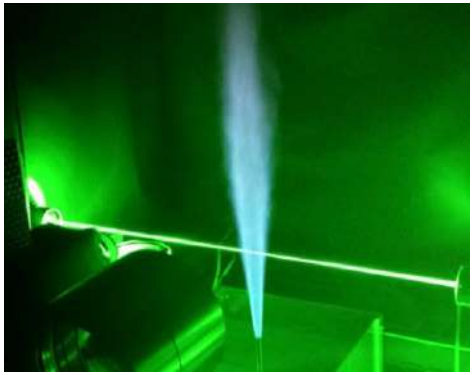

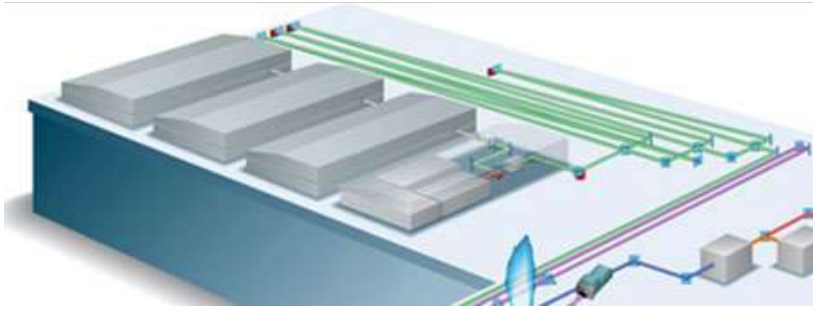

Example of Sandia CRF laser cluster for 1.8 J/pulse output

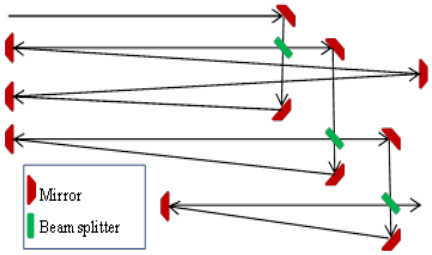

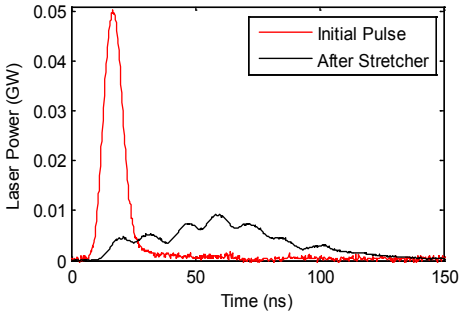

Experimental Setup and Detection

- There are multiple detection strategies ranging from “older” point-based measurements with multiple PMTs (each filtered for a different λ and species) to more modern imaging setups.

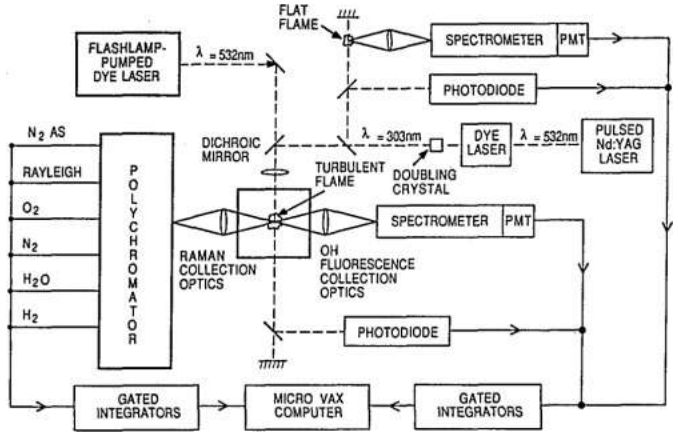

Barlow et al., *Appl. Opt*., 1989

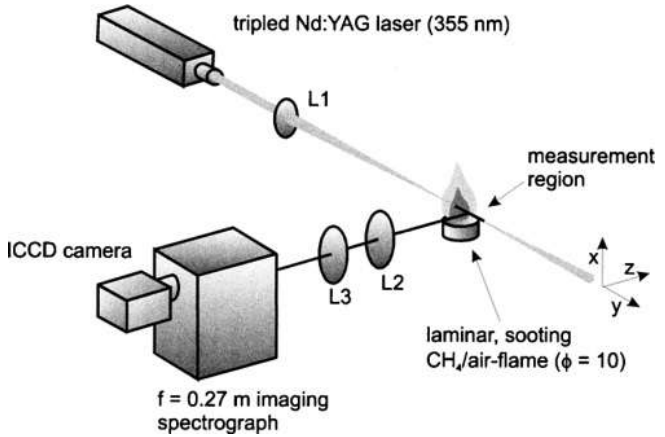

Rabenstein and Leipertz, *Appl. Opt*., 1998

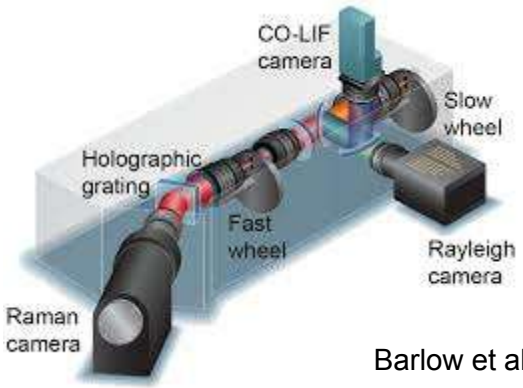

Barlow et al, *Proc. Combust. Inst*., 2008

Raman Measurements in Flames

- Because of the large variation in concentration and scattering cross sections across the species, there are significant signal differences across the flame
- Hydrocarbon flames have more species, more Raman transitions, and hence a more complicated spectrum

Gas species	Raman shift (cm^{-1})
Hydrogen	4160
Methane	2915
	3017
Ethylene	3020
	1623
Oxygen	1556
Nitrogen	2331
Argon	—
Helium	—
Air	—
Freon 22	—
Water vapour	3657
Carbon dioxide	1388
	1285
Carbon monoxide	2145
Nitric oxide	1877

H_2 flame

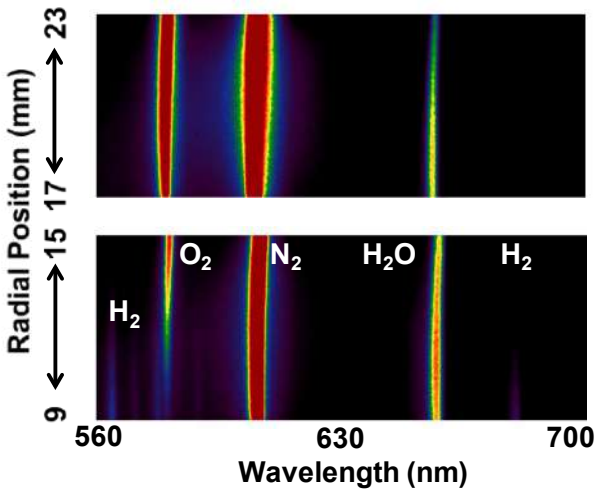

CH_4 flame

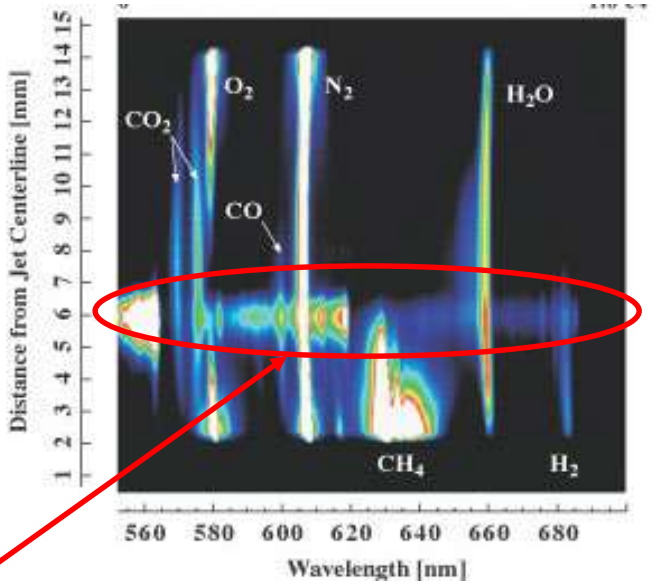

LIF interference in HC flames

http://crf.sandia.gov/combustion-research-facility/reacting-flow/flow-experiments/turbulent-combustion/

Raman Measurements in Flames

- To measure the species that we want, we need to cover approximately 3000 cm^{-1} on an O(1000) pixel camera
- There is a resolution problem!
- In reality the measurements show strong features from the Q branch and a lower "diffuse" signal from the surrounding O and S branches (+ LIF interference)
- Because the resolution is not high enough to separate the spectral features, there will be information from multiple species on a single pixel. This is referred to as "cross talk"
- So, acquiring the signal is only one part of the experimental challenge. A significant amount of effort is spent in data analysis (including calibration)

Behrendt et al. *Appl. Opt.*, 2002

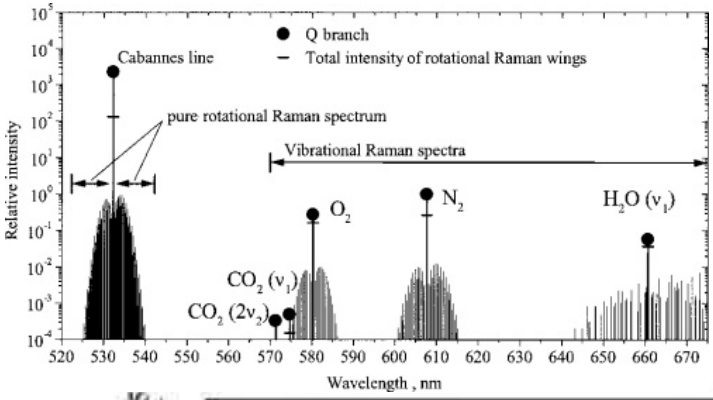

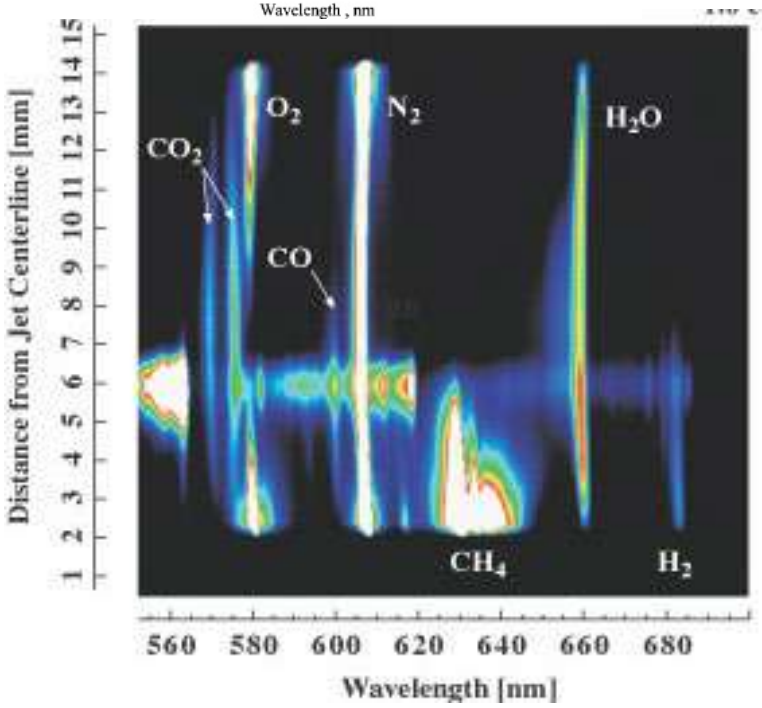

Data Analysis

- There are three primary methods for reducing Raman signal to quantitative measurements of concentration:

  Spectral Fitting: Based on libraries of theoretical spectra (*Geyer, Ph.D. thesis, 2005*). Individual rovibrational Raman transitions are calculated based on Placzek's theory of polarizability for each species and convolved to apparatus function. Species concentrations in turbulent flames are determined by fitting experimental data with libraries (RAMSES).

  Polynomial Matrix Inversion: Raman signals and interferences are integrated across fixed spectral regions (binned pixel regions on camera) to form a signal vector, S_i which is related to species number density via

$$S_i = c_{ij} N_i \qquad \textbf{(237)}$$

  where all matrix elements depend on temperature and experimental setup. The diagonal elements c_{ii} (T) are the Raman responses, whereas c_{ij} (T) are crosstalk between Raman channels, fluorescence interference, and background luminosity. The temperature dependence of each element is based on calibrations and represented as a polynomial. Number densities are determined by inverting Eq. (237) (actually solving via iteration)

Data Analysis

- There are three primary methods for reducing Raman signal to quantitative measurements of concentration:

  Hybrid Matrix Inversion: Based on the polynomial matrix inversion method, but the temperature dependence of the matrix elements c_{ij} are determined from the integration of the spectral libraries (RAMSES) over spectral regions corresponding to the binned Raman channels in the experiment

- Calibration – The matrix elements must be calibrated for use in any particular setup. Thus,

$$\left(c\right)_{i,j} = \left(c_{Ram}\right)_{i,j} \left(c_{SL}(T)\right)_{i,j} \qquad \textbf{(238)}$$

  represents the element-wise multiplication calibration factors $c_{Ram,ij}$ and the matrix elements determined from the spectral libraries $c_{SL,ij}(T)$. The species response and their crosstalks are calibrated in ambient air and calibration flames ranging from lean to rich.

Data Analysis

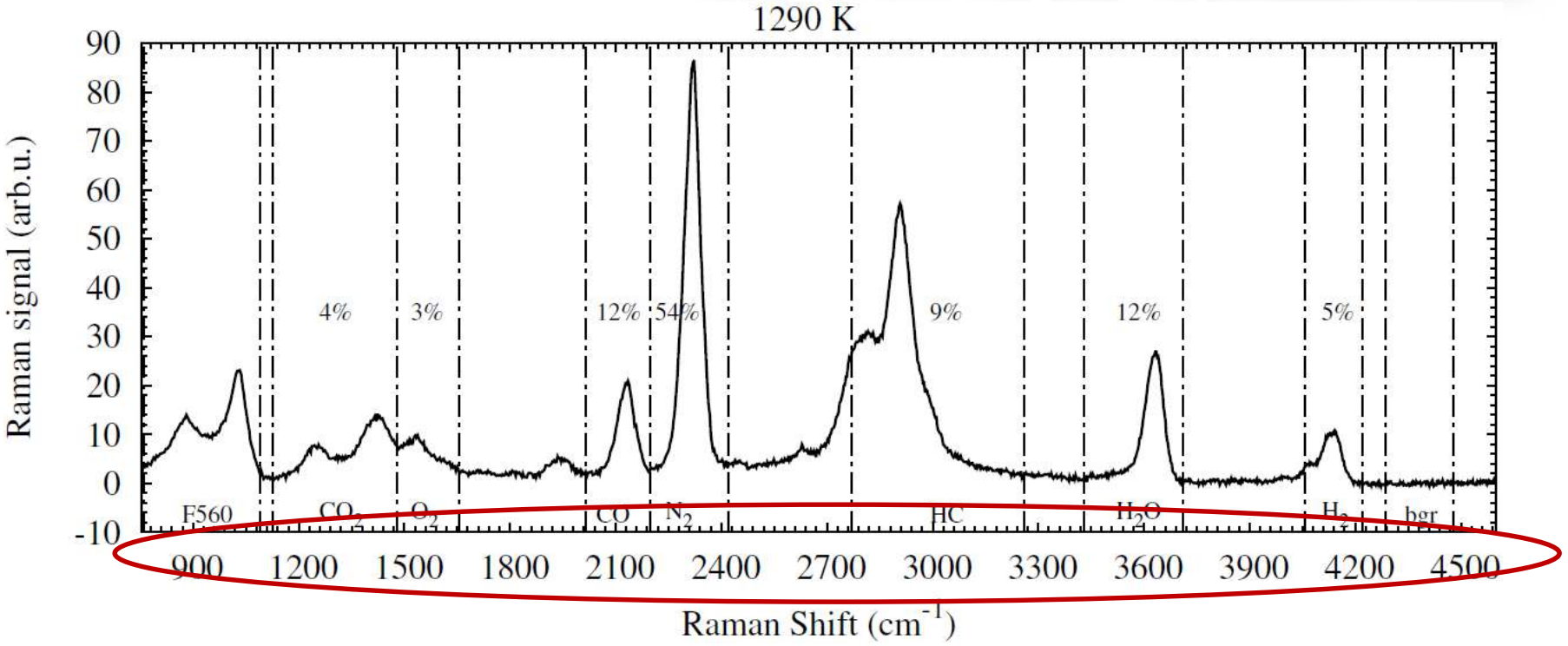

- Define N species and M background channels
- Software or hardware (“on-chip”) binning of signals
- Calibration using cold gases and laminar flat flames with known species composition

Data Analysis

- An example matrix equation with c_{ij} as calibration factors

$$\begin{bmatrix} S_{CO2} \\ S_{O2} \\ S_{CO} \\ S_{N2} \\ S_{CH4} \\ S_{H2O} \\ S_{H2} \\ S_{CO\text{-}LIF} \\ S_{F560} \\ S_{bgr} \end{bmatrix} = \begin{bmatrix} c_{11}(T, pixel) & & & & & & & & & \\ & & & & & & & & & \\ & & & & & & & & & \\ & & & & & & & & & \\ & & & & & & & & & \\ & & & & & & & & & \\ & & & & & & & & & \\ & & & & & & & & & \\ & & & & & & & & & \\ & & & & & & & & & \end{bmatrix} \begin{bmatrix} N_{CO2} \\ N_{O2} \\ N_{CO} \\ N_{N2} \\ N_{CH4} \\ N_{H2O} \\ N_{H2} \\ N_{CO\text{-}LIF} \\ F560 \\ bgr \end{bmatrix} \quad (239)$$

- Crosstalk → off-diagonal matrix elements
- Calibrated $c_{ij}(T, pixel)$ from quantum mechanical calculations → diagonal matrix elements
- Temperature from Rayleigh measurement (Raman species-corrected)
- Iteratively solve matrix equation

Example Calibration

- Consider a series of laminar, H_2/air flames stabilized above the surface of a near-adiabatic Hencken burner
- The initial guess is that $c_{Ram_{i,j}}$ = 1
- Apply matrix elements and iteratively solve. Answers are not that good

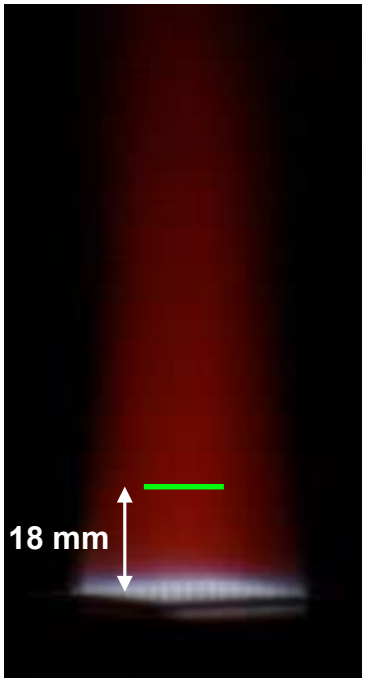

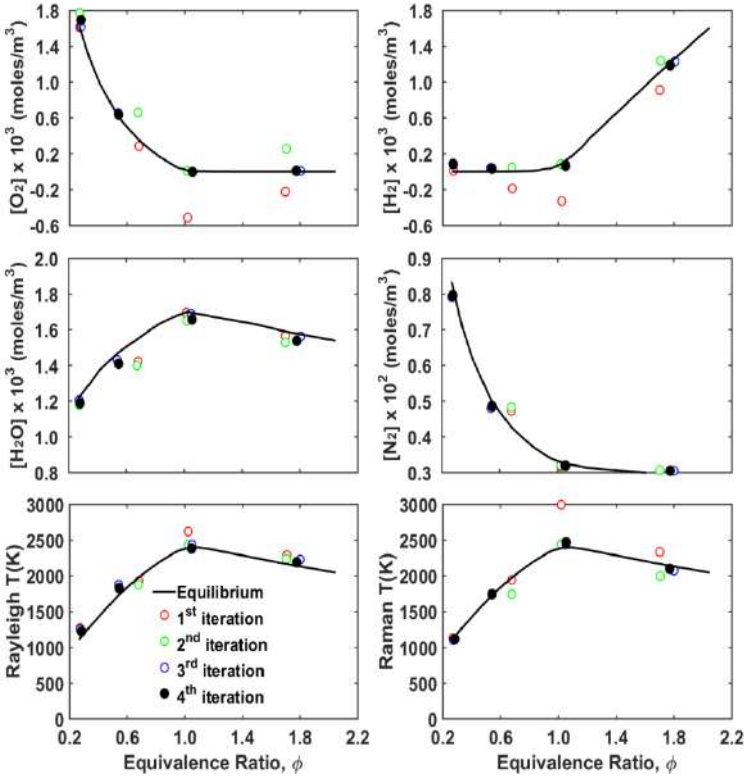

Example Calibration

- The matrix elements can be calibrated based on ambient temperatures and a select number of flame conditions.
- After a 2nd iteration, the answers are better in some places, but still not great.
- The matrix elements are then adjusted via additional calibration and the matrix is inverted again.
- This continues until there is good agreement across flame conditions
- The final values of c_{ij} are ported to turbulent flame measurements and no longer adjusted.

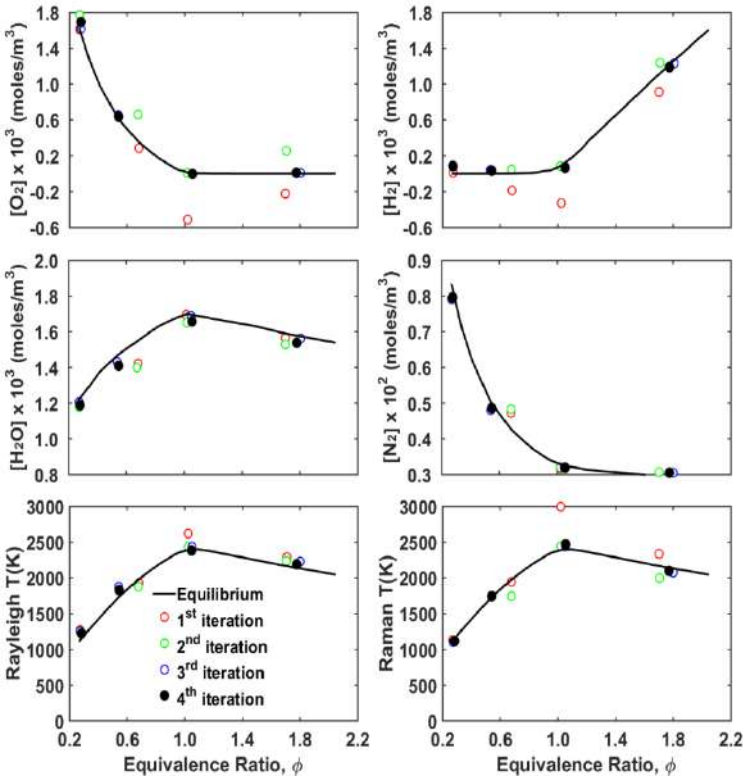

Accuracy

- The accuracy and precision of the method can be evaluated by examining single shot measurements in near-adiabatic, laminar flames (known answer!)

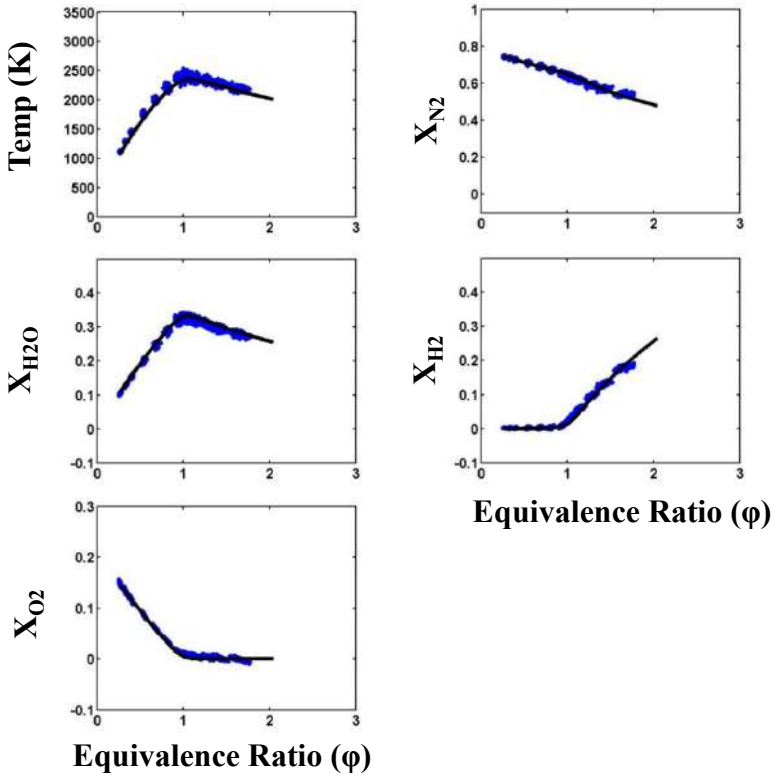

Example Applications

- Most common application is in laboratory-scale turbulent non-premixed or partially premixed flames
- Approach provides detailed measurements of species, temperature, and mixture fraction for model validation

Sandia piloted partially-premixed flame

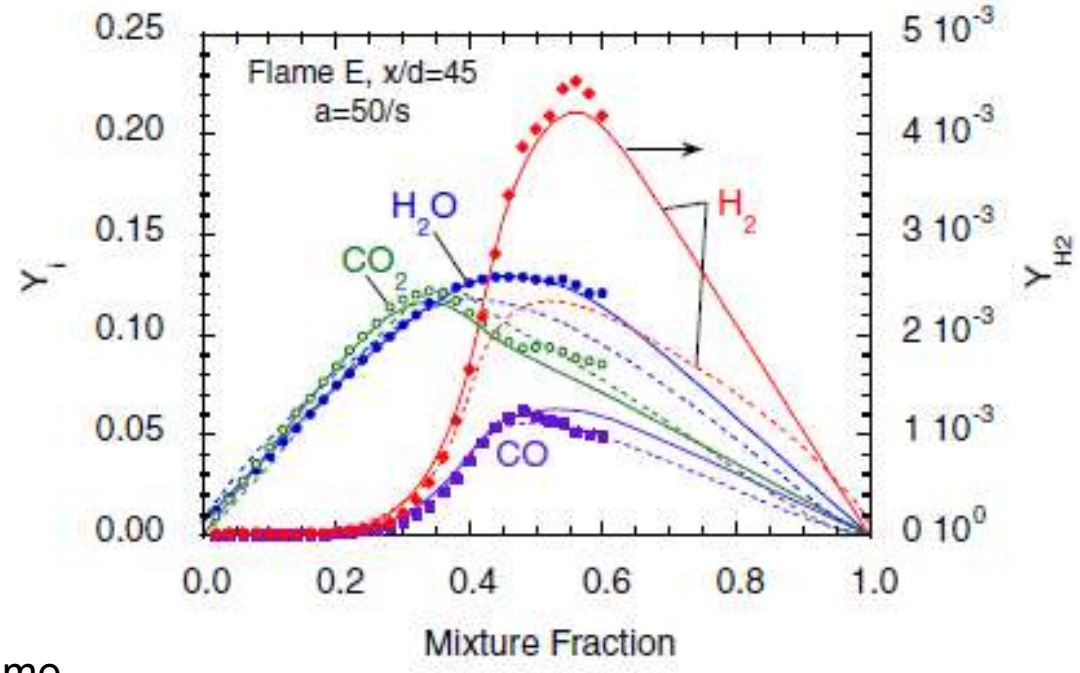

Example Applications

- DLR (German Aerospace) applies spontaneous Raman scattering to complex geometries such as a high-pressure gas turbine

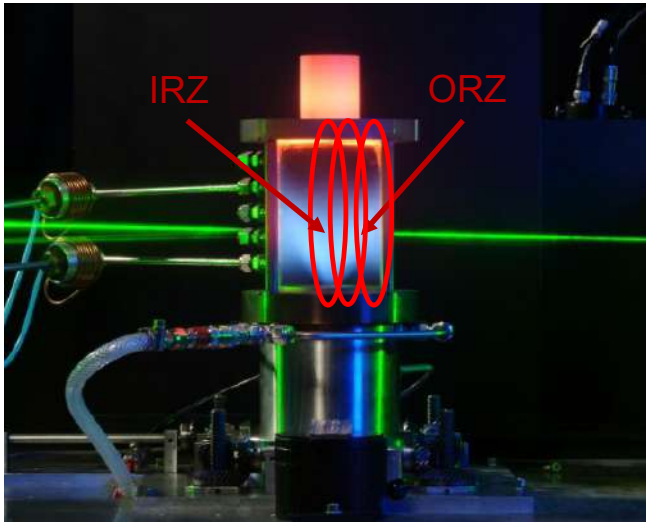

DLR model gas turbine combustor
Wehr et al., 2007

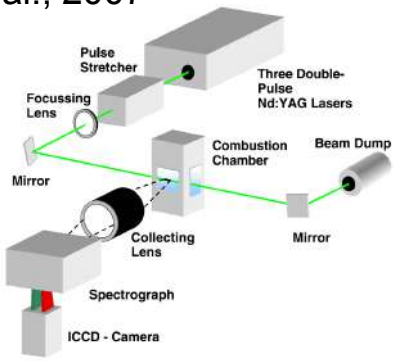

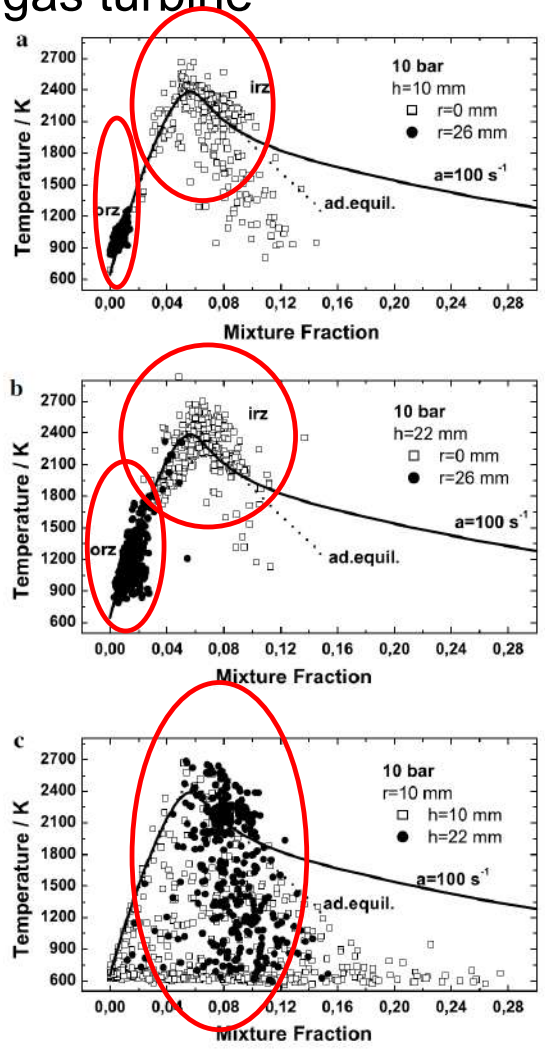

Laser Diagnostics in Turbulent Combustion Research

Jeffrey A. Sutton

Department of Mechanical and Aerospace Engineering
Ohio State University

Princeton-Combustion Institute Summer School on Combustion, 2019

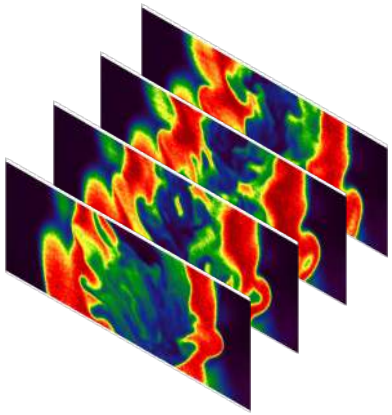

Lecture 14 – Recent Advances

Overview and Outline of Lecture

Goal: Provide an Overview of Recent Advancements in Combustion Diagnostic Development and Application

- High-Speed Imaging
- CEMA/Heat-Release Rate Measurements
- What's Next?

Examples